GENOMIC DISTRIBUTION AND FUNCTIONAL SPECIFICITY OF HUMAN HISTONE H1 SUBTYPES

Lluís Millán Ariño

DOCTORAL THESIS · 2013

Thesis supervisor:

Dr. Albert Jordan Vallès

Molecular Genomics Department

Institut de Biologia Molecular de Barcelona (IBMB) - CSIC

DEPARTMENT OF EXPERIMENTAL AND HEALTH SCIENCES – UPF

6.3. Differential prevalence of H1 variants along the genome

6.3.1. H1.2 is differently distributed in broad genomic regions and correlates with LADs

To further correlate ChIP-chip data of H1 abundance at promoters with ChIP-seq signal, regions of clustered promoters with high H1.2 content, such as the one marked with an asterisk in Figure R.19 (chromosome 1), were examined for input-subtracted H1 variants content, loading our data to the UCSC genome browser (Figure R.23A). The whole domain, delimited by a red square in the figure, was enriched in H1.2 ChIP-seq signal compared to neighboring regions, indicating that H1.2 enrichment was not limited to the promoters of repressed genes within. Interestingly, this domain was characterized by low GC content and the presence of lamina-associated domains (LADs), reported to anchor chromatin segments to the nuclear periphery, thus contributing to the spatial organization of the genome [105]. LADs are typified by low gene-expression levels, representing a repressive chromatin environment. Worth noting, the distribution of the other variants analyzed by ChIP-seq was not as clearly delimited to this domain as H1.2 (Figure R.23A). While H1.2 enrichment was notably restricted within these domains, distribution of other variants was not related with LADs distribution, but was similar among them.

The abundance of different H1 variants at LADs was further analyzed at other genomic regions and genome-wide. When the input-subtracted coverage of H1 variants across LADs was calculated, H1.2 was the only variant showing enrichment and, hence, associated with these domains (Figure R.23B). Further examination of H1 variants signal through several regions containing LADs using the UCSC genome browser confirmed that H1.2 was the variant better correlating with LADs positions and presenting fairly well delimited borders of enrichment (Figure R.23C).

LADs are reported to be highly conserved in different cell lines, although some of them are cell-type specific [106]. So, although LADs positions are available at a database being established in lung fibroblast Tig3 cells, we still find a good correlation with H1.2 enrichment. However, we would expect to increase this correlation if LAD data belonged to the same cell line used in our H1 ChIP experiments (T47D). Still, the differential association with LADs of the different H1 variants analyzed should be maintained, being H1.2 the most related with these domains.

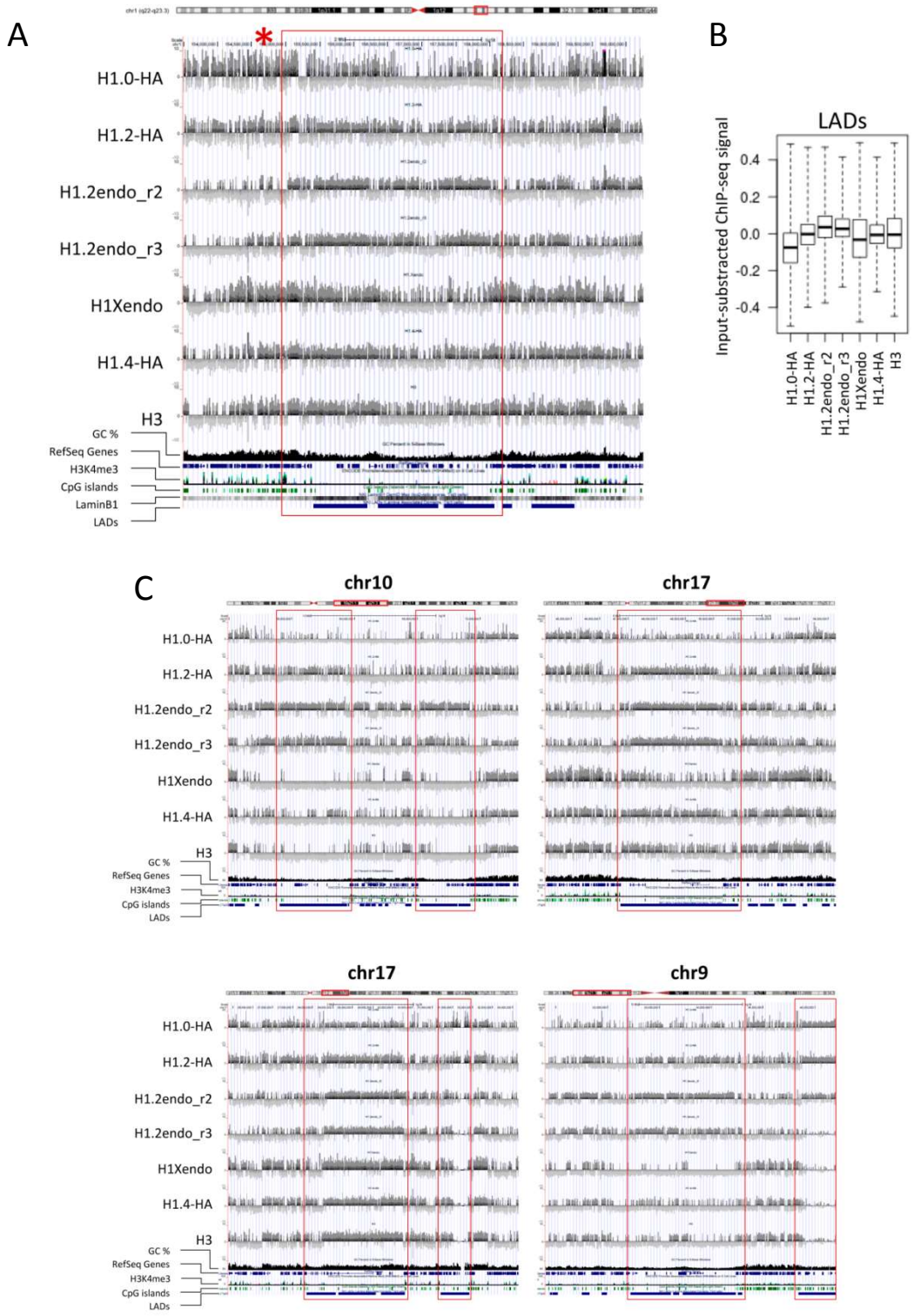

Figure R.23. Distribution of H1.2 in broad chromosome regions is different than other variants, and associates with LADs. (A) *Distribution of H1 variants along a selected region of chromosome 1 (red square) marked with an asterisk in Figure R.19. Input-subtracted H1 variants and H3 ChIP-seq signal viewed in the UCSC genome browser together with GC content, RefSeq genes, H3K4me3 (ENCODE average of 9 cell lines), CpG and Lamina-associated Domains (LADs; data from Tig3 lung fibroblasts).* ***(B)*** *Boxplots showing the occupancy of H1 variants (input-subtracted ChIP-seq signal) within LADs.* ***(C)*** *Distribution of H1 variants along selected LAD-containing regions of chromosomes 9, 10 and 17. Input-subtracted H1 variants and H3 ChIP-seq data viewed in the UCSC genome browser together with GC content, RefSeq genes, H3K4me3 (ENCODE average of 9 cell lines), CpG and LADs.*

6.3.2. H1 correlation with GC content

In order to further determine the relation of H1 variants with CpGs and GC content, we next performed genome-wide correlation analysis between input-subtracted H1 variants signal and GC content. Interestingly, low GC content associated with high occupancy of H1.2, but low occupancy of the other variants, including H1X, and vice versa (Figure R.24A and B). So, in agreement with the observation in Figure R.23A, H1.2 inversely correlated with GC, while other variants where positively correlated. H3 core histone presented also positive correlation, similar to H1.0, H1.4, and H1X. H1.2-HA presented an intermediate behavior between endogenous H1.2 and the rest of H1 variants, including endogenous H1X.

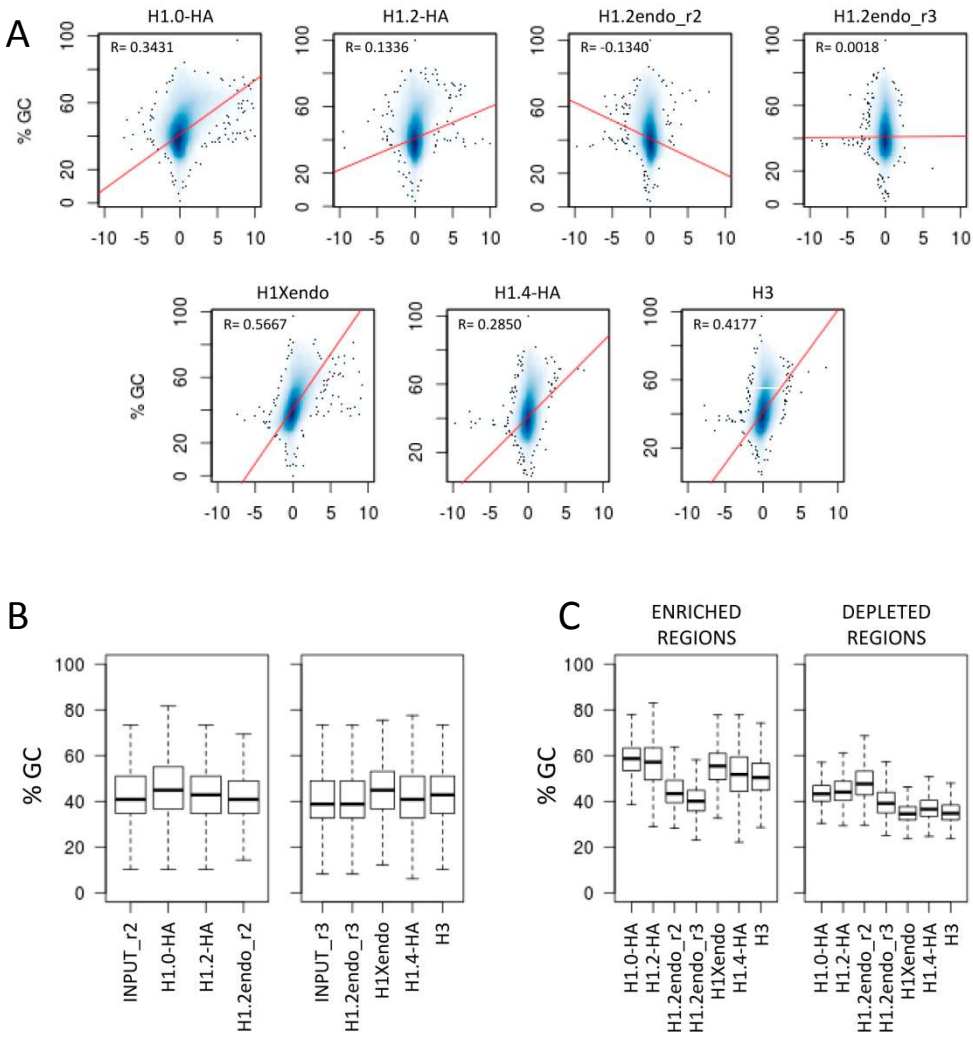

Figure R.24. H1 correlation with GC content. (A) *Genome-wide correlation scatter plots of H1 variants versus GC content. X axes: average input-subtracted H1 variants and H3 ChIP-seq signal (normalized to 1000bp window). Y axes: GC%. R: Pearson's correlation coefficient.* ***(B)*** *Boxplots of the GC content of H1 and input ChIP-seq reads.* ***(C)*** *Boxplots of the GC content of H1 variant enriched and depleted regions (see section 6.4).*

6.3.3. Chromosomal H1 variant abundance

Using the UCSC genome browser, we next examined individual chromosomes for the occurrence of the different H1 variants input-subtracted signal. Abundance of H1 along chromosomes was heterogeneous, showing extensive patches of enrichment or depletion of H1 compared to input (Figure R.25). Interestingly, H1.2 pattern was the most divergent compared to the other variants. Endogenous H1X and HA-tagged variants showed similar distribution patterns, and similar to H3 distribution. HA-tagged H1.2 was more similar to endogenous H1.2 than to other HA-tagged H1s.

In agreement with the heat maps of H1.2 occurrence at promoters shown in Figure R.19A, the gene-poor chromosome 13 was enriched in H1.2 compared with the other variants, and gene-rich chromosomes 17 and 19 were devoid of endogenous H1.2, but occupied by exogenous H1.2-HA. It is worth noting that long genome patches of low GC content were found to be devoid of all H1 variants except H1.2 that was enriched (Figure R.25), in agreement with scatter plots in Figure R.24A.

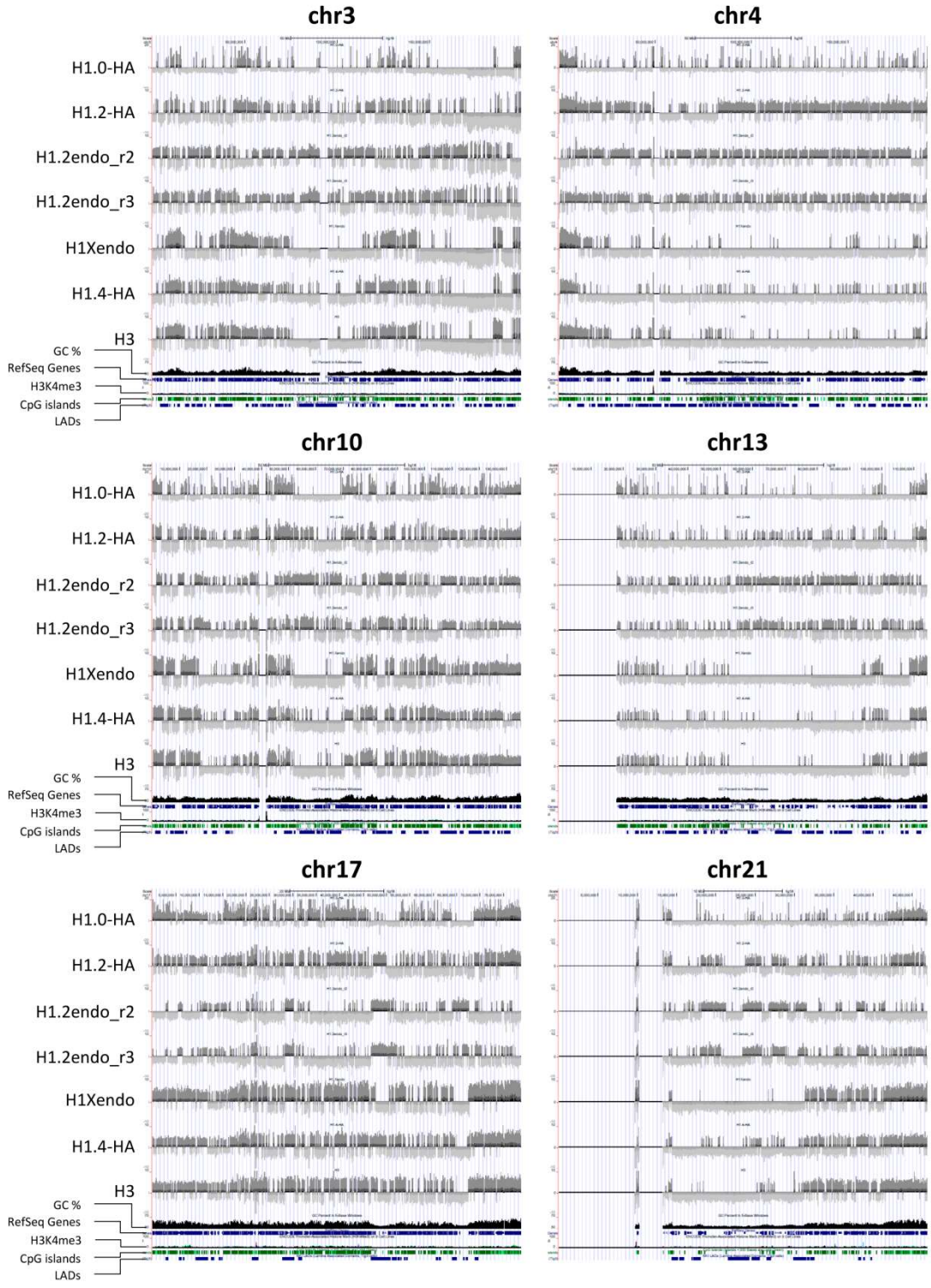

Figure R.25. Distribution of H1 variants along the entire length of chromosomes 3, 4, 10, 13, 17 and 21. *Input-subtracted H1 variants and H3 ChIP-seq signal viewed in the UCSC genome browser together with GC content, RefSeq genes, H3K4me3 (ENCODE average of 9 cell lines), CpG and LADs.*

6.4. Genomic annotation of enriched or depleted regions of individual H1 variants shows that H1.2 preferentially associates with intergenic regions and negatively correlates with CpG islands

Next, we searched for specific regions of the genome either enriched or depleted for each H1 variant over input DNA with a fold change ≥2 using SICER software [251]. The total number of H1 enriched or depleted regions ranged between 7,500-50,000 or 5,700-25,500, respectively, for the different variants (Table R.3), being H1.2 the variant presenting the lowest number of enriched regions. Those regions were further distributed between arbitrary definitions of promoters (-5kb to -1kb from TSS), genes (-5kb from TSS to +3kb from TTS) and intergenic regions (rest of the genome) (Figure R.26A).

A

ENRICHED ISLANDS	H1.0-HA	H1.2-HA	H1.2endo_r2	H1.2endo_r3	H1Xendo	H1.4-HA
Total islands	49320	16059	7500	6911	38782	12478
% intergenic/total	40.97	43.10	54.44	58.10	37.29	42.84
% genic/total	59.03	56.90	45.56	41.90	62.71	57.16
% promoter/gene	22.68	18.01	9.13	6.63	21.75	16.49
Target genes	17116	8332	3602	2789	12589	6183
Target promoters	7591	2176	490	257	6284	1715
% CpG overlap	13.88	10.22	2.37	0.42	11.35	7.53

B

DEPLETED ISLANDS	H1.0-HA	H1.2-HA	H1.2endo_r2	H1.2endo_r3	H1Xendo	H1.4-HA
Total islands	25459	15224	12305	5714	10205	6864
% intergenic/total	46.41	43.44	37.89	42.65	46.65	45.63
% genic/total	53.59	56.56	62.11	57.35	53.35	54.37
% promoter/gene	19.28	26.13	36.35	23.02	11.34	15.06
Target genes	9532	8470	8664	4060	4247	3926
Target promoters	4105	3783	4610	1412	1014	1046
% CpG overlap	2.78	6.15	12.11	3.85	0.55	1.35

Table R.3. Summary of enriched or depleted regions of individual H1 variants and its target genes. *Areas of enrichment* ***(A)*** *or depletion* ***(B)*** *of H1 variants compared to input derived from ChIP-seq data with a fold-change equal or greater than 2 were considered. Genes were defined as comprised between -5kb from TSS to +3kb from TTS, and promoters from -5kb upstream TSS to +1kb downstream TSS. Intergenic regions were defined as those regions not falling in previous definitions of genes and promoters.*

The average size of the enriched or depleted regions (peaks) was ca. 700 bp and 800 bp, respectively, and the peak size distribution was similar between variants (Figure R.26B and C). Most of the enriched and depleted regions ranged between 400 and 1000 bp, although some

of them where slightly shorter (200 bp) and other were larger, up to 1800 bp, or even more in some cases.

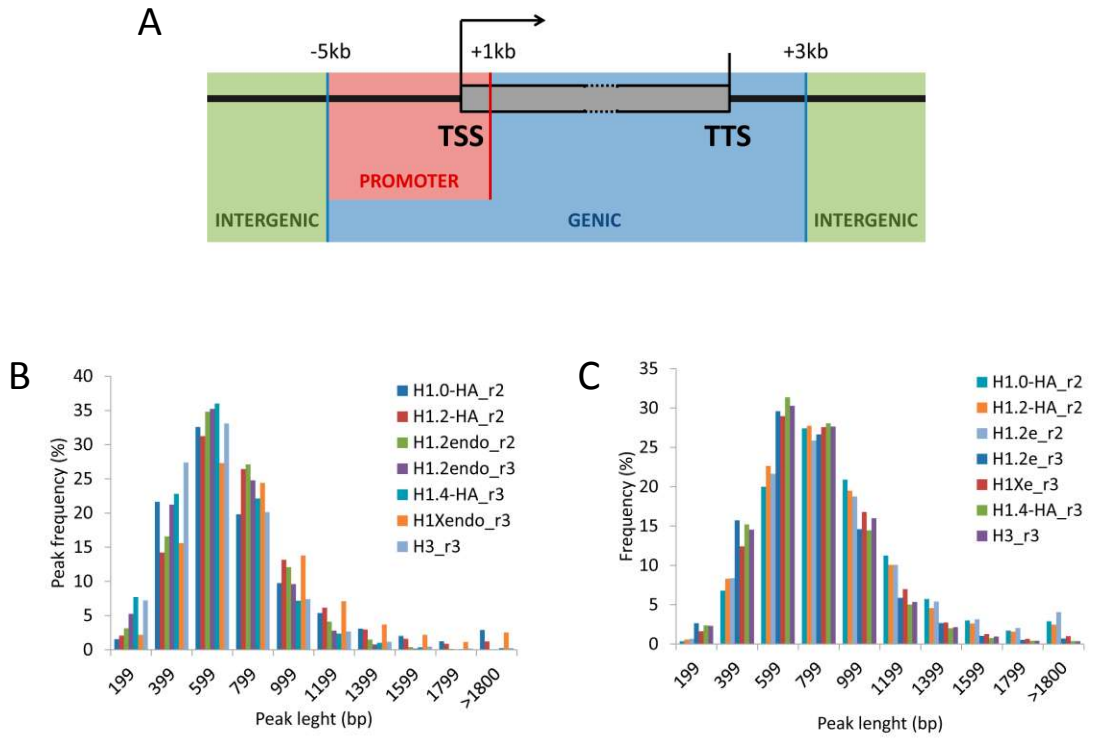

Figure R.26. Characterization of H1-enriched and depleted regions. (A) *Schematic representation of regions defined as promoters (-5kb to +1kb from TSS), genes (-5kb from TSS to +3kb from TTS), and intergenic (rest of the genome).* ***(B and C)*** *Percentages of H1 enriched (B) and depleted (C) regions regarding their length (bp).*

For most of H1s, enriched regions were more abundant inside genes, whereas H1.2 peaks were enriched at intergenic regions, similar to a random distribution according to the relative size of these compartments within the genome (Table R.3 and Figure R.27). On the other hand, all H1-depleted regions were more abundant inside genes, especially for H1.2.

Within genes, H1.2-enriched regions were disfavored at promoters compared to other H1 variants, whereas H1.2-depleted regions were strongly favored (Table R.3). Thus, for H1-enriched regions, the peak tended to be outside the promoter for H1.2, but at the promoter for the other variants, as the percentage of promoter peaks out of total genic peaks (%promoter/gene) was higher for all H1s, except H1.2, indicating that for these variants most of the peaks within genes are located in promoter regions, but nor for H1.2. This is in agreement with ChIP-chip and ChIP-seq data depicted in Figure R.10 and R.21, where high levels of enrichment coinciding with nucleosome +1 were evident for all H1s, except for H1.2,

that was depleted in this region. On the other hand, H1-depleted regions within genes tend to locate at promoters for H1.2, compared with other H1 variants.

Finally, in agreement with the data mentioned above, H1.2-enriched regions presented a low GC content compared to the other variants (Figure R.24C), further supporting the anti-correlation of H1.2 abundance and GC content in T47D cells.

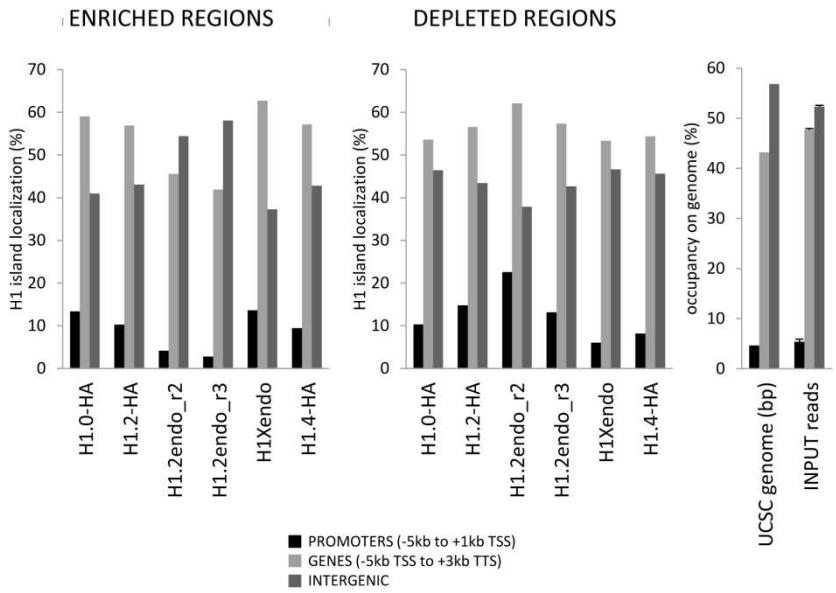

Figure R.27. Annotation of H1 enriched and depleted regions to promoters, genes and intergenic regions. *H1 variants enriched and depleted regions over input were mapped to promoters (defined as -5kb to +1kb from TSS), genes (-5kb from TSS to +3kb from TTS) or intergenic regions (rest of the genome). The percentages of identified regions for the different variants falling into each of these three categories are represented. Notice that 100% is the sum of genic and intergenic regions. The theoretical occupancy of these compartments in the UCSC genome is shown as percentages, as well as occupancy of total ChIP-seq input reads (right panel).*

We further investigated whether the identified H1-enriched and depleted regions fell within genes, proximal regulatory regions, or distal intergenic regions using CEAS software [252]. Again, H1.2 was more differently distributed than the other variants analyzed. H1.0-HA, H1X and H1.4-HA peaks were over-represented in promoters, UTRs, exons and downstream regulatory regions, and under-represented in distal intergenic regions compared to total genome. On the other hand, H1.2-enriched regions were over-represented in intergenic regions, and under-represented in exons and promoters (Figure R.28, left panel). Except H1.2, H1 peaks were as abundant in introns as in distal intergenic regions.

On the other hand, H1-depleted regions were similarly distributed among compartments between all H1 variants, except H1.2-depleted regions, which were more abundant at promoters, and less at intergenic regions, in agreement again with previous data (Figure R.28, right panel).

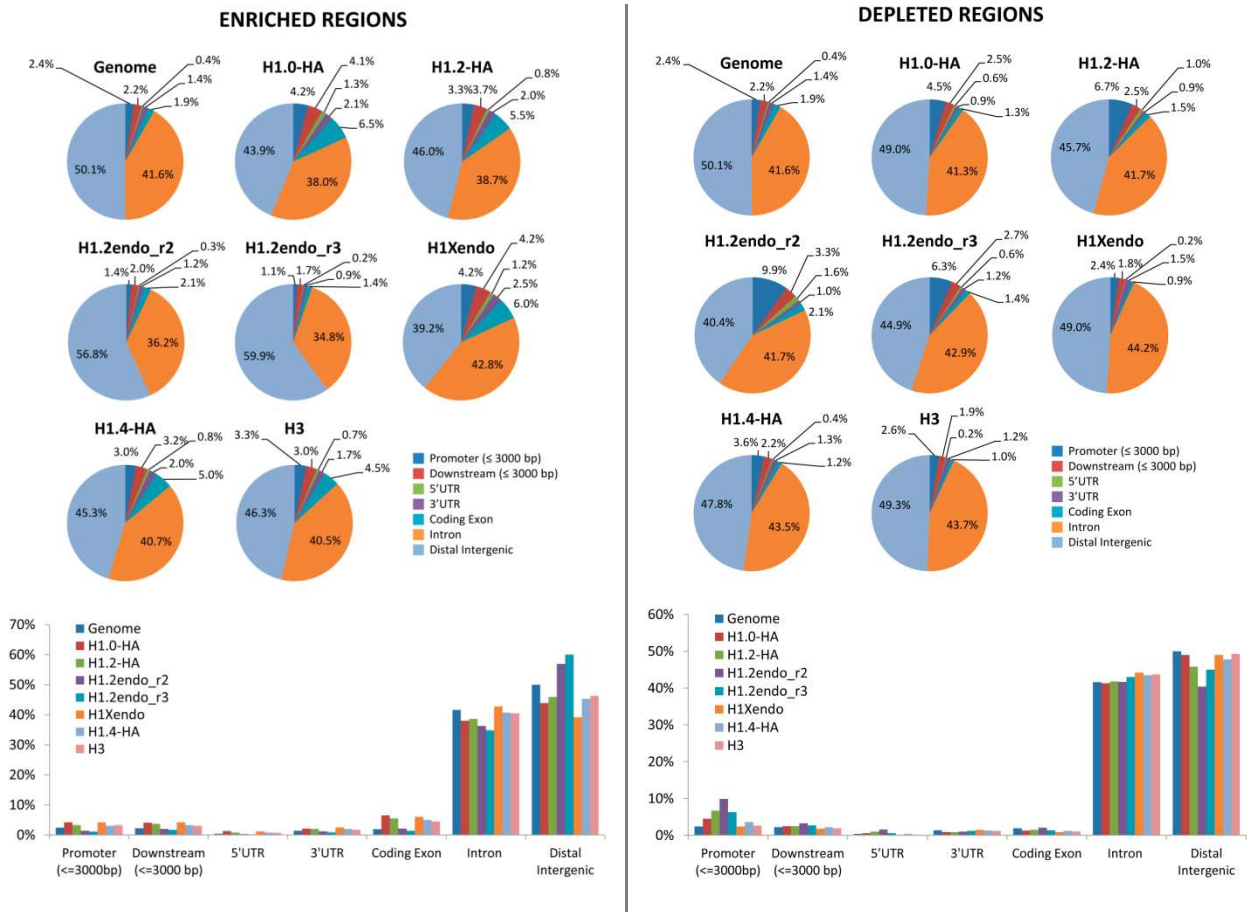

Figure R.28. Genomic annotation of enriched and depleted regions of individual H1 variants. *Pie diagram of the distribution of H1 variants enriched and depleted regions at genes, proximal regulatory regions, and distal intergenic regions. Promoter and downstream regions are defined as 3,000bp upstream TSS or downstream TTS, respectively. As a control, the annotation of all genome base pairs is shown. Two replicas of endogenous H1.2 ChIP-seq experiments are shown.*

Next, to extend the analysis of the relation of H1 variants with CpG regions, we analyzed the physical overlap between H1-enriched and depleted regions with CpG islands (CGIs) (Figure R.29A). Therefore, CpG islands were enriched at H1.2-depleted regions and at regions enriched for the other H1 variants, confirming the anti-correlation between CpG islands and H1.2 abundance, shown in Figure R.22C and D. Moreover, H1 regions overlapped with CpG sites preferentially at promoters, in accordance with the strong association of CpG islands at the 5' regulatory regions around genes. For instance, 42% of H1.0 or H1X-enriched regions located at promoters overlapped with a CpG island, while only 4-8% of regions enriched in these variants

at intergenic regions did (Figure R.29B). Additionally, analyses showed that H1.2 overlap with CpG sites was disfavored compared with other H1s all along the genome, and independently if CpG sites are located at promoters, genes, or intergenic regions.

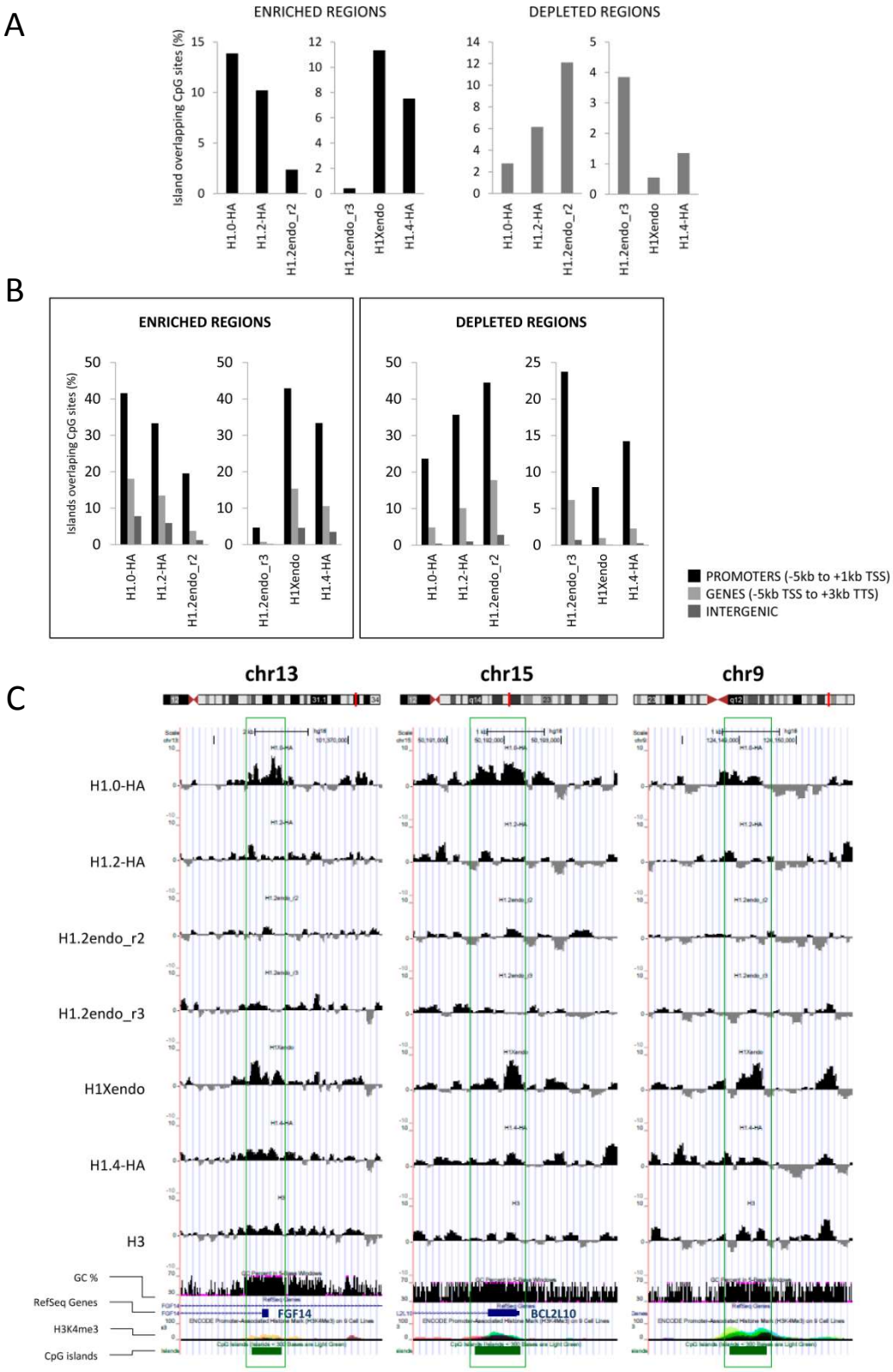

Figure R.29. Co-localization of H1 enriched or depleted regions with CpG islands. (A) *Co-localization of H1 enriched or depleted regions with CpG islands expressed as percentage of total H1 regions overlapping CpG sites. Areas of enrichment or depletion of H1 variants compared to input derived from ChIP-seq data with a fold-change ≥ 2 were considered.* ***(B)*** *Co-localization of previous H1 enriched or depleted regions with CpG islands expressed as percentage of total H1 regions overlapping GpG sites, sorting regions by their correspondence to promoters (defined as -5kb to +1kb from TSS), genes (-5kb from TSS to +3kb from TSS) or intergenic regions (rest of the genome). Areas of enrichment or depletion of H1 variants compared to input derived from ChIP-seq data with a fold-change ≥ 2 were considered.* ***(C)*** *Distribution of H1 variants along selected regions of the genome containing CgG sites and H1 enriched regions identified using SICER software. Input-subtracted H1 variants and H3 ChIP-seq signal viewed in the UCSC genome browser together with GC content, RefSeq genes, H3K4me3 (ENCODE average of 9 cell lines) and CpG islands.*

Examples of the differential H1 enrichment at CpG islands for genic and intergenic regions are illustrated in Figure R.29C for three selected representative genomic regions. In those, CpG islands coincide with a local enrichment of H1.0-HA, H1.4-HA and H1X, but not with H1.2, in gene promoter regions close to the TSS, but also in an intergenic CpG located in chromosome 9 (right panel).

6.5. H1.2 target genes and promoters are associated with repression

In order to obtain enriched or depleted H1 variant target genes, we looked for genes presenting at least one H1-enriched or depleted region comprised between -5kb from TSS and +3kb from TTS (genic region).

Focusing in H1-enriched regions, H1.2 was the variant showing the lowest number of enriched target genes, around 3,000. (Table R.3). Overlap analysis disclosed the number of genes containing peaks of a unique variant or several variants, and we referred as *unique enriched target genes* to genes containing peaks of only one H1 variant. Expression analysis of those unique H1 variant-enriched target genes revealed that genes presenting only H1.2 peaks were less expressed than target genes containing unique peaks of any other H1 variant (Figure R.30), in agreement with data above showing low expression of genes containing elevated levels of H1.2 at distal promoter or coding regions.

On the other hand, as expected, unique target genes presenting H1.2-depleted regions (*unique depleted target genes*) were highly expressed, while unique target genes with depleted regions of H1.0, H1.4 or H1X were expressed below the total transcriptome average.

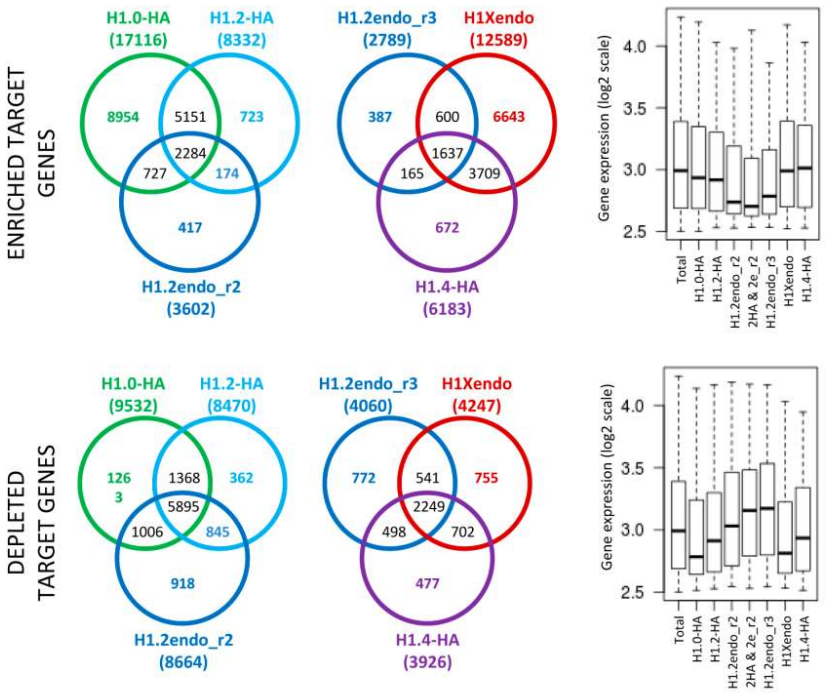

Figure R.30. Analyses of target genes for enriched and depleted H1 regions. *Venn diagrams showing the overlap between genes containing enriched or depleted regions of the different H1 variants. H1 enriched or depleted regions mapping within genes (-5kb from TSS to +3kb from TTS) were used to identify target genes. Comparisons between different H1 variants are shown in two clusters for clarity and coinciding with different ChIP-seq experiments. The expression profiles of target genes containing enriched or depleted regions for a unique variant are shown as boxplots (right panels). The profile of genes containing both H1.2-HA and H1.2endo (replica 2) enriched or depleted regions are also shown (2HA & 2e_r2).*

Similarly, we also looked for H1 variant target promoters by searching promoters that had at least one H1 enriched or depleted region comprised between -5kb and +1kb from the TSS (promoter region).

Again, H1.2 showed less enriched target promoters than other variants (Table R.3), and the associated genes with *unique H1.2-enriched target promoters* were less expressed than the corresponding ones for other H1 variants (Figure R.31). For depleted regions, genes associated with *unique H1.2-depleted target promoters* were higher expressed than unique target promoter-associated genes for other variants or total transcriptome average.

In conclusion, we show again that H1.2 enrichment at promoter or coding regions is negatively correlated with transcriptional status.

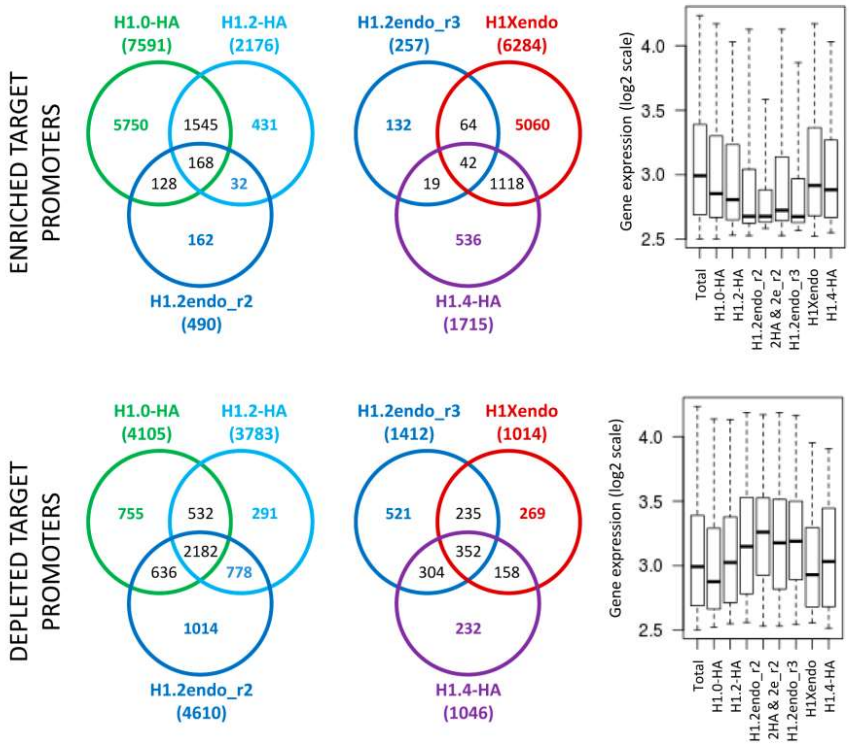

Figure R.31. Analyses of target promoters for enriched and depleted H1 regions. *Venn diagrams showing the overlap between promoters containing enriched or depleted regions of the different H1 variants. H1 enriched or depleted regions mapping within promoters (-5kb to +1kb from TSS) were used to identify target genes. Comparisons between different H1 variants are shown in two clusters for clarity and coinciding with different ChIP-seq experiments. The expression profiles of target promoter-associated genes containing enriched or depleted regions for a unique variant are shown as boxplots (right panels). The profile of promoters containing both H1.2-HA and H1.2endo (replica 2) enriched or depleted regions are also shown (2HA & 2e_r2).*

6.6. Differential binding of H1.0-HA versus H1.2 along the genome

Finally, in order to identify regions of the genome enriched in one variant respect to another, we performed differential binding analysis of H1.0-HA versus H1.2, as these two variants behaved differently in previous analysis and are reported to present divergent features regarding their structure, expression pattern, chromatin binding affinity, gene expression regulation, etc. SICER tools [251] where used again to decipher regions (islands) specifically enriched in H1.0-HA respect to H1.2, and vice versa. Interestingly, much more differentially-enriched islands were found for H1.0-HA than for H1.2-HA or endogenous H1.2 when H1.0-HA was compared with H1.2-HA or with endogenous H1.2 (Table R.4A). Moreover, approximately 10% of the differentially-enriched H1.0 islands were located at gene promoters (defined as -5kb to +1kb from the TSS), while only 1.5-2.4% for the H1.2 differentially-enriched islands were. As expected, it exist a large overlap between promoters differentially-enriched in H1.0-HA, after comparing either with H1.2-HA or endogenous H1.2 (Figure R.32A).

A

	H1.0-HA vs H1.2-HA		H1.0-HA vs H1.2endo		H1.2-HA vs H1.2endo	
	H1.0-HA < H1.2-HA	H1.0-HA > H1.2-HA	H1.0-HA < H1.2endo	H1.0-HA > H1.2endo	H1.2-HA < H1.2endo	H1.2-HA > H1.2endo
DIFFERENTIAL ISLANDS	2958	36624	6106	59375	2119	7236
PROMOTER-RELATED ISLANDS	70	3645	94	6143	22	627
ISLAND % IN PROMOTERS	2.4	10	1.5	10.3	1.03	8.7

B

Gene ontology of H1.0 vs H1.2 differentially island-related genes **(H1.0>H1.2)**.

Biological Process	P-Value	MTC
POSITIVE REGULATION OF NEUROBLAST PROLIFERATION	9.92E-12	1.47E-08
POSITIVE REGULATION OF Wnt RECEPTOR SIGNALLING PATHWAY	1.58E-10	1.17E-07
MULTICELLULAR ORGANISMAL DEVELOPMENT	5.79E-10	2.85E-07
REGULATION OF NEURON PROJECTION DEVELOPMENT	6.49E-10	2.40E-07
REGULATION OF METABOLIC PROCESS	2.42E-08	7.15E-06
NEURON RECOGNITION	2.42E-08	5.96E-06
NERVOUS SISTEM DEVELOPMENT	2.96E-08	6.25E-06
Cellular Component	**P-Value**	**MTC**
CYTOPLASMIC MEMBRANE-BOUNDED VESICLE	9.33E-07	3.52E-04
POSTSYNAPTIC MEMBRANE	5.41E-06	1.02E-03
EXTRACELLULAR REGION	9.75E-06	1.23E-03
PROTEINACEOUS EXTRACELLULAR MATRIX	1.58E-05	1.49E-03
CELL JUNCTION	4.92E-05	3.71E-03

Table R.4. Differential binding analysis of H1.0 vs H1.2. (A) *Differentially enriched islands of one H1 variant in respect to another derived from ChIP-seq data of endogenous H1.2 and HA-tagged H1.0 and H1.2. Total number of enrichment regions found in the genome and the number of promoter-located regions are shown, as well as the percentage of promoter to total regions. Promoter-located regions are defined as being present within a distance -5 kb to +1 kb from TSS.* ***(B)*** *Gene ontology of associated genes to H1.0 vs H1.2 increased differentially enriched promoters according to (A). Overlapping genes in Figure R.32A were used. P-value (adjusted for multiple testing) and MTC is shown.*

Further analysis showed that, in accordance with previously observed association of H1.0-HA with CpG islands (Figure R.22C and D and Figure R.29), H1.0-HA differentially-enriched islands overlapped more with CpG sites than H1.2-HA or endogenous H1.2 differentially-enriched islands, both at gene promoters and genome-wide (Figure R.32B). Similarly, gene ontology (GO) analysis of the genes associated with H1.0-HA differentially-enriched promoters contained CpG regions, and this was not true for H1.2 (Figure R.32C). Finally, gene ontology analysis using GiTools [253] indicated that biological processes such as neuroblast proliferation, neuron development or regulation of Wnt receptor signaling were over-represented among genes associated with differential H1.0-HA-enriched promoters (Table R.4B), in accordance with the reported role of H1.0 during differentiation and development.

Further analyses on this direction comparing other H1 variants will identify regions of the genome specifically enriched in one H1 variant, contributing in understanding the specific function of H1 variants in a certain subset of genes.

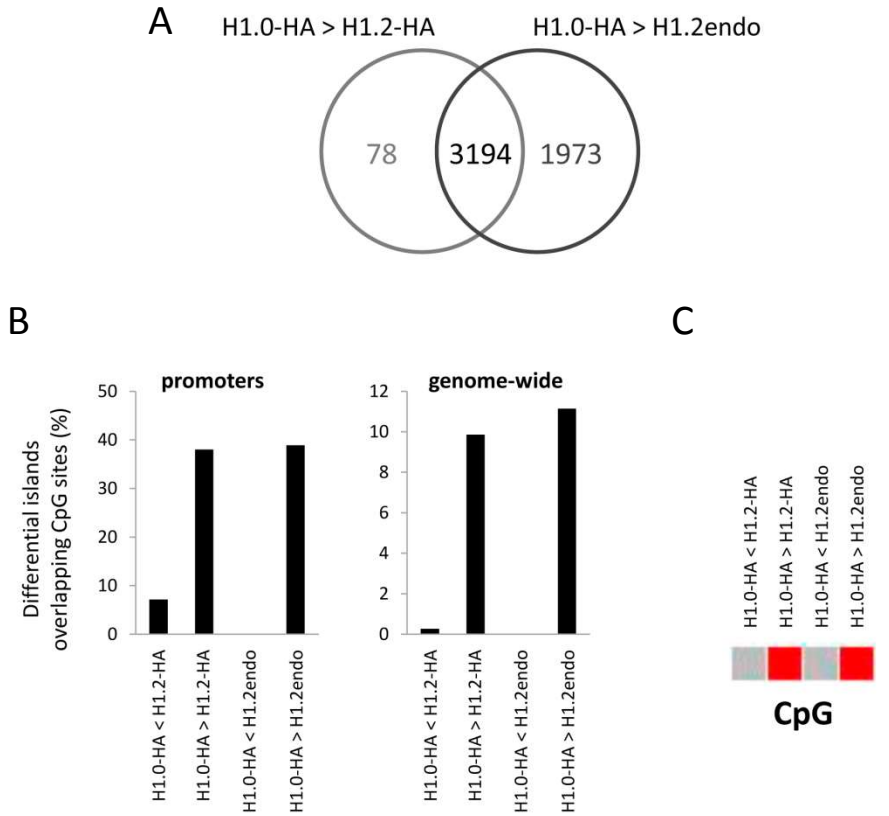

Figure R.32. Islands of differential H1.0 enrichment compared with H1.2 coincide with CpG sites. (A) *Overlap analysis between promoters differentially enriched in H1.0-HA vs H1.2-HA and H1.0-HA vs H1.2endo (see Table R.4A).* ***(B)*** *Percentage of H1.0 versus H1.2, or vice versa, enriched islands that coincide with CpG sites at promoters (left) or genome-wide (right). Promoters were defined as -5kb to +1kb from TSS.* ***(C)*** *CpG island enrichment analysis of the associated genes to the differentially-enriched promoters. Those genes containing differentially increased or decreased H1.0 or H1.2 variants with respect to other at promoter (within -5Kb to +1Kb from TSS) were analyzed for over-representation of promoter associated with CpG sites with FDR cutoff ≤ 0.01. Corrected (FDR) p-values are delineated in a colored heat map, where red signifies over-representation of targets in a particular term.*

RESULTS - CHAPTER II:

FUNCTIONAL SPECIFICITY OF HUMAN HISTONE H1 SUBTYPES

It was previously reported in our group that knock-down of the different H1 variants caused specific effects in breast cancer T47D cells [97]. In particular, upon inducible doxycycline (Dox) H1.2 knock-down, cells proliferated slower because they arrested in G1 phase of the cell cycle. Moreover, depletion of H1.2 caused a reduction in the nucleosomal spacing. This effect was not only restricted to T47D cells, and depletion of H1.2 also caused proliferation alterations in another breast cancer cell line (MCF7), but not in HeLa, 293T or MCF10A cells. On the other hand, knock-down of H1.0, H1.3 and H1.5 did not produce any phenotype in T47D cells, supporting the idea of specific functions for linker histone H1 variants.

However, depletion of H1.4 also affected cell proliferation in a similar extent that H1.2 knock-down. Furthermore, morphology alterations towards a more necrotic phenotype were observed in those cells and cell cycle analysis revealed an increase in the subG1 peak, indicating high mortality in the H1.4 depleted cells. Apoptosis was discarded to occur as several experiments to measure apoptosis (formation of apoptotic DNA ladder, anexin V and TUNEL assays, or caspase 3 activation assays) failed to show differences compared with control cells. So, it was concluded at that time that H1.4 knock-down cells presented a death phenotype, probably by necrosis. Interestingly, H1.4 inhibition in non-tumoral breast MCF10A cells also affected cell proliferation, but not in MCF7, HeLa or 293T cells. Despite all this observations, the phenotype of H1.4 knock-down was not further analyzed.

Finally, expression microarray analysis of all H1 variant depleted cells concluded that a few proportion of the genes were altered upon depletion of individual variants, and inhibition of the different variants leaded to specific changes in gene expression, altering different subsets of genes. Further analysis of these data would be helpful to understand the specific phenotypes after H1 variants inhibition, especially for H1.2 and H1.4.

1. An off-target effect of the shRNA targeting H1.4 affects lamin B2 expression

In an attempt to further explore the phenotype observed in T47D cells upon H1.4 depletion, we realized, based on expression microarray data analysis, that expression of lamin B2 gene (LMNB2) was strongly down-regulated in H1.4 knock-down cells (data not shown). Further verifications using RT-PCR confirmed down-regulation of lamin B2 in T47D, but also in 293T and MCF7 upon H1.4 knock-down (Figure R.33B and C). The family of lamins (lamin A/C, B1 and B2) makes up the nuclear lamina, consisting in a two-dimensional matrix of proteins located next to the inner nuclear membrane. These proteins are involved in nuclear stability, chromatin structure and gene expression.

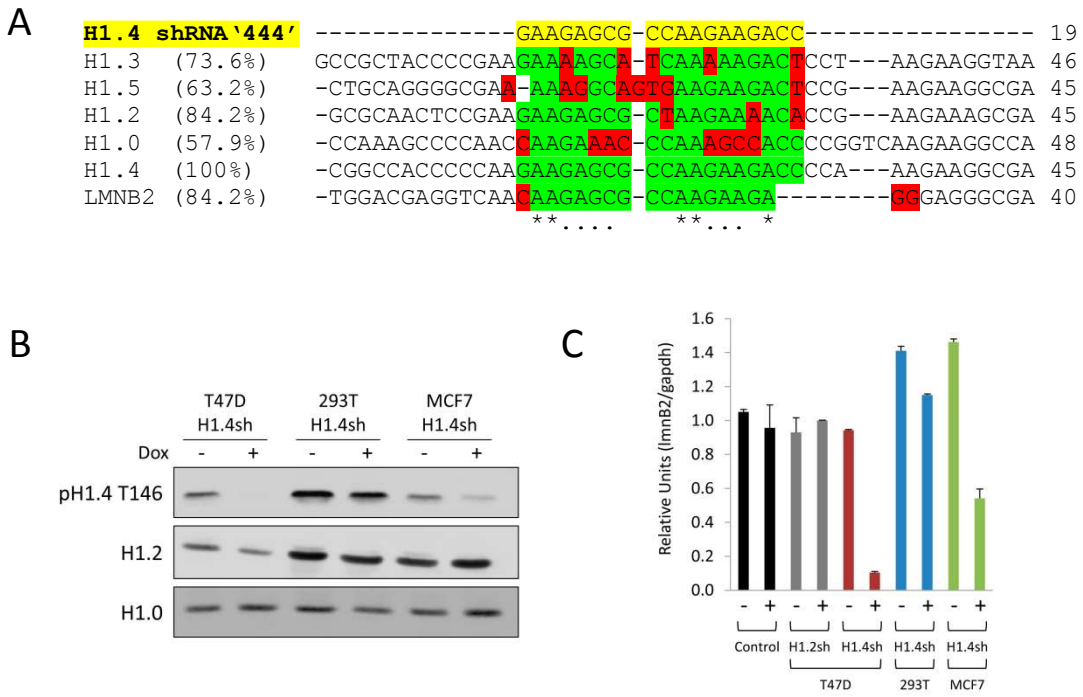

Figure R.33. Lamin B2 expression is impaired upon H1.4 KD in different cell lines. (A) *Nucleotide sequence aligment of H1.4 shRNA with sequences surrounding potential shRNA target sites of several human histone H1 variants and LMNB2 gene. H1.4 shRNA is highlighted in yellow; conserved nucleotides of H1 variants and LMNB2 gene with the shRNA are colored in green; divergent nucleotides are colored in red. Percentages indicate the similarity between the shRNA and the correspondent gene. Aligment was perfomed using ClustalW2 software (EMBL-EBI).* ***(B, C)*** *T47D, 293T or MCF7 cells stably infected with the lentiviral inducible system for the expression of control, H1.2 or H1.4 shRNA were treated for 6 days with Dox or left untreated.* ***(B)*** *Inhibition of H1.4 was tested by Western blot with isoform-specific antibodies on histone H1 preparations obtained by acid extraction.* ***(C)*** *Inhibition of lamin B2 gene was tested by RT followed by qPCR with specific oligonucleotides. RT-PCR values for lamin B2 were normalized to GAPDH expression.*

Additionally, a detailed comparison of H1.4 shRNA sequence with different H1 variants and lamin B2 gene sequences revealed that lamin B2 gene contains a region of 84% similarity with the shRNA used to target H1.4 mRNA (Figure R.33A). This similarity is the same than with H1.2 mRNA, but while H1.2 presents divergent nucleotides alternated through the target mRNA

sequence, lamin B2 mRNA divergence is restricted to the extremes of the shRNA target sequence, thus conserving a large 16 nucleotide region with 100% similarity with the shRNA. Thus, we hypothesize that this characteristic makes LMNB2 gene a potential candidate to be targeted by the H1.4 shRNA, compared with other H1 variants. In conclusion, in light of these observations, it raised the possibility that inhibition of lamin B2 gene upon doxycycline treatment was not consequence of H1.4 depletion, but was an off-target effect of the shRNA.

To prove if lamin B2 depletion was caused by H1.4 down-regulation or was directly targeted by the shRNA, we investigated whether H1.4 shRNA (from now on "444"shRNA) was able to reduce the expression of an exogenous lamin B2 fused to GFP in transient transfection assays in 293T cells. GFP-lamin B2 expression was reported by a specific pair of primers for the transfected GFP-lamin B2, with a forward primer in the GFP sequence and the reverse in the lamin B2 gene. As a control of "444"shRNA inhibition, expression of exogenous H1.4 fused to an HA tag was monitored similarly using a specific pair of primers for exogenous H1.4-HA mRNA. Amplification of other regions of GFP-lamin B2 and H1.4-HA-containing vectors were used to normalize expression values regarding transfection efficiency. As shown in Figure R.34A, expression of GFP-lamin B2 was decreased after co-transfecting cells with "444"shRNA compared with a random shRNA (line 3). However, depletion efficiency was lower than that achieved by four out of five specific shRNAs against lamin B2 (Figure R.34A, lines 5-9). As expected, exogenous H1.4-HA expression was also depleted upon co-transfection with the "444"shRNA (Figure R.34B). The effect of "444"shRNA on GFP-lamin B2 expression was also investigated at protein level by Western blot using a GFP antibody. As in RT-qPCR assays, "444"shRNA inhibited exogenous H1.4-HA (Figure R.34D), and also exogenous GFP-lamin B2 (Figure R.34C). Specific shRNAs against lamin B2 also inhibited expression of the recombinant GFP-lamin B2 protein. In conclusion, the direct effect of "444"shRNA on the expression of exogenous GFP-lamin B2, discarded a possible effect of H1.4 knock-down on lamin B2 expression, and made us to conclude that inhibition of lamin B2 was the consequence of an off-target effect of the "444"shRNA.

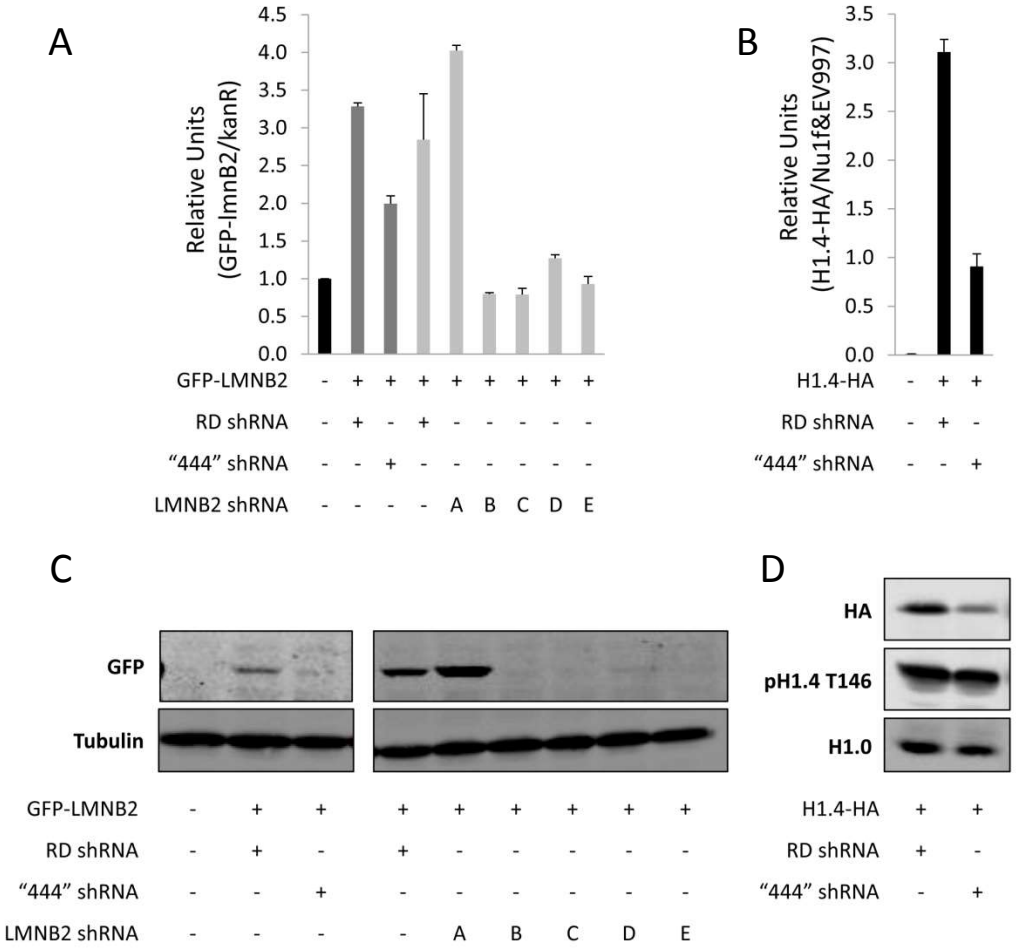

Figure R.34. "444"shRNA targets both H1.4 and lamin B2 mRNA. *Transient transfection assays were performed in 293T cells by transfecting GFP-lamin B2 or H1.4-HA together with random (RD), "444", or different lamin B2 shRNAs (LMNB2 A-E). 48 hours post-transfection, cells were harvested and RNA (A, B), total protein extract (C), or H1 extract (D) was prepared.* ***(A, B)*** *Expression of exogenous GFP-lamin B2 and H1.4-HA was tested by RT-PCR followed by qPCR with specific oligonucleotides for these exogenous forms. RT-PCR values were normalized using primers for regions of the vectors containing GFP-lamin B2 and H1.4-HA ("kanR" and "Nu1f&EV997", respectively).* ***(C)*** *Expression of recombinant GFP-lamin B2 was tested by Western blot of total protein extract using a GFP antibody. Tubulin antibody was used as loading control.* ***(D)*** *Exogenous H1.4-HA inhibition was also tested by Western blot of H1 histone extract using an HA antibody and specific H1 variant antibodies as loading control.*

2. Combined depletion of H1.4 and lamin B2 by "444"shRNA causes altered cell morphology in T47D cells

To further characterize H1.4-lamin B2 knock-down cells (from now on referred as "444"shRNA cells), we followed their growth by microscopy approaches upon Dox treatment. As it has been previously described, these cells failed to reach confluence due to defects in proliferation [97]. After 6 days of Dox treatment, few "444"shRNA cells were found attached to the culture dish, as they did not grow similarly to non-treated cells, and they presented different morphology, being more compacted and refringent (Figure R.35A). Furthermore, by performing time lapse

experiments from day 3 to day 6 after Dox treatment, we were able to follow their growth *in vivo*, and while control cells grew normally forming a monolayer and reaching confluence after 3 days in the plate, the "444"shRNA cells stopped proliferating and, interestingly, grew into cellular clusters together with the neighboring cells. Moreover, they presented a particular morphology different from the wild type cells (Figure R.35B).

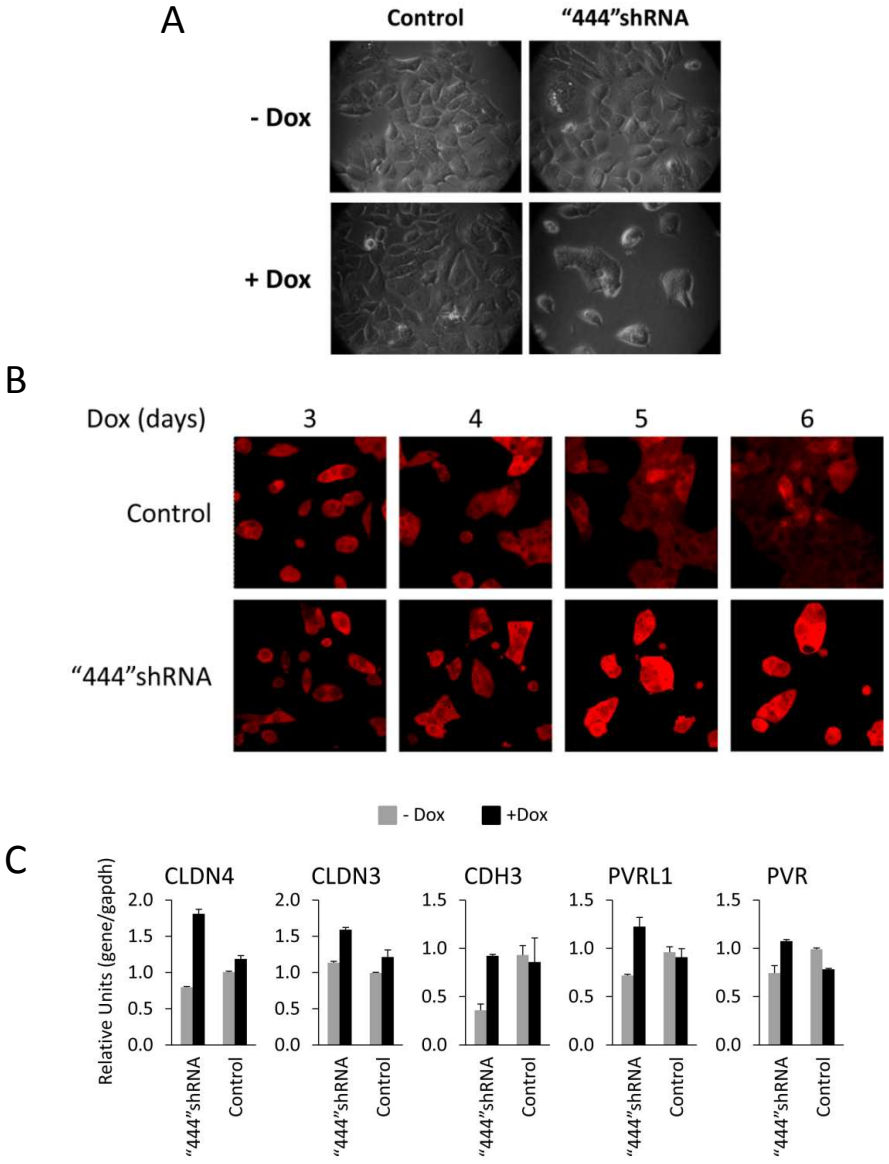

Figure R.35. "444"shRNA cells form cellular clusters. (A) *T47D cells infected with an inducible shRNA-expression system (control and "444"shRNA) were treated for 6 days with Dox or left untreated and observed at the optical microscopy.* ***(B)*** *Growth of control and "444"shRNA cells treated with Dox (RedFP and GFP-positive) was followed from day 3 to day 6 of Dox treatment in a time lapse experiment with the confocal microscope monitoring RedFP self-fluorescence. Images were taken every 10 minutes along 3 days with cells growing at 37ºC and 5% CO_2.* ***(C)*** *Control and "444"shRNA cells were treated for 6 days with Dox or left untreated. Expression of adhseion-related genes was tested by RT-qPCR with specific oligonucleotides. RT-PCR values for candidate genes were normalized to GAPDH expression.*

Finally, in accordance with the observed association of these cells, analysis of gene expression microarray on “444”shRNA cells, showed an overrepresentation of homophilic cell-adhesion related genes and cellular adhesion signaling pathways (data not shown). Overexpression of some of these genes in “444”shRNA cells upon Dox treatment was experimentally validated by RT-qPCR (Figure R.35C), pointing to an increase of cellular adhesion in those cells upon shRNA expression.

3. Specific lamin B2 knock-down cells resemble “444”shRNA cells

In order to discern between the effect of H1.4 and lamin B2 knock-down in the phenotype observed in “444”shRNA cells, we generated constitutively lamin B2 knock-down T47D cell lines. Inhibition of lamin B2 by three different specific shRNAs (Figure R.36B) showed defects in proliferation and increased cell mortality after 5 and 17 days of infection (Figure R.36A). This phenotype resembled the one observed with “444”shRNA KD cells. Furthermore, some genes related with the adhesion phenotype were also up-regulated for some of the lamin B2 depleted cells (Figure R.36C). These observations allow us to hypothesize that the aggregation phenotype observed in the “444”shRNA KD cells is mainly caused by the inhibition of lamin B2, rather than by the depletion of H1.4. Nevertheless, we cannot totally exclude partial effects of H1.4 depletion.

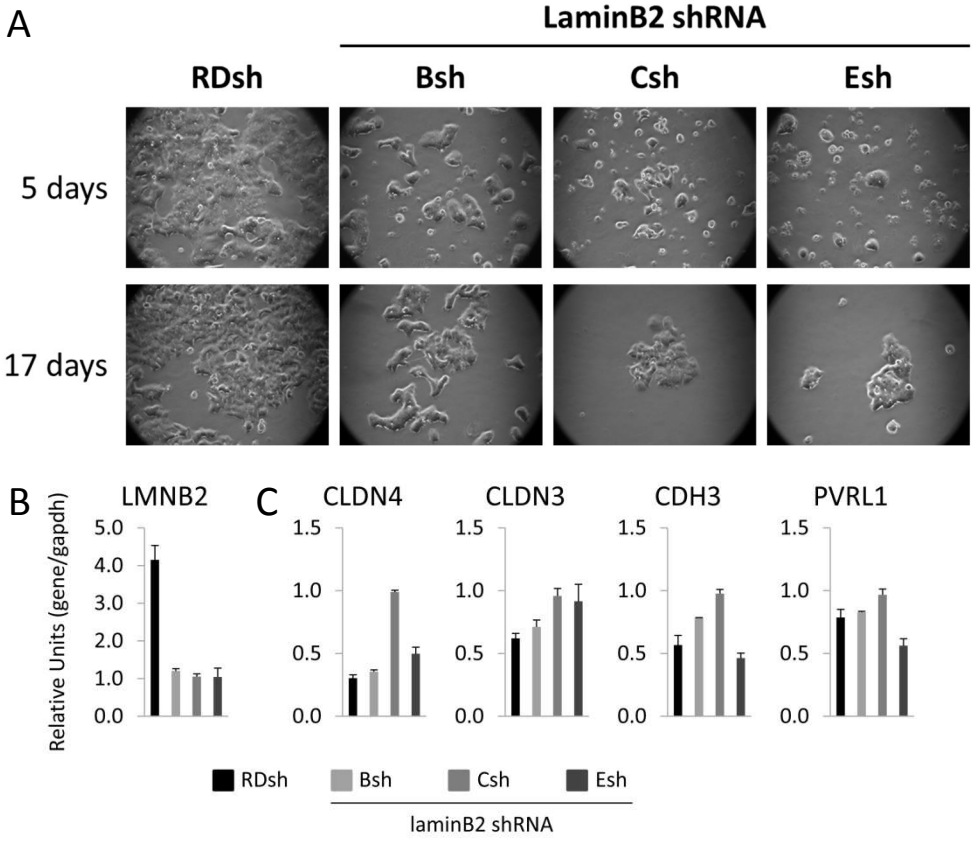

Figure R.36. T47D phenotype after specific inhibition of lamin B2 resembles "444"shRNA KD cells. (A) *T47D cells infected with different constitutive shRNA expression vectors against lamin B2, or random (RD) shRNA, were observed under the optical microscope after 5 and 17 days of puromycin selection of infected cells with virus.* ***(B, C)*** *RNA of random and lamin B2 shRNA infected cells was extracted one week post-infection and expression of lamin B2 (B) and adhseion-related genes (C) was tested by RT-qPCR with specific oligonucleotides. RT-PCR values for candidate genes were normalized to GAPDH expression.*

4. Generation of a new inducible specific H1.4 knock-down T47D cell line and a multi-H1 inducible knock-down cell line

Next, in order to obtain a T47D cell line specifically inhibiting H1.4 avoiding off-target effects, we tested other shRNAs targeting divergent gene regions of H1.4 gene, discarding those with more than 80% similarity with other proteins by using BLAST search of the target sequence (Figure R.37). Inducible knock-down cell lines were generated as previously reported [97] based on a TeT-On strategy (see Materials and Methods). Among several candidates, we obtained a T47D cell line specifically inhibiting H1.4 ("120sh") without major compensatory effects by other H1 subtypes (Figure R.38A and B). Moreover, we also obtained a cell line inhibiting most of the somatic H1 variants at the mRNA level (H1.2, H1.3, H1.4 and H1.5) but, interestingly, only H1.2 and H1.4 at the protein level (Figure R.38A and C). We referred to this cell line as "multi-H1sh" or "mH1sh" cell line, and to the shRNA as "225"shRNA. As it was previously described for H1.2 KD [97], H1.0 was overexpressed upon depletion of H1.4, and also in the combined H1.2 and H1.4 knock-down. Note that none of these new inducible H1 knock-down cell lines inhibits expression of lamin B2 gene (Figure R.38A).

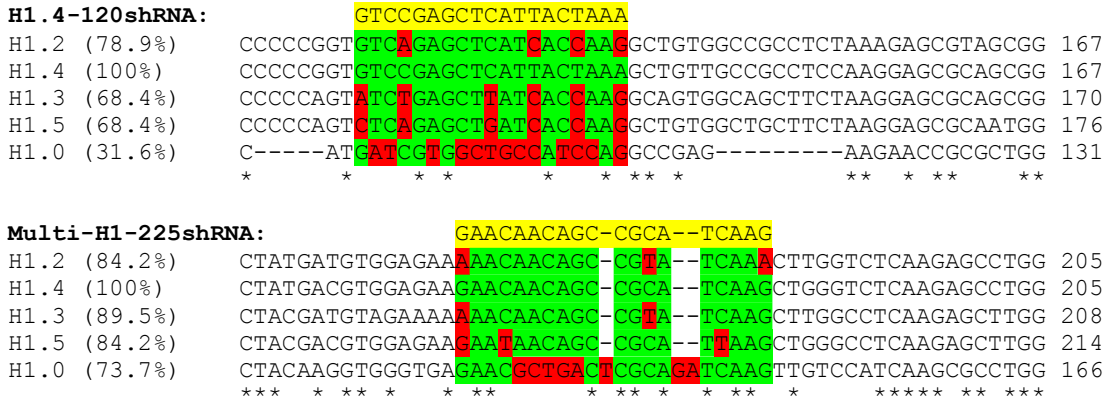

Figure R.37. Selected target sequences for shRNA-mediated inhibition. *Nucleotide sequence aligment of human histone H1 variants at target sites for new H1.4 shRNA and multi-H1 shRNA. shRNAs are highlighted in yellow; conserved nucleotides of H1 variant genes with the shRNA are colored in green; divergent nucleotides are colored in red. Percentages indicate the similarity between the shRNA and the correspondent H1 variant. Aligment was perfomed using ClustalW2 software (EMBL-EBI).*

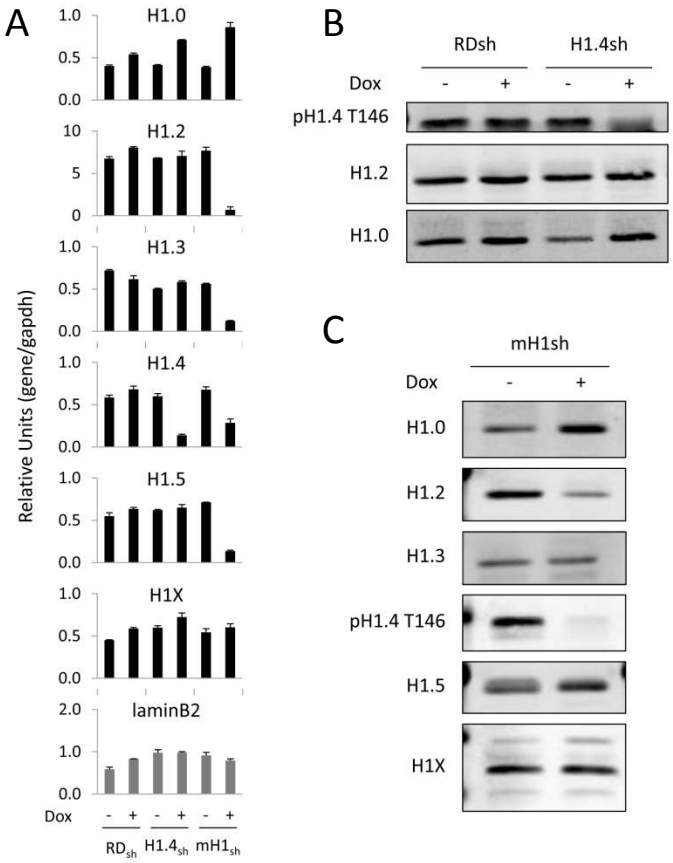

Figure R.38. H1.4 and multi-H1 inducible RNA interference-mediated knock-down in human T47D breast cancer cells. (A) *Inhibtion of H1 expression was tested by RT-qPCR with oligonucleotides specific for the different H1 variants and lamin B2 genes. RT-PCR values were normalized to GAPDH expression.* ***(B)*** *H1.4 depletion in H1.4sh cells was tested by Western blot with isoform-specific antibodies on histone H1 preparations obtained by acid extraction.* ***(C)*** *H1 depletion in multi-H1 KD cells arrested without serum during 24 hours was tested by Western blot with isoform-specific antibodies on total histone preparations obtained by acid extraction.*

5. H1.4 and multi-H1 knock-down resemble H1.2 knock-down in breast cancer cells

Next, we further analyzed the phenotype of both H1.4 KD and multi-H1 KD cells. Upon 6 days of Dox treatment, we observed a deficiency in the growth rate of these cells, mainly for the multi-H1 KD (Figure R.39A, left panel). These cells stopped proliferating, and a closer look to the morphology of the attached cells showed an apparent refringent aspect and an increase in dead cells (Figure R.39A, right panel). To further quantify this defect in cellular growth, we performed proliferation experiments mixing at 1:1 ratio the shRNA expressing cells (RedFP and GFP-positive upon Dox treatment) with parental T47D cells (RedFP and GFP-negative), and we monitored by FACS the proportion between both populations over the time in the presence of Dox (Figure R.39B). Both H1.4 KD and multi-H1 KD cells proliferated slower than the control RD KD cell line, confirming previous observations with the microscope. Furthermore, multi-H1 KD proliferation decreased drastically from day 3 upon Dox treatment, with almost no RedFP and GFP-positive cells on the plate after 2 weeks in culture. In parallel, the cell cycle profile for these cell lines was examined by FACS analysis after propidium iodide-staining of non-treated and Dox-treated cells. Like in the case of previously described H1.2 KD cell line, both H1.4 and

multi-H1 KD cells arrested in G1 and decreased percentage of cells in S and G2/M phases (Figure R.39C). It is worth noting that combined depletion of H1.2 and H1.4 in multi-H1 KD cells presented a stronger phenotype than individual knock-downs separately.

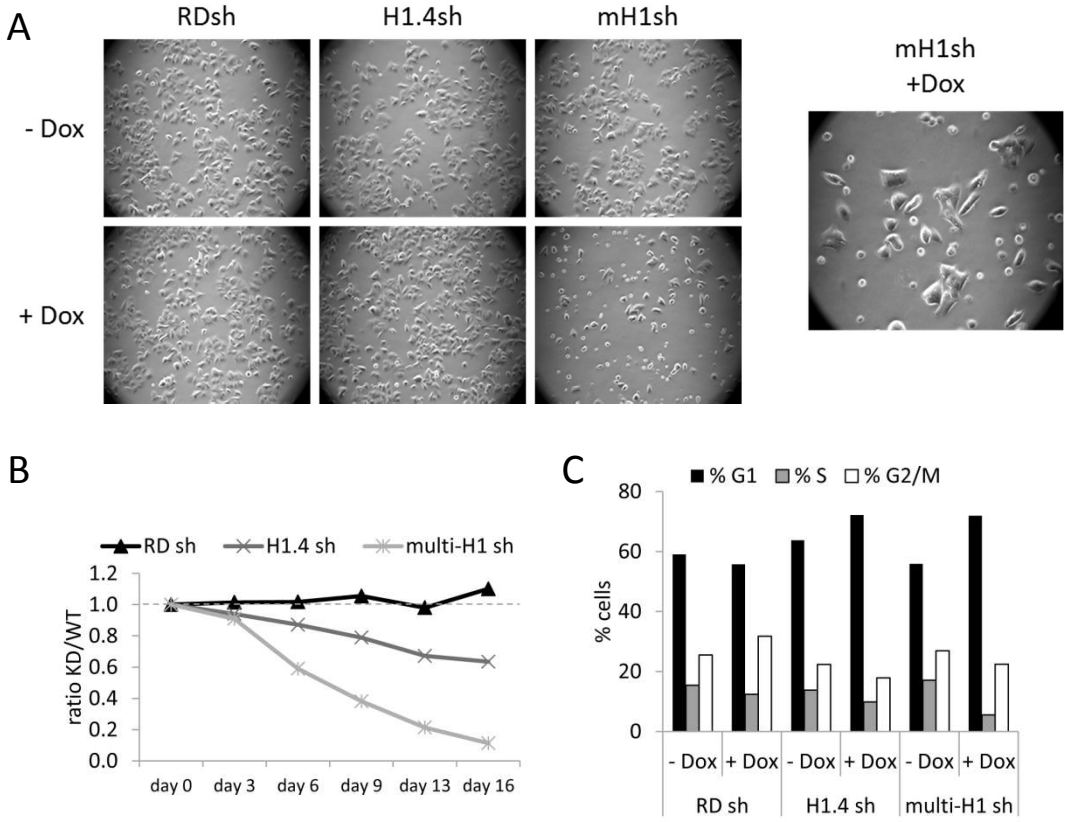

Figure R.39. H1.4 and multi-H1 inhibition causes deffects on cell proliferation and cell cycle progression. (A) *Random (RD), H1.4 and multi-H1 T47D shRNA-expressing cells were treated for 6 days with Dox or left untreated and observed at the optical microscopy. Right panel corresponds to a higher magnification of Dox-treated multi-H1 KD cells.* ***(B)*** *Proliferation assay on RD, H1.4 and multi-H1 KD cells. Knock-down cell lines (RedFP and GFP positive) were mixed 1:1 with parental T47D cells (RedFP and GFP negative) and treated with Dox. Cells were split at the indicated times and the percentage of RFP/GFP-positive cells was measured by FACS. Data is expressed as percentage of variation of the proportion RFP/GFP-positive (KD) versus RFP/GFP-negative (WT) cells along time respect to the initial seeding proportion.* ***(C)*** *Cell cycle profile after propidium iodide (PI) staining of RD, H1.4 and multi-H1 KD cells in the presence (6 days) and absence of Dox. Data is expressed as percentage of cells in G1, S and G2/M phases of the cell cycle.*

Afterwards, we also investigated nucleosomal spacing in these new established cell lines after H1 knock-down. MNase digestion of bulk chromatin from H1.4 and multi-H1 knock-down cells revealed a decrease in the nucleosomal repeat length (NRL) in both cell lines upon H1 depletion (Figure R.40). Again, H1.4 knock-down resembled previously described H1.2 knock-down, and multi-H1 knock-down presented a stronger effect than H1.4 knock-down alone. This observation is also in accordance with the well-known relation of H1 with NRL, where high H1/nucleosome ratios lead to long NRL, while low ratios are related with short NRL.

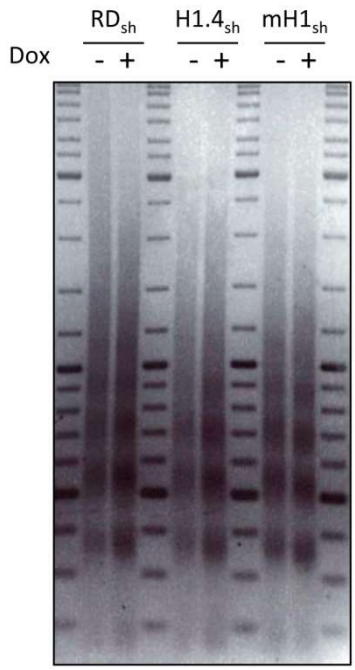

Figure R.40. H1.4 and multi-H1 KD cells present a reduction in nucleosomal spacing. *Nuclei from RD, H1.4 and multi-H1 KD cells treated of not with Dox for 6 days were subjected to MNase digestion and the profile of bulk chromtin resolved in agarose gel eletrophoresis to visualize the nucleosomal repeat length (NRL).*

In conclusion, we established a new H1.4 knock-down cell line in T47D breast cancer cells, different from the previously described one presenting an off-target effect on lamin B2. This newly characterized cell line resembled phenotypically to the already described H1.2 knock-down cells line. Thus, both H1.2 and H1.4 knock-down produced in T47D cells defects in proliferation due to an accumulation of cells in the G1 phase of the cell cycle. Moreover, both of them seemed to be specifically related with chromatin organization as their depletion caused a reduction in the nucleosomal repeat length (NRL). Nonetheless, as already discussed [97], nucleosome spacing and proliferation was not affected in previous H1.0, H1.3 and H1.5 knock-down cells, although these variants represented a similar or higher proportion than H1.2 or H1.4 in this cell line (Box R.1). So, this still points to a specific role of H1.2 and H1.4 in proliferation and chromatin organization of T47D breast cancer cell line. Finally, we have established a new H1 knock-down cell line inhibiting most of H1 variants at mRNA level but only H1.2 and H1.4 at the protein level after 6 days of Dox treatment. The phenotype of this cell line resembled again the phenotypes of H1.2 and H1.4 knock-downs, but, reasonably, caused stronger effects than the individual knock-downs. Due to the unexpected inhibitory effect of this shRNA on H1 variants different to H1.4, it remains to be determined whether this effect is direct on H1 mRNA targets or indirect.

Box R.1. Identification of T47D H1 variants in two-dimensional gels

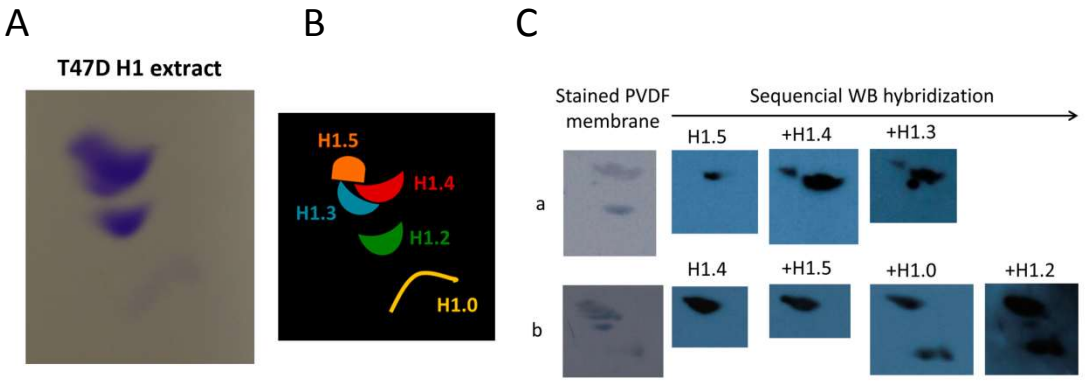

In order to establish a relation in the proportion of H1 variants in T47D human breast cancer cells, we performed two-dimensional gel elctrophoresis with H1 preparations obtained by perchloric acid extraction. Extracts were initially run in an Acetic acid – Urea (AU) gel, followed by a second run in an SDS-PAGE ***(A)****. Then, using specific antibodies for the H1 variants (H1.0, H1.2, H1.3, pH1.4 and H1.5), sequential Western blot hibridizations without stripping lead us to identify which H1 variant corresponded to each band in the gel. "a" and "b" in correspond to different WB membranes.* ***(C)****. A cartoon representation of the gel with the idenfied variants is shown in* ***(B)****.*

6. Morphological alterations of breast cancer cells upon combined H1.2 and H1.4 depletion and H1.4-lamin B2 knock-down

As depicted in Figure R.39A, multi-H1 KD cells lacking H1.2 and H1.4 presented a particular morphology compared with non-Dox treated cells or individual knock-down cells. To better understand such phenomena, we decided to further study this cell line, comparing it with individual knock-downs for H1.2 and H1.4, but also with the previous "444"shRNA cell line, as it presented a similar phenotype (Figure R.35), and because, regarding our ChIP experiments in Chapter 1-Figure R.23 and other similar recent observations [249], H1 could be related with the establishment of LADs. Thus, if H1 is important in the establishment of LADs, H1 knock-down could indirectly impair nuclear lamina organization and cause similar effects as lamin B2 knock-down.

We started by performing time lapse experiments similar to the one in Figure R.35B. By following *in vivo* the growth of knock-down cells between day 3 and day 6 after Dox treatment we confirmed that H1.2 and H1.4 knock-down proliferated slower than RD KD cells, as cellular divisions were more spread along the time and after 6 days of Dox treatment cells did not reach same levels of confluence as random shRNA-expressing cells. On the other hand, both multi-H1 KD and "444"shRNA KD cells almost did not proliferate, as cellular divisions were rare and some cells died during the course of days. Additionally, the characteristic behavior described for "444"shRNA cells in Figure R.35B was also observed for multi-H1 knock-down cell

line, and both of them grew forming compacted cellular clusters (Figure R.41A). Although microarray data points to increased cell adhesion properties of these cells, these phenotype could also reflect an altered cell polarity upon knock-down.

Interestingly, Z-stack reconstruction experiments on those cells showed that both Dox-treated multi-H1 and "444"shRNA KD cells presented a particular and similar morphology under the microscope, with cells imbricated among them, in comparison to the monolayer formed by RD KD cells, but also to H1.2 or H1.4 knock-down cells (Figure R.41B). These cellular clusters formed in multi-H1 KD and "444"shRNA KD cells were higher than the cellular monolayer in individual knock-downs and control cells, as depicted by measurements of cellular Z-reconstruction experiments using the confocal microscope (Figure R.41C). Finally, actin staining with phalloidin of these cells discarded global alterations of the cytoskeleton upon H1 or H1.4-lamin B2 knock-downs (Figure R.41D).

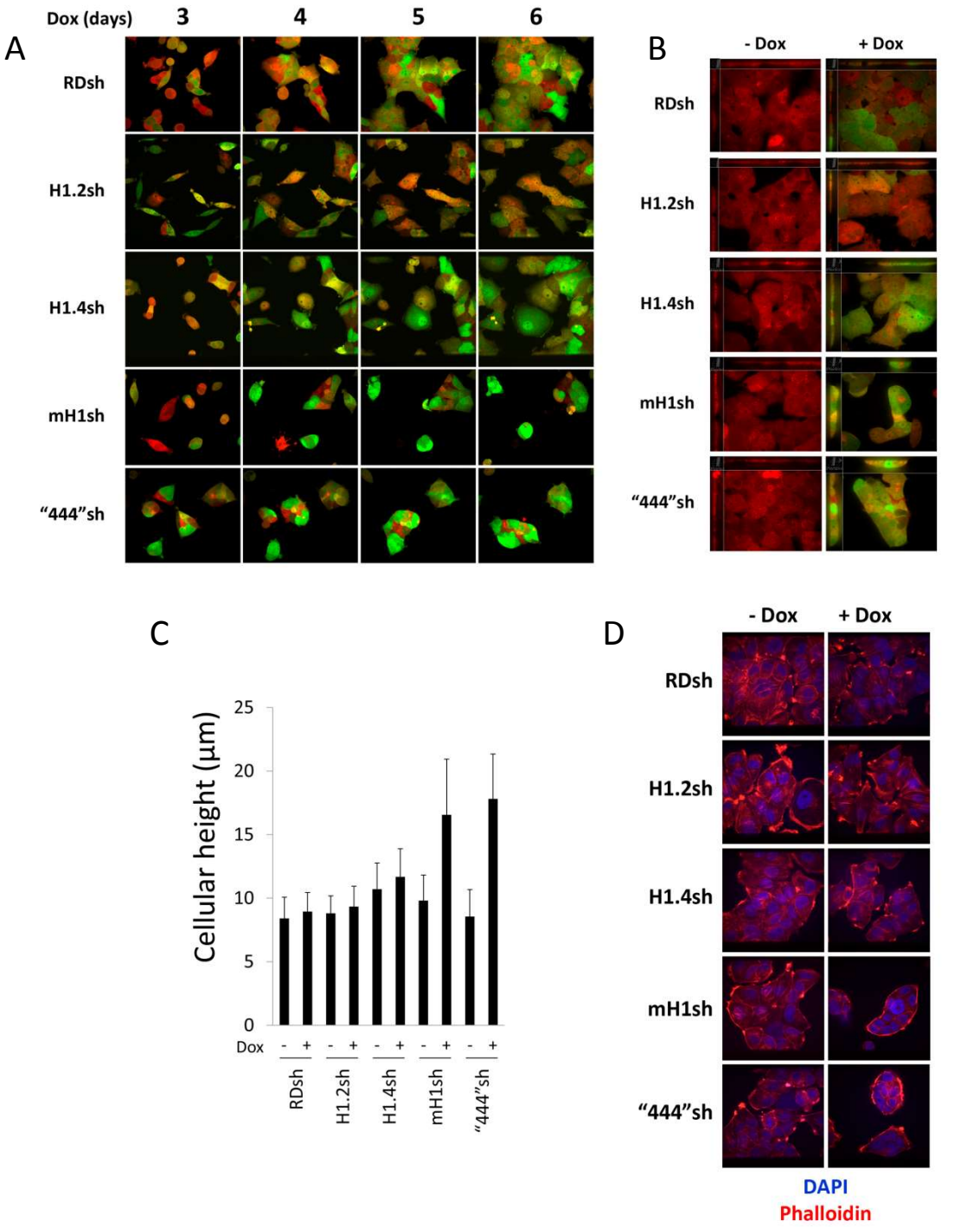

Figure R.41. Morphological alterations in multi-H1 KD and "444"shRNA cells. (A) *Growth of knock-down cells treated with Dox (RedFP and GFP-positive) was followed from day 3 to day 6 of Dox treatment in a time lapse experiment with a Spinning Disk microscope. Images were taken every 10 minutes along 3 days with cells growing at 37ºC and 5% CO_2.* ***(B)*** *Z-stack reconstruction in the Spinning Disk microscope to measure height of living cells at day 6 after Dox treatment. Cells were visualized by RFP (-Dox) or RFP+GFP (+Dox) self fluorescence.* ***(C)*** *Quantification of cellular height in (B) using Volocity Perkin Elmer software. N=50 cells for each condition were quantified.* ***(D)*** *Immunofluorescence experiments in knock-down cells after 6 days of Dox treatment. DAPI (blue) stains nuclei and actin fibers are stained with phalloidin (red).*

Finally, to further correlate the phenotype observed in multi-H1 KD and "444"shRNA cells, we looked for expression of CDH3 (P-cadherin) in multi-H1 KD cells, as it was overexpressed in "444"shRNA and specific lamin B2 knock-down cells (Figure R.35C and R.36B). P-cadherin is a member of the cadherin family, calcium-dependent transmembrane proteins implicated in cell adhesion, by forming adherent junctions within cells. Moreover, P-cadherin has been reported to play a role in breast cancer, as it is aberrantly expressed in ~30 % of breast carcinomas [254, 255]. As seen in Figure R.42A and B, CDH3 (P-cadherin) was overexpressed in both multi-H1 KD and "444"shRNA cells lines upon Dox treatment, compared with untreated cells or individual H1.2 and H1.4 knock-downs.

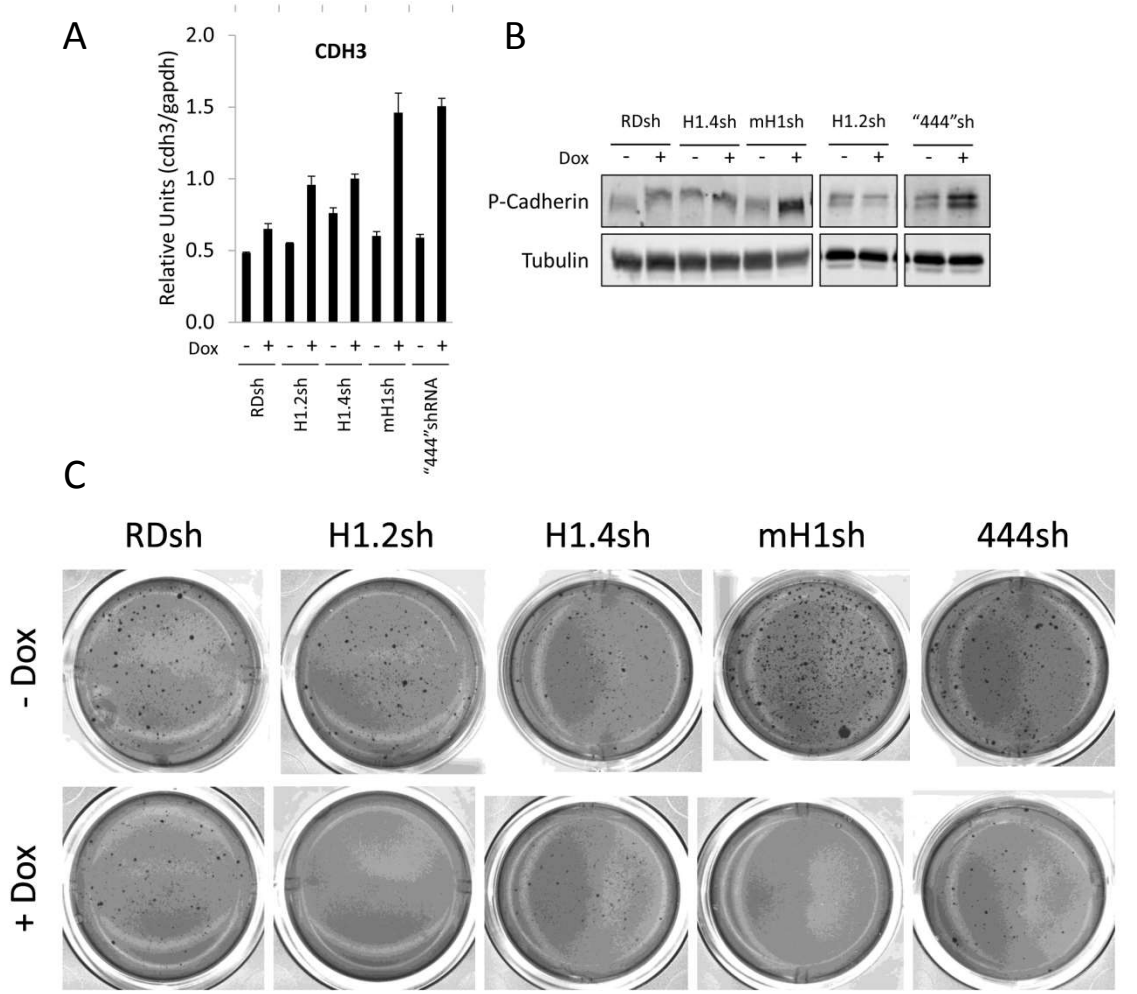

Figure R.42. Multi-H1 KD and "444"shRNA cells overexpress CDH3 and H1.2 depletion inhibits the in vitro clonogenicity of T47D breast cancer cells. (A) *Inducible knock-down T47D cell lines were treated for 6 days with Dox or left untreated. Expression of CDH3 gene was tested by RT followed by qPCR with specific oligonucleotides. RT-PCR values for CDH3 were normalized to GAPDH expression.* ***(B)*** *Expression of CDH3 (P-cadherin) in knock-down cell lines was tested by Western blot of total protein extract using an specific antibody. Tubulin was used as a loading control.* ***(C)*** *Soft-agar colony formation assay in T47D knock-down cell lines. Experiment was done in triplicate.*

Given the fact that cell-cell adhesion and cellular proliferation are processes related with migration, invasion, and tumorogenicity in cancer processes, we decided to interrogate our knock-down cell lines in their ability to grow in colonies independently of the attachment to the cellular matrix. The *in vitro* capability for colony formation in soft-agar resembles the ability of cells to grow into a foreign tissue after a metastatic event, and, hence, it is positive linked with metastatic tumor progression. These soft-agar colony formation assays revealed that WT human T47D breast cancer cells were able to grow into such conditions. However, upon H1 and "444"shRNA-mediated knock-down, the effects were different (Figure R.42C). Interestingly, while H1.4 depleted cells were still able to grow in agar, H1.2 knock-down cells lost this capability. Moreover, the clonogenicity of multi-H1 KD and "444"shRNA cells was also differed, as the double H1.2 and H1.4 knock-down was not able to form colonies, while H1.4-lamin B2 knock-down did. Altogether, it seems that depletion of H1.2 in T47D breast cancer cells, alone or together with H1.4, causes a less tumorigenic phenotype in these cells. On the other hand, H1.4 depletion, alone or in combination with lamin B2, does not cause the same effect. We discarded that absence of colonies in the H1.2 knock-down was just due to its decrease in proliferation, as "444"shRNA KD cells proliferate even slower but colonies were still formed in this cell line after Dox treatment.

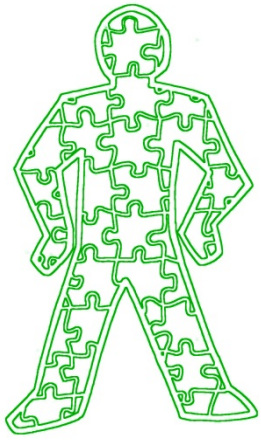

DISCUSSION

DISCUSSION - CHAPTER I:

GENOMIC DISTRIBUTION OF HUMAN HISTONE H1 SUBTYPES

Linker histone H1 family includes in humans 11 *variants* or *subtypes* with different structural features, expression patterns or post-translational modifications. The study of these subtypes has been challenging since they were discovered as lysine-rich histone proteins in calf thymus that differed in sequence composition [256, 257]. The growing heterogeneity of H1 family due to an increasing number of described variants, as well as the lack of specific antibodies for all of them, delayed the precise study of the role of the different H1 variants until not many years ago. However, knock-out and knock-down experiments in several organisms helped in shedding light into the controversial issue regarding the redundancy versus specificity of histone H1 variants. Thus, as it has been previously addressed in the *introduction* part of the thesis, it seems that there is overlapping redundancy between the variants, as knock-out of single or double H1 subtypes in mice caused no apparent phenotype, and animals developed normally because other subtypes compensated the loss of these variants in order to maintain an appropriate H1-to-nucleosome stoichiometry [191]. However, as also previously discussed, increasing studies and observations in the last years support the idea of different functions for the H1 subtypes in more specific processes. The study of the specificity of H1 subtypes has been focused to their structure, expression pattern, chromatin dynamics, regulation of transcription, and post-translational modifications. Additionally, during the last months, two groups succeeded in obtaining the firsts genome-wide comparisons of H1 variants, dodging by different strategies the issue of the inexistence of useful ChIP-grade antibodies for the different H1 variants [248, 249]. The understanding of the precise location of the linker histone H1 variants will help to clarify several aspects of their functionality, regarding their specificity and the role of this histone family in the organization of chromatin and gene regulation.

In an attempt to contribute in elucidating the genome-wide distribution of the somatic H1 variants, we have combined chromatin immunoprecipitation (ChIP) experiments on endogenous H1 variants with ChIP in HA-tagged H1 variants. Thus, in this thesis project, we have investigated the distribution of all somatic histone H1 variants present in breast cancer T47D cells, i.e. H1.0, H1X and H1.2 to H1.5, by combining ChIP with genomic technologies such as tiling promoter array hybridization and high-resolution sequencing. After analyzing many aspects of H1 variant distribution in the genome, we conclude that H1.2 presents distinctive features compared with other H1 variants in the cell line investigated, and we suggest that different variants may be present at different chromatin types, depending on the cell type, differentiation state and whether cells are originated from a neoplastic process.

1. Combination of endogenous and HA-tagged H1 variants in the study of H1 location by ChIP

After testing several H1 variant-specific antibodies that we and others have produced, only H1.2 and H1X commercial antibodies were found to be useful on ChIP-qPCR experiments, and variant specific, as shown by performing ChIP experiments in H1.2 and H1X KD cells (Figure R.3). In those experiments, although the inhibition of H1.2 and H1X in Dox-treated cells was evident, the decrease in the IPed material was not comparable to the signal achieved with an unrelated immunoglobulin (IgG), and H1s were still been immunoprecipitated in low amounts, despite the expression of the shRNA. This observation is explained by the incomplete knock-down of the H1 variants in these cell lines at day 6 upon Dox treatment. We previously showed that, while H1 variant inhibition at the mRNA level was achieved after 2 days of doxycycline treatment, H1 depletion at the protein level was delayed until day 6. This shifting between mRNA and protein degradation by the shRNA may be explained by a long lifespan of most histone proteins, including linker histone H1 variants [258].

Consequently, in order to being able to compare all somatic H1 variants expressed in our cell line, we generated stable T47D-derived cells expressing HA-tagged versions of the H1 variants at protein levels close to or below endogenous levels, despite mRNA levels of exogenous H1 forms were higher (data not shown). Our results and others elsewhere suggest that H1 is tightly post-transcriptionally regulated to control the overall levels of H1 and the proportion between variants, which are diverse among cell types and cell lines. Moreover, H1-HA expressing cell lines were also validated with proliferation assays and cell cycle analysis, which showed that no major differences in growth were observed between H1-HA expressing cells and parental T47D cells. Thus, HA-tagging allowed us to perform ChIP of all variants with the same antibody, discarding variability due to diverse antibody specificity or affinity.

As a result, by combining chromatin immunoprecipitation assays in both HA-tagged H1 variants and endogenous histone H1 variants (H1.2 and H1X) we show a complete picture of the distribution of H1 variants in the genome of breast cancer cells, controlling the effect of reporting H1 distribution using exogenously expressed recombinant proteins by comparison with some endogenous proteins.

Regarding with this fact, we have noticed that H1.2-HA was not exactly distributed as endogenous H1.2, and showed intermediate features somehow close to the other H1-HAs. For instance, at the promoter level, H1.2-HA resembled endogenous H1.2 distribution, as in ChIP-

chip and ChIP-seq analysis, both of them are less present at the TSS than other H1-HAs or endogenous H1X (Figure R.10B and R.21). Furthermore, visualization of genomic distribution of H1 along entire chromosomes showed that both endogenous and exogenous H1.2 proteins distribute similarly, but different from other H1 subtypes (Figure R.25). On the other hand, in other studies such as in correlation analysis of H1 variant abundance at distal promoter regions, H1.2-HA presented and intermediate behavior between endogenous H1.2 and other H1-HA proteins (Figure R.14). We believe that this recombinant protein has the H1.2 structural features that direct it to the natural H1.2-occupied sites, but due to its overexpression it may also locate at distinct sites normally occupied by other H1 variants. We have noticed by ChIP-qPCR that upon knock-down of endogenous H1.2, exogenous H1.2-HA occupancy was increased, suggesting a re-location to H1.2 sites (Figure D.1). All together, we believe that caution has to be taken when interpreting data generated with exogenous histone variants fused either to the Dam domain or to peptide tags, strategies used until now to decipher the distribution of H1 variants [248, 249].

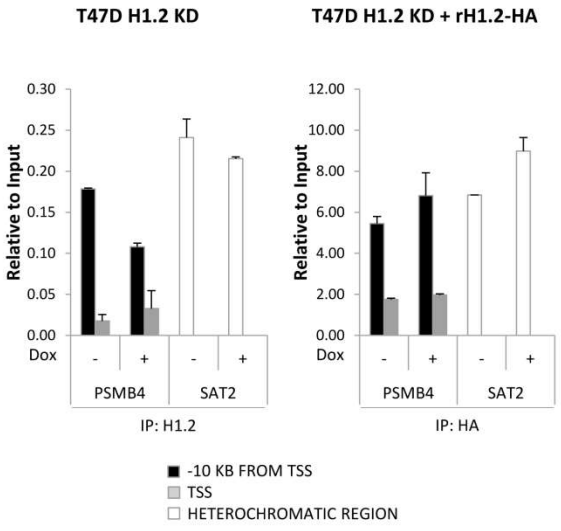

Figure D.1. Exogenous H1.2-HA relocates to endogenous H1.2 occcupied sites upon H1.2 knock-down. *T47D-derived cells stably harboring an inducible system for shRNA expression against H1.2 (left), and same cells overexpressing a shRNA-resistant form of H1.2 (rH1.2-HA) (right) were treated with doxycicline for 6 days or left untreated. Then, ChIP was performed with H1.2 specific antibody (left) or HA antibody (right), and the IPed material was quantified by qPCR with oligonucletotides corresponding to distal promoter regions, TSS, or satellite heterochromatic regions (SAT2). IP was corrected by input DNA amplification.*

2. H1 abundance at promoters inversely correlates with gene expression, being H1.2 occupancy the best reporter of transcriptional repression

After different approaches by ChIP-qPCR, ChIP-chip and ChIP-seq, we corroborated previous observations reporting a depletion of H1 at the TSS of active genes. By ChIP-qPCR experiments, we showed that in selected active promoters previously reported to have an “H1 valley” at the TSS [170], the H1 depletion was not variant specific, as all H1 variants were

depleted into a similar extend (Figure R.5). Moreover, we showed that H1 depletion at the TSS is related with the presence of H3K4me3, and an open-chromatin state measured by FAIRE, both of them general characteristics of active promoters. In addition, H1 depletion at the TSS is also related with the existence of a nucleosome-free region, investigated by H3 core histone occupancy (Figure R.6). On the other hand, H1 variant depletion at the TSS was not observed in transcriptionally silenced genes, whose promoter is fully occupied with H1, thus preventing binding of the transcriptional machinery and other coactivator proteins.

Taking ChIP-chip and ChIP-seq analysis into account, an inverse correlation of H1 occupancy at promoter regions with the transcription status of the genes was seen for all the H1 variants and also for H3 (Figure R.10B and R.21). However, H1.2 is the variant that better correlates with transcription, as depicted by many analyses demonstrating that genes with high content of H1.2 are mainly repressed, while genes with few H1.2 tent to be activated. For instance, in Figure R.13, sorted promoters by H1 variant abundance at the distal promoter region (-3200 to -2000 bp from TSS) showed a clear inverse correlation with expression for H1.2, but not for other variants. Moreover, 10% highly enriched H1.2 promoters are expressed below the total transcriptome average, and 10% lowly enriched promoters are above the mean. Furthermore, expression of clustered genes in defined chromosome regions is directly linked with abundance of H1.2 within these clusters, and H1.2 abundance reflects the mean expression level of the embedded genes in a given chromosome (Figure R.19). Additionally, H1.2 is the variant presenting a clearer correlation with histone PTMs. Genomic regions enriched in active histone marks are devoid of H1.2, while regions enriched in repressed marks present higher levels of H1.2. Note that data on histone PTMs comes from databases in HeLa cell line, so we expect that better correlations would be found if using data from T47D cell line. Finally, H1.2 enriched target genes or promoters are less expressed than other H1 target genes, and, vice versa, H1.2 depleted target genes or promoters tent to be highly expressed (Figure R.30 and R.31). Altogether, H1.2 occupancy inversely correlates with gene expression in T47D cells.

3. H1 depletion from promoters and coding regions is more pronounced than core histone H3 and shows differences between variants

As the effect of histone H1 on gene expression is thought to be explained by its action on gene promoters, most of the reports on H1 distribution focus in elucidating H1 occupancy around TSS and gene bodies. That an H1 valley exists close to the TSS of active genes has been reported since the firsts genome-wide studies of total human and *Drosophila* H1 [170, 246]. Later, studies of Cao et al. and Izzo et al. reproduced this observation for all H1 variants

studied [248, 249], and Cao et al. extended the study towards gene bodies, showing that genic H1 occupancy is lower at active genes compared with inactive ones. In our analysis we further confirm these observations, emphasizing a different behavior for H1.2 and comparing the H1 distribution with nucleosome occupancy, reported by H3 ChIP.

Strikingly, by both ChIP-chip and ChIP-seq analysis, we show that the removal of all H1s from active promoters, with their maximum depletion close to TSS, extends several nucleosomes upstream beyond the reported nucleosome-free region (NFR) [98, 100], and within the coding regions. While H3 depletion at TSS is localized in the region comprised between the TSS and no more than -500 bp upstream, in accordance with recent data suggesting that the NFR may accommodate multiple nucleosomes [100], H1 depletion extends into a broader range, starting from further than -1000 bp upstream the TSS (Figure R.10B and R.21). H2A.Z and H3.3 histone variants have been reported to locate at active promoters surrounding the nucleosome free-region, where they positively regulate transcription [56, 65, 259]. Moreover, it has been demonstrated weaker histone H1 binding in H2A.Z-containing nucleosomes [260] and negative genome-wide correlation between H1 and H3.3 [246]. So, we claim that H1s are depleted from H2A.Z and H3.3-enriched nucleosomes at promoter regions, favoring an open-chromatin state necessary for the binding of transcription factors, co-activators, and RNA polymerase during transcription initiation events. This observation and previous reports indicate that H1 removal is part of the chromatin remodeling events occurring upon promoter activation to facilitate binding of transcription factors and the RNA polymerase machinery. For instance, phosphorylation and PARylation have been involved in H1 ejection from promoters, contributing to the dynamic regulation of gene expression [82, 171, 172].

Moreover, at a more genome-wide level, comparison of H1 occupancy with H3 has shown that all H1s except H1.2 follow the distribution of the core histone, whether this represents nucleosome enrichment, stability or defined positioning through the cell population. Nonetheless, H1 depletion at promoters and also at regulatory sites (CTCF or p300 binding sites) is more extensive than H3, denoting again that nucleosomes might be ejected from very delimited sites such as those NFR at TSS, but H1 might be ejected from larger regions encompassing several nucleosomes. This is again in agreement with previous reports showing that dips of low H1 occupancy at TSS and regulatory sites are not due to lack of nucleosomes as they show enrichment of the core histone variant H3.3 [246].

Furthermore, the shape of the H1.2 (and H1.2-HA) valley at the TSS in ChIP-chip and ChIP-seq data (Figure R.8, R.10 and R.21) was slightly different from those of other H1 variants. H1.2

signal did not present a local enrichment immediately after the TSS as other variants did. Instead, H1.2 depletion extended downstream of the TSS. This local enrichment of other H1 variants just after the TSS may coincide with a well-positioned nucleosome (+1), flanked by phased nucleosomes, as it is reported for yeast but also for human genes [98, 100]. This indicates that such nucleosome may contain any H1 variant except H1.2. Additionally, H1.2 was unabundant around the TSS of repressed genes even in non-protein-coding transcripts, suggesting that TSS of genes is epigenetically marked in T47D breast cancer cells, including the absence of H1.2. Overall, we have shown a strong rejection of H1.2 from the TSS of most genes.

Interestingly, we have also found that immediate-early (IE) responsive promoters, under non-stimulating conditions, are prepared to respond to stimuli by keeping the TSS free of H1 (Figure R.7), indicating that other mechanisms different from transcription initiation might dictate H1 clearance. In this case, there is also a histone H3 depletion at the TSS compared to a distal promoter region in the absence of stimuli, indicating that the nucleosome-free region might be maintained to allow rapid response after stimulation of those genes. Promoter regulation of immediate-early (IE) genes such as *Jun* and *Fos* includes H3 phosphorylation at serine 28 or 10 upon activation of the ERK and p38 MAPK pathways, and chromatin remodeling by SWI/SNF [261-263]. Supporting our hypothesis, it has been recently proposed that transcription factors (TF) interact with DNA in a dynamic way, and some TF-DNA interactions are established prior to the stimuli, especially at IE genes [264]. Our observation of a maintained NFR in IE genes independently of transcription has not been reported previously to our knowledge, and would help to further explain how this kind of genes are able to start transcription immediately after being stimulated.

Apart from the TSS, the transcription terminator site (TTS) is also characterized by a reduction in the nucleosome occupancy in many organisms including mammals, a feature that could be important in transcription termination or in anti-sense initiation [265, 266]. Our data shows that H1 is depleted around the TTS in the same extend that H3 (Figure R.21). However, interestingly, both H1.2 (H1.2endo and H1.2-HA) present almost no depletion around the TTS, pointing again like in the case of the TSS, to a different behavior of H1.2 in its localization around nucleosome depleted regions, compared with other H1 subtypes.

Finally, at coding regions, the differential content of H1 in active versus repressed genes is more pronounced than those of H3, especially towards the 5’ of genes. While H3 occupancy into the gene body is constant in all gene groups, independently of the transcriptional status

of the gene, the H1 occupancy is higher in the repressed groups of promoters compared with the active ones (Figure R.21), mainly for H1.2, indicating again that a reduced H1.2 occupancy, not only in the promoter region, but also in the whole gene body, favors gene expression. Cao et al. also showed a differential H1 content in gene bodies of active genes compared with repressed gens, and suggested that H1s are depleted from broad domains at regions of active transcription because H1 levels at active genes remained diminished up to 200 kb from the TSS [248]. In accordance with their hypothesis, we show that a general depletion of H1.2 along active genes fits with the fact that H1.2 abundance correlates with clusters of differential gene expression along chromosomes (Figure R.19). Moreover, H1 abundance in chromosomes seems to be related with their distinct radial organization in the nucleus regarding gene density and transcriptional activity. For instance, H1.2 is poorly present in chromosome 19, a gene-rich chromosome reported to localize towards the center of the nucleus [250]. Consequently, clustered gene-rich domains might adopt an overall decondensed chromatin structure devoid of H1.2. Nonetheless, at active genes, H1 is less abundant in promoters than in coding regions, indicating that H1 presence might be more restrictive for transcription initiation than for elongation.

4. Abundance of H1 at promoters differs between variants and does not correlate with altered genes upon H1 knock-down

Initial experiments by ChIP-qPCR indicated that all H1 variants were present at all tested promoters (Figure R.4 and R.5). Nonetheless, hybridization of ChIP material with a promoter array visualized that promoters might present differential H1 variants abundance (Figure R.14). The most streaking difference is between H1.2 and the other H1s, including H1X. H1.2 abundance at distal promoter regions negatively correlates with abundance of other variants. To prove this, subsets of genes with the strongest abundance of one variant and the lowest of another have been identified comparing H1.2 with H1X and H1.0-HA, e.g. high or low H1.2/H1X ratio. Overall, expression of genes presenting these features is different, relating H1 variant content with gene expression (Figure R.15 and R.16). Worth noting, relative abundance of H1.2 and H1X in selected promoters was conserved at the distant HeLa cell line, but not in MCF7 cells (Figure R.17). We propose that the relative promoter abundance of H1 variants is related with the relative content of the variants in a given cell line. In T47D and HeLa cells the ratio of H1.2/H1X content compared with that of MCF7 cells could explain the differences in the promoter occupancy of such variants, as MCF7 cells present higher levels of H1X than T47D, and even more than HeLa, which has very low levels (Figure R.17C).

The preferential targeting of H1 variants to certain promoters could be determinant in regulating the expression of their related genes. It can be easily hypothesized that if a promoter is controlled by the presence of a single H1 variant, its depletion would deregulate its expression. By taken advantage of previously reported gene expression microarray experiments in T47D specific H1 knock-down cell lines, we investigated if genes up- or down-regulated by inhibition of a certain H1 variant were preferentially loaded by this variant at the distal promoter region. Interestingly, there was no clear over-representation of an H1 variant in genes up-regulated upon knocking-down this variant (Figure R.20). However, for H1.2, expression levels of deregulated genes were above the mean, especially for down-regulated ones. According to previous analysis showing an inverse correlation of H1.2 abundance and gene expression, low abundance of H1.2 would be expected in those down-regulated genes, compared with up-regulated genes that presented lower expression levels. Instead, H1.2 occupancy at distal promoter regions was higher in down-regulated genes than in up-regulated ones, suggesting that may be H1.2 has a positive role in those promoters. Further analysis should be carried on to prove this hypothesis.

Therefore, although differential H1.2 and H1X abundance at distal promoter regions is related with distinct biological processes in gene ontology (GO) analysis (Table R.1), alternative mechanisms of regulation different from the abundance of an H1 variant in the overall promoter should be considered. So, it may be conceivable that the total amount of H1 variants in the promoter is not the determinant in controlling gene expression, and more precise mechanisms are involved in fine tuning transcription at certain promoter regions. For instance, although H1 histone PTMs are not still broadly studied, the combination of specific H1 variant modifications may control the expression of different subsets of genes. In this direction, a recent report mapping H1.4-K34 acetylation shows accumulation of this modification at the TSS of active genes, where it has a positive role in transcription [168]. Alternatively, H1 variant function in regulating gene expression could be linked with specific deposition at certain delimited promoter regions, such as transcription factor binding sites, rather than with its presence in the whole promoter. For instance, H1 positively regulates transcription of the MMTV by favoring nucleosome stability in a delimited region of its promoter (nucleosome B) during early progesterone response [161, 162].

5. Genome-wide distribution of H1.2 differs from other variants in breast cancer cells and coincides with broad repressed genomic regions

According to what is shown in ChIP-chip and ChIP-seq experiments, we conclude that all H1 variants are widely distributed along the genome and within promoters with few differences between HA-tagged H1.0, H1.3, H1.4 and H1.5. Nonetheless, endogenous H1.2 presents striking differences, already discussed for promoter regions. We discard that this differential distribution is due to antibody usage or protein overexpression as endogenous H1X presented an occurrence similar to HA-tagged variants and exogenous H1.2-HA resembled more to its endogenous counterpart than to the other H1-HAs.

As a result, we report that in the cell line investigated, H1.2 presents a variant-specific distribution and may play differential functions. In fact, we reported elsewhere that H1.2 KD [97], and now also H1.4 KD (see Results – Chapter II), produced unique effects, i.e. cell cycle arrest at G1 and decreased nucleosome spacing, not seen in other H1 KDs and, not only in T47D cells, but also in MCF7 cells. Nonetheless, this feature was not general as it was not seen in other tested cell types, including HeLa cells, were H1.2 is highly abundant, indicating that H1 variants may have cell-type dependent specific effects. Moreover, H1.2, in comparison with H1.4, seems to be related with the tumorigenic capacity of breast cancer cells, as depicted by in vitro soft-agar colony formation assay (Figure R.42C). Thus, the importance of H1.2 in clonogenicity could be explained by a differential function of this variant in T47D breast cancer cells, linked to a particular genome-wide distribution of H1.2 in comparison with other H1 variants. How a differential prevalence of H1.2 in the genome would explain the outcome of differential phenotypes upon specific knock-down should be further studied in the future.

Instead, our data cannot rule out that the rest of variants may share redundant functions and distribution in breast cancer cells. Genomic distribution of Dam-H1.1 to H1.5 in lung fibroblasts IMR90 cells found that H1.1 is the unique subtype showing divergent features [249]. H1.1 is not expressed in breast cancer cells or in many other cell types. Instead, H1.2 and H1.4 are the unique variants that have been found in all tested cell lines tested up to now [217, 267]. Although this is a too short sampling, these results suggest that different H1 subtypes may play different roles in different cell types, along development or in cancer cells, inviting further investigation of H1 variants occurrence in different cell lines or cellular states.

Furthermore, after extending the study to the whole genome by ChIP-seq, we show that H1 variants are not uniformly distributed along the genome. Instead, H1 abundance alternates broad genomic regions of local enrichment and depletion (Figure R.19, R.23, and R.25). This is accordance with other genome-wide H1 variant studies [247, 249]. Both reports showed H1 variants organized in defined blocks of H1 enrichment and depletion. In T47D cells, the negative correlation observed between gene activity and H1.2 content found at promoters extended upstream towards the whole genomic region around. Patches of H1.2 enrichment seem to be associated with gene repression, gene-poor regions (including entire chromosomes, e.g. chromosome 13), low GC content or Lamina associated domains, features related with chromatin compaction (Figure R.19 and R.23). Moreover, H1.2 enriched regions were frequently found at intergenic regions (Figure R.27 and R.28). This distribution of H1.2 is somehow similar to H1.5 distribution in IMR90 fibroblasts, where H1.5 target genes are clustered together and present a transcriptionally repressed state [247]. Similar results were also found in other reports, linking histone H1 to repressive and compacted regions of the genome and suggesting a role for H1 in three-dimensional organization of the genome. Cao et al. described some of these features for mouse $H1c^{Myc}$ and $H1d^{FLAG}$, the closest orthologs of human H1.2 and H1.3, and Izzo et al. for human Dam-H1.2 to H1.5 [248, 249]. On the other hand, we found that other H1 variants are more abundant at promoters and genic regions (Figure R.28). In conclusion, we show that distribution of H1.2 in T47D breast cancer cells is different than that of other H1 variants studied. While distribution of most of the variants resembles distribution of H3, H1.2 occupancy is different and directly related with a repressed chromatin state. Interestingly, analysis by Izzo et al. on IMR90 lung fibroblasts also showed differential distribution of H1 variants. While Dam-H1.2 to H1.5 distribution was similar among them, H1.1 presented a DamID binding profile distinct from the other subtypes. H1.1 was more abundant at promoters and less at intergenic regions compared to the other variants, was not depleted from active regulatory regions or CpG-rich regions, absent in LADs or HP1-associated chromatin, and associated with polycomb-type domains. In our case, H1X, H1.0-HA and H1.4-HA at least, differed from H1.2 genomic distribution and were similar among them. They were more associated with higher GC content, genes, its promoters and CpG islands, and were not enriched in LADs. In some extent, this resembles the distribution of H1.1 in IMR90 fibroblasts described by Izzo et al. On the other hand, H1.2 prevalence at T47D was more similar to Dam-H1.2 to H1.5 distribution in IMR90 cells.

It is conceivable that at least two groups of H1 variants with different distribution are found in each cell type, so that all together histone H1 covers the whole genome, being present in

most of the nucleosomes. Although the paradigm of one H1 molecule per nucleosome was longer thought, studies of stoichiometry in different cell types and the high mobility of H1 within the nucleus rejected it [146]. Still, in average, H1 might be present genome-wide.

Whether a same variant may present distinct features in different cell types instead of having intrinsic properties is an intriguing question. Factors involved may be the relative and absolute abundance of each variant and whether a genome needs more plasticity or is progressively silenced, i.e. pluripotency versus terminal differentiation. So, taking into account the importance of H1 in chromatin structure and compaction, differential expression and/or distribution of H1 variants could mediate the transition between different chromatin states, and explain for intance the more "open" chromatin state of undifferentiated cells, which contributes to the maintenance of pluripotency by creating a poised chromatin state that leads to rapid activation of lineage-specific genes when differentiation is induced. ES cells have considerably less heterochromatin than differentiated cells, present less genomic loci enriched in repressive chromatin marks such as H3K9me3 and H3K27me, and present higher promoter histone acetylation [268-270]. Moreover, it is reported that architectural chromatin proteins, HP1 and histone H1, are hyperdynamic and bound loosely to chromatin in ES cells [271, 272]. Supporting our hypothesis, Li et al. described the existence of blocks of H1.5 enrichment in differentiated fibroblasts but not in embryonic stem cells [247]. Additionally, we have previously reported progressive changes on the expression and abundance of H1 variants along differentiation of human embryonic stem cells or reprogramming of differentiated cells to iPS, in opposite directions [224]. In fact, it is proposed that different "anti-silencing" mechanisms, including incorporation of specific histone variants such as H3.3, are involved in the maintenance of open chromatin in ES cells [67].

Cancer is another cellular state presenting global chromatin rearrangement. In fact, abnormal nuclear morphology is one of the characteristics of cancer cells. Tumor-originated cells accumulate genetic and/or epigenetic differences compared to non-tumoral cells, and chromatin is reorganized leading to altered gene expression programs and higher plasticity (Figure D.2). The hallmark of cancer is de-differentiation and genome deregulation. DNA methylation and histone modifications are two epigenetic mechanisms that are altered in cancer cells [273-276]. Thus, it is conceivable that in such reorganized nucleus, histone H1 variant distribution could be different than that of non-malignant cells. In the same way, the poised state of chromatin to allow transcription upon response to environment might be the

reason to find in our study most of the H1 variants in genomic regions associated with more active and open chromatin.

So, we hypothesize that the differences in H1 variant distribution in breast cancer cells may help to explain the dysregulated epigenome of cancer cells, pointing to a possible role of the different H1 subtypes in chromatin reorganization during tumorigenic processes (Figure D.3). In fact, LOCKs (large organized chromatin lysine modifications) are reduced in cancer [277] and genes encoding proteins of the nuclear membrane present altered alterations in many cancer types [278], indicating that LADs might be partially disorganized in cancer cells, according to the large scale chromatin decondensation occurring in cancer.

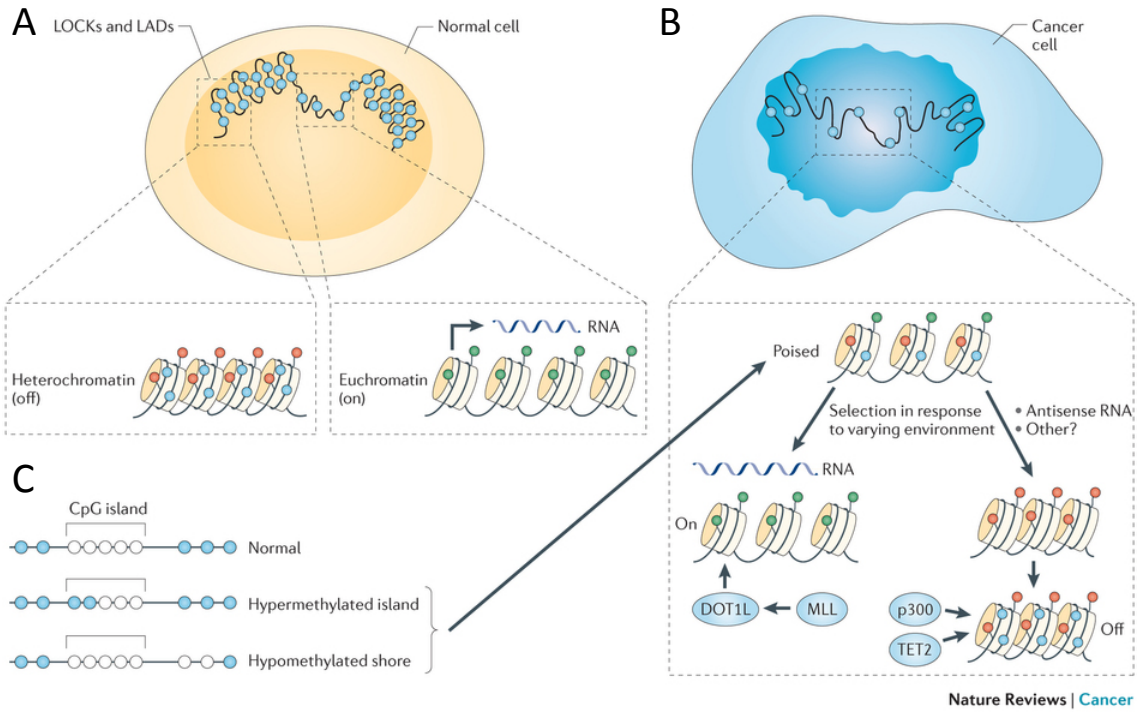

Figure D.2. A dysregulated epigenome in cancer processes, resembling the "open" chromatin state in pluripotent cells, increases expression plasticity. (A) *Normal somatic cells present large organized chromatin lysine modifitications (LOCKs) and lamin-associated domains (LADs) associated with the nuclear membrane, in a hetrochromatic state and with DNA highly methylated. Active genes present a more chromatin relaxed state, while inactive genes are in close chromatin regions. Moreover, differently histone PTMs (green=on; red=off) mark active and inactive genes. DNA methylation (blue) is increased in silent genes.* ***(B)*** *In cancer, there is a reduction of LOCKs, and a general disorganization of the nuclear membrane. Global hypomethylation of the genome in cancer corresponds mainly to LOCKs and LADs [279]. As a result, chromatin is in a more stem cell-like state with the ability to differenctiate into euchromatin and hypomethylated genes, or into heterochromatin and hypermethylated genes, in response to the cellular environment. These epigenetic alterations may be the result of mutation of epigenetic modifiers (DOT1L, MLL, p300 or TET2).* ***(C)*** *DNA methylation is also affected in cancer. CpG island (CGI) shores are regions around 2kb on either sides of a CGI. It has been recently reported that most methylation differences between tissues occur within these regions, rather than in CGI themselves. Cancers lose the boundary stability of methylation at CpG islands leading to hyper o hypomethylated CpG shores, which will affect gene expression. Figure taken from [275].*

Regarding ours and Izzo et al. observations of the association of H1 with LADs, we hypothesize that H1 could be a key player in the establishment of LADs in normal cells, but could also participate in the rearrangement of such domains in cancer cells, by a different prevalence of H1 variants within these domains. Alternatively, LADs reorganization in cancer cells could cause H1 variant redistribution in these genomic domains. Further experiments extending the comparison between normal and cancer cells would prove these hypotheses.

Thus, chromatin containing H1s other than H1.2 might support a level of compaction that facilitates a rapid conversion into either an active or repressed state and, consequently, these variants are allowed at TSS of genes before activation. In fact, a particular post-translational modification in H1.4 (K34ac) has been found to locate around the TSS of active genes [168]. Instead, we have described another behavior for H1.2, more related with transcriptional repression, and being H1.2 occupancy at distal promoter the best predictor of gene repression. This study would direct towards the inclusion of H1.2 as a repressive mark and associated with more compacted chromatin in breast cancer cells. In this regards, H1.2 has been found included in a p53-containing repressive complex in HeLa cells [240], and murine H1.2 has been found to be developmentally up-regulated in the retina, promoting facultative heterochromatin formation in mature rod photoreceptors [280].

6. H1 variant occupancy and DNA methylation

DNA methylation is an epigenetic modification directly related with gene regulation and other cellular processes. Most of DNA methylation occurs within CpG islands, but it can also happen outside this context. CpG islands (CGI) are sites of transcription initiation, including thousands that are remote from annotated promoters. They may contribute to destabilize nucleosomes by facilitating binding of proteins that create a transcriptionally permissive chromatin state. Silencing of CpG island-containing promoters is achieved through dense CpG methylation. Nucleosome positioning and DNA methylation at CpG present a bidirectional relationship, where nucleosome positioning directs DNA methylation patterns, and DNA methylation is also able to determine nucleosome positioning [281-283].

Tumor cells are characterized by a different methylome from that of normal cells (reviewed in [23, 284]). Global DNA hypomethylation in cancer causes genomic instability, activation of transposable elements, and loss of genomic imprinting. On the other hand, hypermethylation of particular promoters, including tumor-supressor genes, housekeeping genes, or tissue-specific genes, leads to changes in transcriptional activity. In our analysis, we found that CpG

islands (CGI) contain H1.0, H1X, and in a minor extent H1.4, but not H1.2 (Figure R.22D and R.29). This might reflect the relative abundance of these variants at promoters and suggests that promoter occupancy by H1 variants different from H1.2 is more permissive for transcription regulation in breast cancer cells. Alternatively, as H1.2 prevalence in intergenic CGIs is also lower than that of other variants (Figure R.29B), we cannot discard a direct role of the different H1 variants in CpG island regulation in breast cancer cells. Thus, differential binding of H1 variants around CGI may help to explain the altered DNA methylation pattern observed in tumor cells within CGI and CGI shores (Figure D.2C).

Similarly, within a long region of genomic sequence, genes are often characterized by having a higher GC-content in contrast to the background GC-content of the entire genome. We found that H1 variants except H1.2 associate with higher GC-content regions (Figure R.24), in agreement with the preferential location of H1-enriched regions within genes (Figure R.27 and R.28). H1.2 presents an inverse correlation with GC content at a genome-wide level, unlike H1.0-HA, H1.4-HA and H1X, which correlate positively. Moreover, H1.2-enriched regions are associated with low percentages of GC content compared with other variants (Figure R.24C). In our analysis, H3 also associates preferentially with higher GC-content regions, in agreement with reports describing a higher nucleosome-space occupancy coinciding with active transcription and higher GC contents [285]. Altogether, in breast cancer cells, H1 variants are differentially associated with CpG islands and GC content. This, again, does not correspond exactly with previous reports on genome-wide distribution of H1. Cao et al. showed in their report that both H1d and H1c were negatively correlated with GC content, although comparison of specific peaks for those variants revealed that H1d (human H1.3) was more associated with GC-rich regions than H1c (human H1.2). Izzo et al. also investigated H1 occupancy at CpG islands, and showed depletion of Dam-H1.2-H1.5 but enrichment of Dam-H1.1 at high-, intermediate-, and low-CpG promoters (HCPs, ICPs, and LCPs). Interestingly, HCPs were H1-free even when the genes were repressed. They also showed a positive correlation of H1 binding at promoter CGI with DNA methylation. High CGI DNA methylation was related with higher amounts of H1. However, this was not the case for CGI located at gene bodies, where DNA methylation was negatively correlated with H1 occupancy, except for H1.1 that went in the opposite direction. Thus, they end concluding that there is not a simple correlation between H1 binding and DNA methylation, and the presence of H1 at methylated sites depends on the genomic region and the chromatin context. So, we propose that the characteristic methylome profile of cancer cells is related with a differential prevalence of H1

subtypes at high/low GC-content regions compared to normal cells, providing to H1 variants a potential role in establishing or maintaining this methylation profile in breast cancer cells.

Other studies have related H1 with DNA methylation, sometimes with partial contradictory results [286-291]. The lack of distinction of H1 variants in some of these studies and their *in vitro* character using purified H1 and naked DNA instead of nucleosomes, could explain these discrepancies regarding H1 prevalence in DNA methylated regions. More recently, *in vivo* studies in mouse ES cells with 50% depletion of H1 content showed altered expression in some DNA methylation regulated genes. Although global methylation in those cells was not altered, methylation of specific CpGs within the regulatory regions of some of the H1 regulated genes was reduced [96]. A subsequent report based on those mouse H1 TKO ES cells showed that H1 variants are involved in the formation of epigenetic silencing marks at H19 and Gtl2 imprinted control regions (ICR), by promoting DNA methylation through the recruitment of DNMT1 and DNMT3B in those loci, and also by preventing the production of active methylation marks on histone H3K4 [292]. Interestingly, H1c (human H1.2) and H1(0) (human H1.0) did not interact with DMNTs, and H1c re-expression in TKO H1 cells was not able to rescue the overexpression of H19 and Gtl2 as H1d (human H1.3) did. Thus, H1d, and probably other H1 subtypes, can promote DNA methylation by interacting (through their CTD) and recruiting DNMT1 and DNMT3B to chromatin. They also showed that H3 interacted with both DNMT1 and DNMT3B. These observations in ES cells fit with our data, as H1.2 is the variant with lower correlation with methylation events at CpGs, while other variants present similar characteristics and are associated with CpGs. It would be necessary to further study the methylation state of the CpGs in our cellular model in order to better understand the link between H1 variants and DNA methylation at GC regions. Additionally, it would be also interesting to address if human H1 variants interact differently with DNMTs in our breast cancer cells, and if H1.2 is the variant with weaker interaction with DNMTs. Strikingly, DNMT3B is overexpressed in many breast cancer cell lines [293].

So, we hypothesize that redistribution of most of histone H1 variants in cancer, may help to establish a differential chromatin state, but also an altered methylation pattern (Figure D.3). In fact, as addressed in the *introduction* part, H1 variants are differently related with several cancer types. Regarding to DNA methylation and breast cancer, it has been reported recently that breast cancer cells present aberrant methylation, in accordance with other cancer types [294]. Comparison of human mammary epithelial cells (HMEC) with eight different human breast cancer cell lines (BCC), including T47D cells, showed global massive reduced

methylation, particularly at CpG-poor regions, and hypermethylation occurring at CpG-rich gene-related regions. Furthermore, the majority of hypermethylated CpGs were related to gene promoters, at regions proximal to the TSS. According to our hypothesis, the observed local enrichment of H1.0, H1.3-H1.5, and H1X immediately downstream of the TSS could be related with the reported hyermethylation at those regions in breast cancer cells. Aberrant methylation of first exons has also been reported in cancer, explaining in part, together with H1 enrichment at CGI, this local enrichment of H1 downstream the TSS. In fact, around 35-40% of the H1-enriched regions overlapping CpG sites coincided with promoters, except for H1.2 (Figure R.29B). Additionally, Ruike et al. also reported that hypermethylation observed at gene-related regions was not only restricted to CGIs, and 53% of hypermethylated CpGs in BCC lines corresponded to non-CGI regions. This fits with the positive genome-wide correlation observed for most of H1s with GC-content (Figure R.24). Thus, we propose that most of H1 variants would relocate to promoter regions in breast cancer to maintain gene-related CpG-rich regions at high methylation state, while H1.2 would preferentially locate at intergenic CpG-poor regions maintaining CpGs unmethylated (Figure D.3). Another study in breast cancer cells demonstrated, in discordance of what it was previously believed, that these hypomethylated regions were associated with repressive chromatin, gene silencing, and H3K9me3 and H3K27me3 histone PTMs [295], in accordance with our association of H1.2 with gene repression. Moreover, interestingly, repressed hypomethylated regions corresponded mainly with intergenic, late-replicating, and LADs, coinciding again with the enrichment of H1.2 in these regions in breast cancer cells. Further analysis of our H1 ChIP data compared with T47D DNA methylation data, would provide more clues about the precise role of H1 variants in the establishment of specific methylation patterns in breast cancer. Finally, if our hypothesis is true, then we expect to find slightly differential H1 occupancy in different tumor types or subtypes within breast cancer, as it has been reported that different gene expression patterns and methylation profiles may contribute to breast cancer heterogeneity [296-298].

7. Histone H1 prevalence in different chromatin types and role in chromatin spatial organization

High-throughput profiling of chromatin marks and components has recently allowed defining chromatin states [108, 299]. In *Drosophila* cells, five principal chromatin types have been described, being H1 (unique variant) present in all of them in different proportions [108]. H1 was abundant in HP1- and Polycomb-containing chromatin types, as well as in the silent 'black' chromatin, associated with lamin and occupying long domains. Transcriptionally active

euchromatin was divided in two types, being H1 more abundant in the one that associates better with transcription elongation than in the one containing high density of regulatory complexes. Although this may represent general features of H1 occurrence, in cells presenting several H1 subtypes a differential distribution of subtypes among different chromatin types may occur, as is suggested in our study. We have found that H1.2 is the variant that better associates with LADs and low GC content, features related to chromatin compaction, while chromatin associated with the other variants presents features of a more plastic chromatin. It would be interesting to further analyze the co-localization of the different human H1 variants with chromatin marks and components that better define the diverse chromatin states, although this type of comparisons are limited by the availability of high-throughput data on coinciding or related cell types.

There are nowadays increasing evidences of a three-dimensional organization of the genome within the cell nucleus. Interphase chromatin is organized in big chromosome territories defined as "topological domains", which can interact between them despite being several megabases faraway [104, 115]. These domains are stable across different cell types and highly conserved across species. It is already reported that embedded genes in these domains are in a transcriptionally similar status and associated with transcriptionally-related histone marks and chromatin features. So, it is not illogic to speculate that H1 could be involved in the formation or maintenance of such domains due to its role in chromatin structure. In fact, Izzo et al. showed different association of H1 variants to four epigenetically different classes of topological domains [249]. Further similar studies in our breast cancer cell line will determine if these features are maintained in a different cellular state. Therefore, it seems that H1 could play a role in the spatial organization of the genome.

8. Model for H1 variant distribution in breast cancer cells and summary of H1.2 differential features

A cartoon model of the distribution of H1 variants in breast cancer cells compared with distribution in normal IMR90 fibroblasts reported by Izzo et al (Figure D.3), and a table summarizing the differential features of H1.2 versus other H1 in T47D breast cancer cells (Table D.1), is shown below.

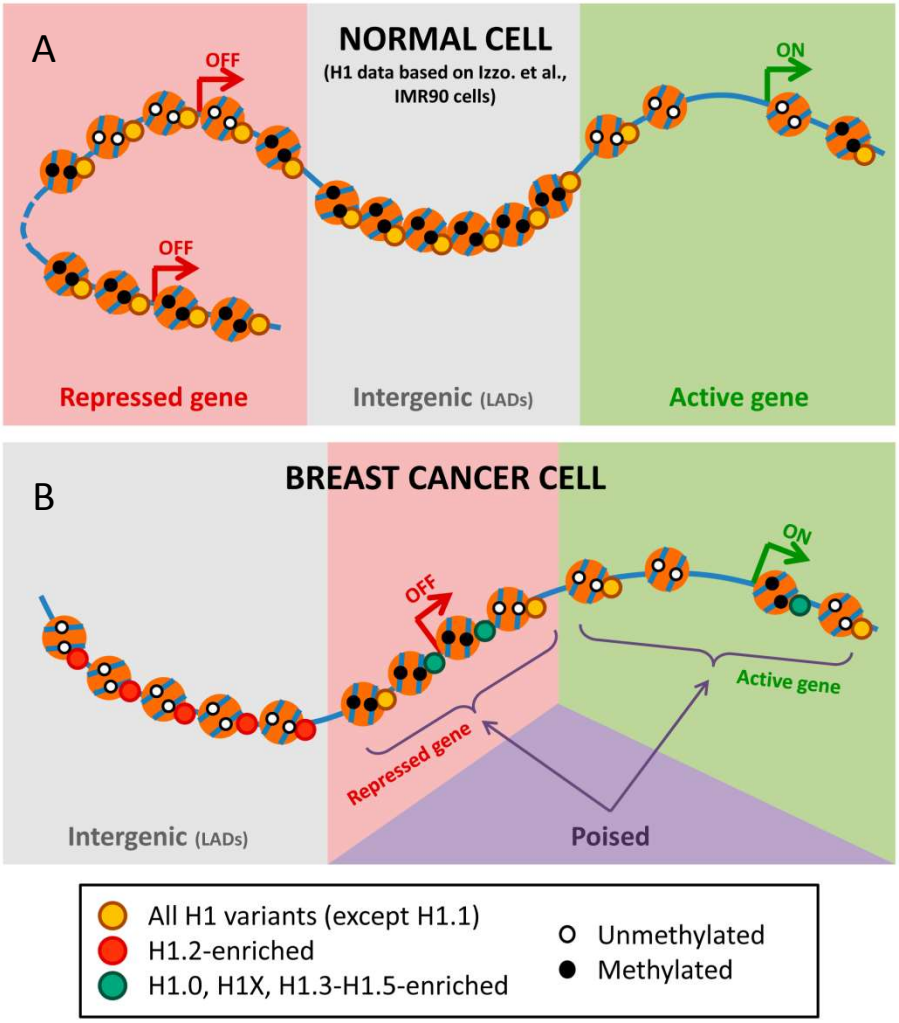

Figure D.3. Proposed hypothetical model for normal cell versus breast cancer cell genome-wide distribution of H1 variants (based in our data of H1 distribution in breast cancer cells and other data in the literature).

(A) *In normal somatic cells, H1.2-H1.5 variants distribute similarly in the genome, being more abundant at intergenic regions and overrepresented at LADs, where chromatin is more compacted. Active genes are depleted of H1 at their promoter, concomitantly with the presence of a NFR. On the other hand, repressed genes are fully occupied with H1. DNA methylation in normal somatic cells is context-dependent. Promoter CpG islands usually remain unmethylated, in order to allow gene transcription. Only genes that should be kept in a repressed state for a long time are methylated at the promoter, while other repressed genes that may change between active-inactive states remain unmethylated. Additionally, DNA methylation within gene bodies avoids spurious transcriptional initiations and stimulates transcriptional elongation. Finally, DNA methylation of repetitive sequences at intergenic regions prevents genomic instability in normal cells*

(B) *We propose that, in breast cancer cells, H1 variants redistribute their location in accordance with chromatin rearrangement. H1.2 is more related with transcriptional repression and is enriched at intergenic GC-poor regions, where it also correlates with LADs. Global DNA hypomethylation, causing genomic instability and transposon activation, is a hallmark of cancer. In breast cancer it coincides with intergenic regions and LADs, where H1.2 is enriched. On the other hand, at genic regions, active genes show an H1 valley at the TSS. Inactive genes present all H1s except H1.2 at the TSS and Nuc+1, coinciding with CGIs. Genic regions, in cancer, are maintained in a poised state in order to activate or repress genes in response to the environment. CpG islands around gene proximal promoters are hypermethylated, blocking transcription of many genes, including tumor-suppressor genes. On the other hand, gene bodies lack DNA methylation and aberrant transcription from incorrect TSS occurs.*

FEATURE	H1.2	H1.0, H1X, H1.3-H1.5
Presence at promoters/TSS		
Active genes	no	no
Inactive genes	no	yes
Coincidence with Nuc+1	no	yes
Depletion at TTS	no	yes
Presence at enhancers and insulators	no	no
Coincidence with repressive histone PTMs	yes	no
Negative correlation with gene expression	yes	medium
Coincidence with high GC content	no	yes
Coincidence with CGIs	no	yes
Coincidence with LADs	yes	no
Enriched regions	intergenic	genes and promoters
Abundance at gene-rich chromosomes	no	yes
Abundance at gene-poor chromosomes	yes	no

Table D.1. Summary of differential features of H1.2 compared with other H1 variants in T47D breast cancer cells.

DISCUSSION - CHAPTER II:

FUNCTIONAL SPECIFICITY OF HUMAN HISTONE H1 SUBTYPES

A common widespread strategy to study protein function is by altering its amount in the cell, either by over-expression or by down-regulation. Histone H1 function has been studied in the last years by depleting H1 content in many organisms. These studies have been essential in reassessing the role of linker histone in gene expression. Classically, H1 histone has been seen as a transcriptional repressor due to its role in chromatin compaction. However, knock-down and knock-out studies in several organisms show that H1 depletion has an impact in a discrete subset of genes and, interestingly, H1 depletion does not only cause over-expression in those genes, as it should be expected, but also down-regulation in many of them, pointing to a positive role of H1 in regulation of certain genes. We and others have also addressed the controversial role of histone H1 variants, showing that different H1 variants are involved in regulating different subsets of genes, and supporting the idea that H1 variants have specific roles in some cellular processes.

After a first trial in studying the phenotype of T47D breast cancer cells upon individual depletion of most of the H1 variants expressed within this cell line (H1.0, H1.2, H1.3, H1.4 and H1.5), we pursued in understanding the characteristics of those cells upon H1 knock-down.

1. Off-target effect of the H1.4 KD ("444"sh) against lamin B2

By analyzing data of expression microarrays for all the H1 knock-downs, we realized that expression of lamin B2 gene (LMNB2) was heavily impaired in H1.4-depleted cells (Figure R.33C). Although specific shRNAs for the H1 variants were designed in order not to find any other target human mRNA with 100% homology, a closer analysis of the H1.4 shRNA ("444"sh) sequence using BLAST software, revealed that this sequence was 84% homologous to a sequence region of the lamin B2 gene, with 16 continuous nucleotides directly matching LMNB2 mRNA (Figure R.33A). Consequently, we performed transient transfection assays with an exogenous lamin B2 protein, fused to GFP, to elucidate if lamin B2 depletion is consequence of H1.4 depletion, or is the consequence of an off-target effect of the H1.4 shRNA. Those experiments (Figure R.34) revealed that H1.4 shRNA ("444"sh) targets lamin B2 mRNA by homology with the previously referred mRNA region. Thus, we had to reconsider the specific phenotype observed in H1.4 knock-down cell lines.

Silencing of protein expression based on RNA interference (RNAi) has been broadly used since its development. However, several handicaps are associated with this technology, including the lack of specificity by off-target activity, which leads to misinterpretation of the phenotypic effects in gene-silencing experiments. Since the first recognized off-target activity of siRNAs in

2003 [300], the reasons for this phenomena have been addressed and suggestions have been proposed to overcome this problem (for a review, see [301, 302]).

To further explore the effects of H1.4 depletion in our cellular model, we designed again shRNAs specifically inhibiting these H1 variants, and we developed a new cell line specifically inhibiting H1.4 but no other H1 variants ("120"shRNA) (Figure R.37 and R.38). Moreover, we also obtained another cell line down-regulating the mRNA of most of the H1 variants (H1.2-H1.5) (Figure R.38).We referred to this shRNA as "225"shRNA. As shown in Figure R.37, although this shRNA is only 100% homologous to H1.4, but not for other H1s, most of them are down-regulated upon Doxycycline treatment. Even more interesting is the fact that, though most of H1s are affected at the level of mRNA, only H1.4 and H1.2 present reduced protein levels at day 6 of Dox treatment. Future analysis on this direction are needed to elucidate the relation between H1 expression and H1 protein levels in the cell, as several evidences suggest a complex post-transcriptional regulation for linker histones.

2. The new H1.4 knock-down ("120"sh) arrested cells in G1 and reduced the NRL, similarly to H1.2 KD

By inducible shRNA-mediated down-regulation, we have characterized a new H1.4 knock-down cell line ("120"sh). These cells presented a decreased proliferation rate compared with control cells, as cells were arrested in G1 phase of the cell cycle. Moreover, nucleosome spacing was also affected in these cells. MNase digestion of bulk chromatin from H1.4 knock-down revealed a decrease in the nucleosomal repeat length (NRL) compared with non Dox-treated or control cells. All these observations in the new H1.4 knock-down cells resemble the previously described phenotype observed for H1.2 knock-down cells [97]. Thus, after this work, we conclude that H1 variant depletion in T47D cells causes specific phenotypes for both H1.2 and H1.4 variants, while knock-down for other variants (H1.0, H1.3 and H1.5) does not cause similar effects. It is worth noting that most of cell types express both H1.2 and H1.4, while other subtypes are sometimes absent or in low amounts [217], pointing to a basal function of these two variants compared with others. Accordingly, bi-dimensional gel electrophoresis (Box R.1) and other data coming from gel electrophoresis and immunobloting (data not shown) estimates that H1.2 and H1.4 present similar relative proportions that other H1 variants in T47D (H1.0=9%, H1.2=23%, H1.3=13%, H1.4=24%, and H1.5=31%), discarding that phenotypes observed in H1.2 and H1.4 knock-down cells are consequence of a high prevalence of those variants compared with others. In summary, H1.2 and H1.4 are present in all cell types tested but are not necessarily the most abundant H1 types in all cells.

Although a similar phenotype is observed upon H1.2 and H1.4 knock-down, further analysis on these cells will determine if they control different processes. For instance, preliminary gene expression microarray analysis in the new H1.4 KD cells reveals, as previously reported for other H1 variants, that H1.4 controls the expression of different subsets of genes compared to H1.2 (data not shown). Thus, we still point to the idea that different H1 variants play distinct roles in specific functions. Furthermore, we also reported that inhibition of H1.2 and H1.4 affects differently the clonogenicity of T47D breast cancer cells (Figure R.42), suggesting different roles of these variants in tumor progression (see below). Finally, we have also shown a different genome-wide distribution of these variants in breast cancer cells (Results – Chapter I).

3. Effect of H1 depletion on nucleosome spacing

Regarding the effect of H1.2 and H1.4 in the nucleosomal repeat length (NRL), it is well know the importance of linker histone in determining nucleosome spacing. Several studies impairing H1 expression report a reduction in the NRL [96, 144, 145]. Although H1 is distributed all along the genome, it is not present at a 1:1 ratio respect to nucleosomes. Instead, histone H1/nucleosome ratio varies within cell types, cellular states, and even among different chromatin regions in the same cell. Thus, high H1/nucleosome ratios are related with longer NRL and more compacted chromatin, while low ratios cause short nucleosome spacing, characteristic of open-chromatin regions. In mouse ESCs, associated with open hyperdynamic chromatin, the H1/nucleosome ratio is around 0.5 and the NRL is decreased, while differentiated cells present higher rations, around 0.8, and the NRL is increased [96, 145, 146, 225]. In parallel, transcriptionally active genes present linker DNA about 40 bp shorter than repressed or noncoding sequences [92]. The linear relationship between H1 stoichiometry and NRL is explained in terms of maintaining an intranuclear electrostatic balance, taking into account that DNA phosphate backbone is negatively charged and H1 is enriched in positively charged aminoacids. Thus, if the amount of H1 per nucleosome is reduced, charge homeostasis tends to be restored by a reduction in nucleosome spacing, and the other way around [146]. Our results point to a different contribution of H1 variants in chromatin organization and functioning, as only depletion of H1.2 and H1.4 alters nucleosome spacing in breast cancer cells. According with our data, it has been recently published, based on H1 reconstitution experiments in *Xenopus* oocytes, that H1 subtypes differently affect nucleosome spacing *in vivo* [147]. In this report, H1.2 and H1.4 presented different behaviors, as H1.4 expression resulted in higher increase of the NRL compared with H1.2. However, coming back to the fact that H1 variant depletion had different outcomes in different cell

types, we claim that H1 variant contribution to chromatin structure could be also different among cell types or cellular states. Furthermore, we have previously shown that upon differentiation, relative amounts of H1 variants progressively change, increasing H1.0 expression and decreasing H1.3 and H1.5 [224]. Thus, a global increase of H1 together with a different composition on H1 subtypes may dictate different chromatin organization in pluripotent versus differentiated cells.

4. Phenotypic similarity between knock-down cells for H1.4 and lamin B2 ("444"sh) and multi-H1 KD ("225"sh)

Several approaches showed similar phenotypic effects between the knock-down cell line inhibiting H1.4 and lamin B2, as a consequence of an off-target effect ("444"sh), and the multi-H1 KD cell line ("225"sh), depleted of H1.2 and H1.4. Proliferation of both cell lines was drastically reduced, although only multi-H1 KD cell line was arrested in G1 (Figure R.35 and R39). Moreover, both of them presented an increase in dead cells upon 6 days of Dox treatment. Finally, analyses in the microscope revealed morphological alterations in these cells, together with an increased expression of P-cadherin (CDH3) (Figure R.41A-C and R.42A and B).

As specific knock-down of H1.4 ("120"sh) did not cause such phenotype (see above), we claim that in "444"shRNA cells, inhibition of lamin B2 may be the main responsible of all these alterations. Moreover, stable down-regulation of lamin B2 by different specific shRNAs also caused an increased cell mortality, proliferation defects, and over-expression of some cell-adhesion-related genes (Figure R.36). According to the death phenotype observed in these cells, lamin B1 and laminB2 have been identified as essential genes in HeLa cells [303], and apoptosis has been shown to be induced upon B-type lamin disassembly [304]. Apart with lamina proteins, a link between H1 and cellular progression and DNA damage has also been established. In fact, an appropriate content of H1 is essential for mouse development, as triple KO mice embryos died during gestation [145], and also for fly viability [183, 200]. Further studies on mouse triple KO cells also showed hyper-resistance to DNA damage [214]. Moreover, H1.2 has been found to participate in p53-dependent apoptosis in response to DNA damage in MCF7 cells [188, 305], and H1.5 depletion in IMR90 cells caused decreased cell growth, G1 arrest, and up-regulation of cell death and apoptotic-related genes [247]. The study on dH1 depletion in *D. melanogaster* also showed that dH1 knock-down caused DNA damage and genomic instability, marked by increased γH2Av detection, leading to strong reactivity of αcaspase-3 and apoptosis [183]. Altogether, it seems that histone H1 depletion

induces p53-dependent apoptosis in response to DNA damage. Thus, it has been proposed that both core and linker histones are dissociated from chromatin and accumulate in the cytoplasm to transmit apoptotic signaling in response to DNA damage [187]. Finally, loss of H1 has also been observed in cellular senescence, a tumor-suppressing mechanism, like apoptosis, that stably blocks the growth of stressed cells [306]. In conclusion, according to the literature, H1 and lamin B2 depletion could cause similar apoptotic outcomes. However, interestingly, many approaches failed to detect apoptotic events in our "444"sh KD and H1 KD cells (data not shown), probably due to the expression of a functionally defective p53 in these cells. However, we have been able to detect slightly increased γH2A.X staining in H1 knock-down cell lines compared with T47D control cells, mainly for multi-H1 knock-down cells (data not shown).

The nuclear lamina (NL) is a filamentous meshwork underneath the inner nuclear membrane (INM) and intranuclear structures. It is composed by two types of lamins: lamin A/C, found only in differentiated cells, and lamins B1 and B2, found in all cell types. It has been reported that the NL is in molecular contact with some genomic regions, participating in chromosome organization and transcriptional regulation [307]. In fact, cells lacking lamin B1 showed abnormal positioning of the chromosomes [308, 309], and cells with mutated lamin A presented reduced heterochromatin amount [310]. Lamin B1 has also been recently related with chromatin reorganization during senescence [311]. Hence, it is proposed that interactions between the NL and lamina-associated domains (LADs) help to organize chromosomes inside the nucleus. Although many chromatin proteins, including core histones H2A/H2B, have been reported to interact with lamins, the precise mechanism by which LADs are formed is still elusive [312, 313].

So, given that H1 could participate in the maintenance and establishment of lamina associated domains (LADs) (see Results – Chapter I and [249]), we hypothesize that H1 depletion could cause similar effects than lamin B2 depletion, if knocking-down H1 impairs the proper organization of the nuclear lamina. However, further analyses need to be done in order to prove deregulation of the nuclear lamina in multi-H1 KD cells. Nevertheless, Izzo et al. showed delocalization of lamins in H1.4 knock-down breast cancer MCF7 cells [249]. In conclusion, the interplay between H1 and the nuclear lamina could explain the similar phenotypes observed upon impairment of these proteins. A detailed observation in the microscope of the nuclear lamina structure will reveal possible differences between T47D WT and H1 knock-down cells. However, given that the nuclear membrane is reported to be probably disorganized in cancer, we should first determine the degree of organization of the nuclear lamina in our breast

cancer cell model, in comparison with a normal breast cell line. Despite of this, Izzo et al. showed lamina A/C staining in the nuclear periphery in wild-type MCF7 breast cancer cells.

5. P-cadherin over-expression in H1.4/laminB2 KD and multi-H1 KD cells

Knock-down cell lines for H1.4/laminB2 and H1.2/H1.4 presented other similarities besides of defects in proliferation and a death-like phenotype. A closer look into the confocal microscope of those cells that remained attached to the plate after 6 days of Dox treatment revealed a characteristic morphology. Z-reconstruction experiments showed that unlike control or individual H1 knock-down cells, that grew forming a typical monolayer of cells, those two knock-downs formed higher cellular clusters with cells imbricated among them (Figure R.41B and C). According to what it seems an increase in the cell-to-cell contacts, “444”sh KD cells showed over-expression of cell adhesion-related genes (Figure R.35C), and we also proved overexpression of P-cadherin (CDH3) in “444”sh KD and multi-H1 KD cells upon Dox treatment (Figure R.42A and B). Further functional experiments to prove an increased cell-to-cell adhesion are needed to corroborate these observations. Nonetheless, the observed phenotype could also fit with altered cell polarity in these knock-down cells. In fact, P-cadherin over-expression has been related with decreased cell polarity [314, 315].

Cadherins participate in the maintenance of cell polarity, differentiation, cell growth, and cell-cell adhesion in epithelial cells. In tumors, these proteins are usually altered. For instance, E-cadherin down-regulation is a characteristic feature of epithelial-to-mesenchymal transition (EMT). P-cadherin overexpression in breast cancer has been associated with poor patient prognosis and high histological grade tumors, and it is positively related with increased tumor cell motility and invasiveness. However, this invasive phenotype is dependent on the concomitant expression of E-cadherin [316, 317]. Only when E-cadherin is expressed, P-cadherin shows increased invasion function. It is proposed that, when over-expressed, P-cadherin interacts with E-cadherin and disrupts the interaction between E-cadherin and both p120ctn and βctn, promoting cancer cell invasion. On the other hand, P-cadherin is able to suppress invasion in the absence of E-cadherin by strong interaction with catenins, surrogating the role of E-cadherin in cell-cell adhesion. T47D cell line is both E- and P-cadherin-positive, although it is considered as a low invading luminal-like epithelial breast cancer cell line. On the other hand, basal A-like epithelial breast cancer cell lines, such as BT-20, present higher levels of P-cadherin and are considered to have higher invasion capacity than previous ones [315]. Thus, the overexpression of P-cadherin in our T47D knock-down cell lines may alter the balance between E- and P-cadherin, leading to altered properties regarding cell migration,

invasiveness, or cell motility. As results obtained until now are very preliminary, further experiments, such as wound healing migration or matrigel invasion assays, are needed to establish a relation between cadherin balance alteration and the tumorigenic capacity of these cells. Nevertheless, P-cadherin overexpression in MCF7 cells, with similar E- and P-cadherin expression levels as T47D cells, is associated with an increase in cell invasion, cell motility and cell migration, as well as with altered morphology [315]. Moreover, regarding the association of P-cadherin expression with different gene expression profiles in breast cancer, extended analysis of gene expression microarray data will show if our knock-down cells switch their luminal gene expression profile to a more basal-like phenotype.

The mechanisms by which lamin B2 and/or H1 would regulate P-cadherin expression should be also studied in the future, as direct or indirect effects after depleting these proteins could lead to CDH3 gene activation. P-cadherin expression has been shown to be negatively associated with ERα (estrogen receptor) signaling, and expression of CDH3 gene is regulated by chromatin remodeling events, including binding of several identified transcription factors (C/EBPβ, p63, BRCA1/c-Myc complex), and DNA methylation at the proximal CDH3 promoter [318-320]. However, by chromatin immunoprecipitation-qPCR, we have not been able to show enrichment of any of the H1 variants in CDH3 promoter regions reported to bind transcription factors (data not shown).

Finally, we cannot exclude the possibility that other altered genes upon H1 and/or lamin B2 knock-down are the responsible of different phenotypic outcomes in these cells. Both H1 and lamin B2 proteins participate in chromatin organization and transcriptional regulation, and their depletion affects the expression of a considerable amount of genes. In fact, soft-agar colony formation assays showed a different behavior of “444”sh and multi-H1 KD cells (Figure R.42C). These experiments revealed that upon H1.2 inhibition, breast cancer cells acquired a less tumorigenic phenotype, as both individual H1.2 and double H1.2/H1.4 knock-down lost the capability of forming colonies in soft agar. Interestingly, on the other hand, H1.4 inhibition alone or in combination with lamin B2 did not affect the properties of T47D regarding tumorogenicity. Further analyses such as matrigel invasion assay are needed in order to understand the phenotype of all knock-down cells.

In conclusion, an initial approach in studying the consequences of H1 and lamin B2 depletion in T47D breast cancer cells raised the possibility to consider these proteins as regulators of genes involved in cell adhesion, migration, invasion, and motility. Hence, under the context of a breast cancer event, their down-regulation could lead to the alteration of the tumorigenic

properties of a given breast cancer type. However, as previously considered, several functional assays should be performed in the future to understand in more detail the phenotype observed upon H1.4/lamin B2 and H1.2/H1.4 knock-down. Additionally, comparison of gene expression microarrays of the different knock-down cell lines will also help to further understand the behavior of these cells, and, hence, H1 function.

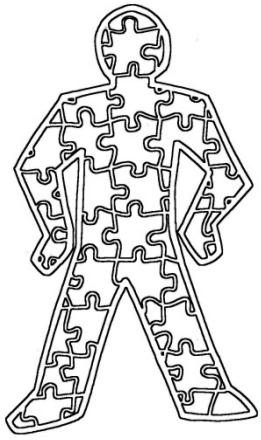

CONCLUSIONS

CHAPTER I: GENOMIC DISTRIBUTION OF HISTONE H1 SUBTYPES

1. Chromatin immunoprecipitation in T47D breast cancer cell lines expressing HA-tagged versions of somatic H1 variants, combined with ChIP on endogenous variants, are useful approaches to study H1 variant distribution in the genome.

2. H1 variants are depleted from the transcription start site (TSS) in active genes, forming an 'H1 valley', and coinciding with H3K4me3, nucleosome depletion, and an open chromatin state.

3. In immediate-early responsive genes, both the H1 valley and the nucleosome free region (NFR) are pre-formed before stimulation. Histone H1 is further depleted from the TSS upon activation by stimuli.

4. Depletion of H1 at promoters is clearly dependent on the transcriptional status of the gene and differs among variants. In T47D cells, H1.2 is depleted from the transcriptional start site (TSS) even in repressed genes, while other H1 variants are present at the TSS and show a local enrichment coinciding with nucleosome +1 downstream of the TSS.

5. H1 depletion at promoters extends further than the nucleosome free region (NFR) reported by H3 ChIP.

6. H1 prevalence at the transcription terminator site (TTS) is also variant-dependent. While most of H1s are depleted at this region, H1.2 is not. At coding regions, H1 abundance towards the 5' is also related with the transcriptional level, especially for H1.2.

7. H1.2 abundance at (distal) promoter of genes inversely correlates with gene expression, better than other H1 variants. Genes with high content of H1.2 are mainly repressed, while genes presenting low H1.2 levels tend to be activated. H1.2 abundance also correlates with clusters of differential gene expression along chromosomes, being enriched in transcriptionally inactive gene clusters or in gene-poor transcriptionally silent chromosomes.

8. H1.2 abundance at distal promoter negatively correlates with the presence of other H1 variants. This suggests that it may be enrichment of different variants for certain promoters, depending on the transcriptional state of such promoter, and maybe also on the H1 variant relative content of a cell type.

9. Genes specifically deregulated by knock-down of particular H1 variants are not enriched in such variant at the promoter.

10. Regulatory regions such as enhancers and insulators are depleted of H1. Additionally, H1.2 is depleted from regions over-represented in active histone marks, but present at regions containing repressive marks.

11. H1.2 and other H1 variants are differentially associated with CpG islands and GC content. All H1 variants, except H1.2, are enriched at GC-rich regions and CpG islands.

12. Genome-wide distribution of H1.2 is different than that of other H1 variants in T47D breast cancer cells. While H1.2 is enriched at intergenic regions and repressive chromatin domains such as lamina-associated domains (LADs), other H1 variants are more abundant at promoters and genic regions, and not enriched at LADs.

13. Regions of differential binding between variants exist. Genes differentially enriched in H1.0 versus H1.2 are related with developmental processes, and enriched in CpG islands.

CHAPTER II: FUNCTIONAL SPECIFICITY OF HISTONE H1 SUBTYPES

14. An off-target effect of the shRNA targeting H1.4 ("444"sh) affects lamin B2 expression.

15. A new H1.4 knock-down breast cancer cell line ("120"sh) presents defects in proliferation, arrest in the G1 phase of the cell cycle, and reduced nucleosomal repeat length (NRL), similarly to a previously reported H1.2 KD. These effects are magnified in a cell line inhibiting both H1.2 and H1.4 ("225"sh).

16. Combined depletion of H1.4/lamin B2 ("444"sh) and H1.2/H1.4 ("225"sh) cause a similar phenotype in T47D breast cancer cells. Increased cellular mortality, morphological alterations, and P-cadherin over-expression is observed in these cells.

17. H1.2 and H1.4 knock-down differently affect tumorogenicity of T47D cells. H1.2 depletion, but not H1.4, reduces the ability of T47D cells to grow in soft-agar colony formation assays.

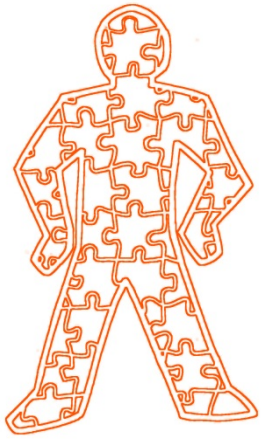

MATERIALS & METHODS

1. PLASMIDS

Several plasmids were used for the generation of T47D-MTVL derivative cells.

For the lentivirus vector-mediated drug-inducible RNA interference system we used pLVTHM (contains GFP) and ptTR-KRAB-Red (contains DsRed), both provided by Dr. Didier Trono (University of Geneva). We also used pVSVG (Clontech), which codifies for viral envelope proteins, and pCMVΔR8.91 (Dr. Trono), which codifies for viral *gag* and *pol* genes, both necessary for the production of viral particles in the case of lentiviral vectors.

The pGEMT (Invitrogen) and pCDNA$_4$-HA (courtesy of Dr. Reinberg) were used as intermediate vectors to clone somatic H1 variants upstream of the HA tag. Subsequently, the pEV833 lentiviral HIV-derived vector (courtesy of Dr. Eric Verdin) was used to generate stably HA-tagged H1 variants expressing cell lines.

pLKO.1 vector (Sigma) was used for generation of constitutive shRNA knock-down cells, after selection with puromycin.

A pEGFP-C1 vector containing laminB2 gene fused to EGFP (GFP-lmnB2) was kindly provided by Dr. Broers (University of Maastricht).

All plasmids were transformed into electrocompetent *E.coli* STBL2 bacteria and positive clones were selected by restriction analysis and sequencing. STBL2 strain, which grows at 30ºC, is used for the cloning and maintenance of unstable vectors as retroviral sequences. Non-viral plasmids were transformed in competent *E.coli* DH5α bacteria, growing at 37ºC.

2. OLIGONUCLEOTIDES

All used oligonucleotides for qPCR are listed below, indicating if they are designed to amplify genomic DNA sequences (“gDNA”) in ChIP experiments, complementary DNA (“cDNA”,with primers in different exons) in RT-PCR assays, or designed in the same exon of the coding region and useful to amply both genomic DNA and cDNA (“cDNA/gDNA”). Primers to amplify recombinant proteins cloned in a vector or sequences of the vector are indicated as “recDNA”.

GENE	REGION	NAME	SENSE	SEQUENCE FROM 5' TO 3'	USE
H1.0	gene	RT2 H1.0 fw	forward	CCTGCGGCCAAGCCCAAGCG	cDNA/gDNA
		RT2 H1.0 rv	reverse	AACTTGATCTGCGAGTCAGC	
H1.1	gene	H1.1_up	forward	CTCCTCTAAGGAGCGTGGTG	cDNA/gDNA
		H1.1_low	reverse	GAGGACGCCTTCTTGTTGAG	
H1.2	gene	H1.2 fw	forward	GGCTGGGGGTACGCCT	cDNA/gDNA
		H1.2 rv	reverse	TTAGGTTTGGTTCCGCCC	
H1.3	gene	H1.3RT1 fw	forward	CTGCTCCACTTGCTCCTACC	cDNA/gDNA
		H1.3RTm rev	reverse	GCAAGCGCTTTCTTAAGC	
H1.4	gene	H1.4RT(3) fw	forward	GTCGGGTTCCTTCAAACTCA	cDNA/gDNA
		H1.4RT(3) rv	reverse	CTTCTTCGCCTTCTTTGGG	
H1.5	gene	H1.5RT(3) fw	forward	CATTAAGCTGGGCCTCAAGA	cDNA/gDNA
		H1.5rt(3) rv	reverse	TCACTGCCTTTTTCGCCCC	
H1X	gene	H1x_up	forward	TTCCTTCAAGCTCAACCG	cDNA/gDNA
		H1x_low	reverse	TGCCTTCTTCGCTTTGTG	
GFP-LMNB2	EGFP LMNB2 gene	gfplamB2_RT up	forward	GGATCCACCGGATCTAGATAAA	recDNA
		gfplamB2_RT low	reverse	GTGGTCACCTCCTCCTTCTCT	
pEGFP-C1	kanR	kanR up	forward	AGACAATCGGCTGCTCTGAT	recDNA
		kanR low	reverse	AGTGACAACGTCGAGCACAG	
H1.4-HA	pLVTHM H1.4 gene	H1.4pEV833 up	forward	TCATTTCAGGTGTCGTGAGG	recDNA
		H1.4pEV833 low	reverse	AGGCGGCAACAGCTTTAGTA	
pLVTHM	Nuf1 EV997	8 up	forward	AGTAGTGTGTGCCCGTCTGT	recDNA
		9 low	reverse	TCGCTTTCAGGTCCCTGTTCG	
LMNB2	gene	lamB2_RT2_up	forward	ATCAAGGCGCTGTACGAGTC	cDNA
		lamB2_RT2_low	reverse	CCCTCAGCTTCCCAATCTCT	
CLDN4	gene	cldn4 S	forward	GGCTGCTTTGCTGCAACTGTC	cDNA
		cldn4 AS	reverse	GAGCCGTGGCACCTTACACG	
CLDN3	gene	cldn3 S	forward	CTGCTCTGCTGCTCGTGTCC	cDNA
		cldn3 AS	reverse	TTAGACGTAGTCCTTGCGGTCGTAG	
CDH3	gene	cdh3 S	forward	AACCTCCACAGCCACCATAG	cDNA
		cdh3 AS	reverse	GTCTCTCAGGATGCGGTAGC	
PVRL1	gene	pvrl1 S	forward	GGAAAGCCTCACTCTCAACG	cDNA
		pvrl1 AS	reverse	TGATGGGTCCCTTGAAGAAG	
PVR	gene	pvr S	forward	GCACCTGATTCTCACAGCAA	cDNA
		pvr AS	reverse	GAGCCAGACCCTGTCTCAAG	
YY1	promoter	YY1 prom up	forward	AGGGAAACAATGGCTGACTG	gDNA
		YY1 prom low	reverse	TGGGAGGATGTCCGTTATTC	
	gene	YY1 gene up	forward	GGAGGAATACCTGGCATTGA	cDNA/gDNA
		YY1 gene low	reverse	TTCTGCACAGACGTGGACTC	
CXCL12	gene	cxcl12 up	forward	TGAGAGCTCGCTTTGAGTGA	cDNA/gDNA
		cxcl12 low	reverse	CACCAGGACCTTCTGTGGAT	
PCAF	gene	pcaf up	forward	ACATCTGCCATTCCCAACTC	cDNA/gDNA
		pcaf low	reverse	TAGCCATTTGCAGGGTTCTT	
GAPDH	gene	gapdh fw	forward	GAGTCAACGGATTTTGGTCGT	cDNA
		gapdh rv	reverse	TTGATTTTGGAGGGATCTCG	
	gene	gapdh_same ex fw	forward	ACCCAGAAGACTGTGGATGG	cDNA/gDNA
		gapdh_same ex rv	reverse	TTCAGCTCAGGGATGACCTT	
β-ACTIN	promoter	ACT2 ChIP - F	forward	GCTGTTCCAGGCTCTGTTCC	gDNA
		ACT2 ChIP - R	reverse	GCTCACACGCCACAACATG	
nucB-MMTV	nucB nucB	NucB up	forward	GGGCTTAAGTAAGTTTTTGGTTACA	gDNA
		NucB V low	reverse	GCAAGTTTACTCAAAAAATCAGCACTCTT	
CCND1	promoter	ccnd1 -50 up	forward	CGGGCTTTGATCTTTGCTTA	gDNA
		ccnd1 -50 low	reverse	ACTCCCCTGTAGTCCGTGTG	
11β-HSD2	promoter A	11β up (-1778)	forward	GGGGTGCTGTGTCTGCCTCCAAG	gDNA
		11β low (-1596)	reverse	GCCATGACCCTGTGTGTGCAAGT	
ALF REP	repeats	α1	forward	AGACAGAAGCATTCTSAGAA	gDNA
		α4	reverse	ATCACAAAGNAGTTTCTSAGAAT	
SAT2	repeats	hsSat2 repeat F1	forward	ATCGAATGGAAATGAAAGGAGTCA	gDNA
		hsSat2 repeat R1	reverse	GACCATTGGATGATTGCAGTCA	
SATa	repeats	hsSat alpha F1	forward	AAGGTCAATGGCAGAAAAGAA	gDNA
		hsSat alpha R1	reverse	CAACGAAGGCCACAAGATGTC	
NANOG	distal promoter -2KB	nanog prom dist F	forward	GACAGGGTTTCACCATGTTGGT	gDNA
		nanog prom dist R	reverse	CCGAGCCAGGTGCATCAT	
	TSS -160bp	nanog prom prox F	forward	CGGTTTTCTAGTTCCCCACCTA	gDNA
		nanog prom prox R	reverse	CCAAGGCCATTGTAATGCAA	
	gene	nanog_RT_same ex up	forward	CAAAGGCAAACAACCCACTT	cDNA/gDNA
		nanog_RT_same ex low	reverse	TCTGCTGGAGGCTGAGGTAT	

OCT4	distal promoter -2.5KB	oct4 prom dist F	forward	CTTGGCAGACAGCAGAGAGATG	gDNA
		oct4 prom dist R	reverse	ATCTCAATCCCCAGGACAGAAC	
	TSS -150bp	oct4 prom prox F	forward	CAGTTGTGTCTCCCGGTTTTC	gDNA
		oct4 prom prox R	reverse	CGAAGGATGTTTGCCTAATGG	
	gene	oct4_RT_same ex up	forward	GCAAAGCAGAAACCCTCGT	cDNA/gDNA
		oct4_RT_same ex low	reverse	GGCTGATCTGCTGCAGTGT	
ITPR1	promoter -10KB	itpr1 upstr fw	forward	GTGCCACTCTTTTGCTTCAA	gDNA
		itpr1 upstr rev	reverse	GAGGCACCAACGTTAAAAAGA	
	TSS	itpr1 tss fw	forward	ACTGAGGTCGCGGTTTGTAT	gDNA
		itpr1 tss rev	reverse	AAGGAGCCGTGTTGTGACTT	
	gene	itpr1_RT up	forward	TGAGGCTGTTTCATGCTGAG	cDNA/gDNA
		itpr1_RT low	reverse	ACAGGGCTTTTGAACTGGTG	
STC1	promoter -10KB	stc1 upstr fw	forward	TTGTCAGCAGCAGAGAGAGC	gDNA
		stc1 upstr rev	reverse	CCTGATGAAGCAGCTTAGGG	
	TSS	stc1 tss fw	forward	AAGCCTGCATTGACACCTCT	gDNA
		stc1 tss rev	reverse	TGCTGACAGTTGGAGGACAG	
PSMB4	promoter -10KB	psmb4 dist fw	forward	CACCACGCCGACTAATTTTT	gDNA
		psmb4 dist rev	reverse	ACGAGGTCAGGAGATCGAGA	
	TSS	psmb4 prox fw	forward	CTCCCTCCTCCTTGAATCGT	gDNA
		psmb4 prox rev	reverse	GACCGAGACAGGGAGTTGAA	
	gene	psmb4_RT up	forward	GAGCTTCTGGGAGATGGACA	cDNA/gDNA
		psmb4_RT low	reverse	GATGACCATGGTGTTCCACA	
ABHD2	promoter -10KB	abhd2 upstr fw	forward	TGACTCCAAATCCCCTTGTC	gDNA
		abhd2 upstr rev	reverse	CATTGGTAAGCAGGGGAGAG	
	TSS	abhd2 tss fw	forward	GCCTCCACTCTGAGGAACAG	gDNA
		abhd2 tss rev	reverse	TTGTTCATTGGGCAGTTCAG	
	gene	abhd2_RT up	forward	TGTATGGGAAGATGGGAAGG	cDNA/gDNA
		abhd2_RT low	reverse	CAACACAGTGCTCAGCCAAG	
PTBP2	promoter -10KB	ptbp2 upstr fw	forward	TGGCTAGACCACTACAATCTCAA	gDNA
		ptbp2 upstr rev	reverse	TGCTCAATTTTCCATAACATCAAA	
	TSS	ptbp2 tss fw	forward	CAATGGCAGAAACAAGAGCA	gDNA
		ptbp2 tss rev	reverse	CACTCAGCATTCCGTCTTGA	
	gene	ptbp2_RT up	forward	GATGGTGCTCCTTCTCGTGT	cDNA/gDNA
		ptbp2_RT low	reverse	TCAGCATAAGGATGTTGGTCA	
JUN	promoter -10KB	jun upstr up	forward	CCTTTTTGTCCCTCCAAACA	gDNA
		jun upstr low	reverse	TCTAGGAACTGAGCCCTCCA	
	TSS	jun tss up	forward	GGGTGACATCATGGGCTATT	gDNA
		jun tss low	reverse	GCCCGAGCTCAACACTTATC	
	gene	jun_RT_same ex up	forward	CAGGTGGCACAGCTTAAACA	cDNA/gDNA
		jun_RT_same ex low	reverse	TTTTTCTCTCCGTCGCAACT	
FOS	promoter -10KB	fos upstr up	forward	TTGTTTGGTGAAACCGTTGA	gDNA
		fos upstr low	reverse	TGAAATAGGCTGGGGAAATG	
	TSS	fos tss up	forward	GAGCCCGTGACGTTTACACT	gDNA
		fos tss low	reverse	CAGATGCGGTTGGAGTACG	
	gene	fos_RT_same ex up	forward	AACTTCATTCCCACGGTCAC	cDNA/gDNA
		fos_RT_same ex low	reverse	GGCCTCCTGTCATGGTCTT	
MYC	promoter -10KB	myc upstr up	forward	GCATTTGCTTTTCGGTCAAT	gDNA
		myc upstr low	reverse	CTTGCTTCGGTTCCATCAAT	
	TSS	myc tss up	forward	TAGGCGCGCGTAGTTAATTC	gDNA
		myc tss low	reverse	CAGCCGAGCACTCTAGCTCT	
	gene	myc_RT_same ex up	forward	TCAGAGAAGCTGGCCTCCTA	cDNA/gDNA
		myc_RT_same ex low	reverse	CTGTCGTTGAGAGGGTAGGG	
CDK2	promoter -3KB	3kb cdk2 prom fw	forward	CAGCGAGGAAAGTCACATCA	gDNA
		3kb cdk2 prom rev	reverse	TGGGGTGAGGGTAGTTTCTG	
	TSS	cdk2 prom fw	forward	GCGGCAACATTGTTTCAAGT	gDNA
		cdk2 prom rv	reverse	GTCGGGATGGAACGCAGTAT	
	gene	cdk2_RT up	forward	CCAAAAGGTGGAAAAGATCG	cDNA/gDNA
		cdk2_RT low	reverse	CACCTCTCCCGTCAACTTGT	
COX7C	promoter -3KB	COX7C_A fw	forward	AGAAGCTGCAAGGCTTTTGA	gDNA
		COX7C_A rv	reverse	CCTTAGTGACCGGATTGACC	
	promoter -300/-100KB	COX7C_B fw	forward	CCCCAGGAATCCTAGACCTAA	gDNA
		COX7C_B rv	reverse	CGAAGGATTGTGGGAAATGT	
	promoter -100/+100KB	COX7C_C fw	forward	CCCCATTTCCCATCTTTCTT	gDNA
		COX7C_C rv	reverse	GCACCTCACCAAGACCTTTT	
	promoter +100/+300KB	COX7C_D fw	forward	CCGTAGGAGCCACTATGAGG	gDNA
		COX7C_D rv	reverse	AGCCTGGTTTCTGGCTATCA	
RPS19	promoter -3KB	RPS19_A fw	forward	GGATGGTCTCCATCTCCTGA	gDNA
		RPS19_A rv	reverse	CGGTGAAACCCCCTCTCTAC	

	promoter -300/-100KB	RPS19_B fw RPS19_B rv	forward reverse	GAAGGACGGAAGATGATAGCC GACAGGGAACCTAGGGGAAG	gDNA
	promoter -100/+100KB	RPS19_C fw RPS19_C rv	forward reverse	TCTCCACCACTGTTCCTTCC GGGAACTTGGCTTCGTTTG	gDNA
	promoter +100/+300KB	RPS19_D fw RPS19_D rv	forward reverse	TACACTCCGGGAGAAGGAAA GGTGTCTAGTGAGGGGTGGA	gDNA
GHITM	promoter -3KB	GHITM_A fw GHITM_A rv	forward reverse	ACCCAAGCAGAGTCAAATGG TTGTTTGCACCCTTCGAGAT	gDNA
	promoter -300/-100KB	GHITM_B fw GHITM_B rv	forward reverse	TTCTTATAGCTGCGGCGAGT ATCTTTGTTTTGGGCAGTGG	gDNA
	promoter -100/+100KB	GHITM_C fw GHITM_C rv	forward reverse	CCCTGCAACAATCCTCAACT GCAACATCGAAAGGACGTAAA	gDNA
	promoter +100/+300KB	GHITM_D fw GHITM_D rv	forward reverse	AGGTGCTGAGTCATCCTTGC CTTCCCTGTCAACCCACAAC	gDNA
ZAP70	promoter -3KB	ZAP 70_A fw ZAP 70_A rv	forward reverse	GTGGATCACGAGGTCAGGAG GACGGAGTTTCACCGTTAGC	gDNA
	promoter -100/+100KB	ZAP 70_C fw ZAP 70_C rv	forward reverse	GCCTGTGATTTTCCTTGAGC CCTATTTCCTGGATGCGAAG	gDNA
PCDHGC4	promoter -3KB	PCDHGC4_A fw PCDHGC4_A rv	forward reverse	GTTGCAGTGAGCCAAGATCA TGCCAGCCATATGATTCTCC	gDNA
	promoter -100/+100KB	PCDHGC4_C fw PCDHGC4_C rv	forward reverse	GGGGAAAGGGAGATAGGTGT ATCTGCCCACAAACGTAACC	gDNA
PSCA	promoter -3KB	PSCA_A up PSCA_A low	forward reverse	CCCTGAGCTGGAATAAGCAG TTCTCACGTGGGTGACTCTG	gDNA
	promoter -300/-100KB	PSCA_B up PSCA_B low	forward reverse	GGTCTTGAGGACGTTTCAGC CTACCCAGGGCCATATCTCA	gDNA
	promoter -100/+100KB	PSCA_C up PSCA_C low	forward reverse	CCCCATTTGAGGCCATATAA ACAGCCTTCGTGGTCACTG	gDNA
	promoter +100/+300KB	PSCA_D up PSCA_D low	forward reverse	GAAGGAGGAAGGGAGAGGAA CAAGAGCTTCCCTGGAGGA	gDNA
GRM7	promoter -3KB	GRM7_A fw GRM7_A rv	forward reverse	GAAACATGGTCCCGGATAAA TGAGGGTAAGGGCTGGGTAT	gDNA
	promoter -300/-100KB	GRM7_B fw GRM7_B rv	forward reverse	AAGGGTGGGGAGAGAAGGA GAGAGGGCAGGGACTGCTAT	gDNA
	promoter -100/+100KB	GRM7_C fw GRM7_C rv	forward reverse	ATAGCAGTCCCTGCCCTCTC CTGCTCGCTCTCTCCAACA	gDNA
	promoter +100/+300KB	GRM7_D fw GRM7_D rv	forward reverse	ATGGTCCAGCTGAGGAAGC GCAGGGGAACTTCATCAAAG	gDNA
TMEM204	promoter -3KB	TMEM204_DistP fw TMEM204_DistP rv	forward reverse	GAGGCACTGGAACAAGAAGC AGCTTCTGCAGGACCTTTGA	gDNA
TUBGCP5	promoter -3KB	TUBGCP5_DistP fw TUBGCP5_DistP rv	forward reverse	TCGCCAGGTGACATTTTG TCCTGGTGGGCCATCATA	gDNA
COL4A3	promoter -3KB	COL4A3_DistP fw COL4A3_DistP rv	forward reverse	TTGGTGAATGTGGGATCTGA CTAAAATGGCTGGAGGCAAG	gDNA
CUGBP2	promoter -3KB	CUGBP2_DistP fw CUGBP2_DistP rv	forward reverse	GCCTTTTGTTTGGGAAATGA AGCTGCATTGTGGAAAAACC	gDNA

3. ANTIBODIES

Polyclonal antibodies specifically recognizing human H1 variants, including those generated in our laboratory [97], and other used antibodies are:

ANTIBODY	HOST	COMPANY	REFERENCE
anti-H1.0	Mouse	Abcam	ab11079
anti-H1.2 (ChIP-grade)	Rabbit	Abcam	ab4086
anti-H1.2	Rabbit	Abcam	ab17677
anti-H1.3	Rabbit	Abcam	ab17679
anti-H1 phospho-T146	Rabbit	Abcam	ab3596
anti-H1.5	Rabbit	Abcam	ab18208
anti-H1X	Rabbit	Abcam	ab31972
anti-H3	Rabbit	Abcam	ab1791
anti-HA tag	Rabbit	Abcam	ab9110
anti-H3K4me3	Rabbit	Abcam	ab8580
anti-total H1 (clone AE-4)	Mouse	Millipore	05-457
anti-GFP	Mouse	Sigma	G6539
anti-Tubulin	Mouse	Sigma	T4026
anti-P-cadherin	Mouse	BD Biosciences	610227

4. CELL LINES AND CULTURING CONDITIONS

Breast cancer **T47D-MTVL** cells (carrying one stably integrated copy of luciferase reporter gene driven by the MMTV promoter), or derivative cells stably expressing hemagglutinin (HA)-tagged H1 variants (H1-HA) or inducible shRNAs against H1 variants, were grown at 37ºC with 5% CO_2 in RPMI 1640 medium, supplemented with 10% FBS, 2mM L-glutamine, 100 U/ml penicillin, and 100 µg/ml streptomycin, as described previously [97].

HeLa or HeLa H1 knock-down cell lines, derived from human cervix carcinoma, were grown at 37ºC with 5% CO_2 in DMEM-GlutaMax medium containing 10% FBS and 1% penicillin/streptomycin.

MCF7 or MCF7 H1 knock-down cell lines, derived from human mammary carcinoma, were grown at 37ºC with 5% CO_2 in MEM medium containing 10% FBS, 1% penicillin/streptomycin, 1% non-essential amino acids, and 1% sodium pyruvate and 1% glutamine.

HEK 293T or 293T H1 knock-down cell lines, derived from human embryonic kidney, were grown at 37ºC with 5% CO_2 in DMEM-GlutaMax media containing 10% FBS, and 1% penicillin/streptomycin.

GP2.293 packaging cell line, drived from HEK 293 cell line, was grown at 37ºC and 5% CO_2 in DMEM-GlutaMax media containing 10% FBS, 1% penicillin/streptomycin, and 2% glutamine.

5. TREATMENTS

For H1 knock-down cell lines, **doxycycline** (Sigma) was added at 2.5 µg/ml when indicated. Along a 6-day treatment with Dox, cells were passaged at day 3.

For **hormone treatment** experiments with R5020 (PerkinElmer Life Sciences), cells were plated in phenol red-free medium supplemented with 10% dextran-coated charcoal-treated FBS and, 24 hours later, the medium was replaced by fresh serum-free medium. After 24 hours under serum-free conditions, cells were treated with R5020 (10 nM) for different times at 37ºC.

For **PMA experiments**, serum-containing RPMI 1640 media was replaced by serum-free media. After 24 hours under serum-free conditions, cells were treated with PMA (100 nM) for the indicated time at 37ºC.

6. shRNA CLONING, VIRUS PRODUCTION, AND CELL INFECTIONS

For **constitutive knock-down** cell lines, specific laminB2 shRNAs cloned in pLKO.1 vector were purchased from Sigma. GP2.293 packaging cell line, already expressing the viral *gag* and *pol* genes, was used for the production of viral particles. $2.5x10^6$ cells were seeded in 100 mm plates the day before transfection. To produce infectious particles, we co-transfected GP2-293 with the pLKO.1-shRNA vector (10 µg) and pVSVG plasmid (5µg), expressing the VsVg envelope protein, using calcium phosphate. Medium was collected every 24 hours for 2 days and ultracentrifuged for 1 h 30 min at 26,000 rpm and 4ºC in a sucrose gradient, to concentrate viral particles. Pellet containing the viruses was dissolved in medium and used for the infection. Cells were infected using the spinoculation system, with centrifugation at 1,200 rpm for 2 hours at RT. Cells infected with shRNA-expressing pLKO.1 vector were selected with 2 mg/ml puromycin (Sigma) 24 hours after infection.

For the **inducible knock-down** system, the 64-mer oligonucleotides for H1 variant shRNA cloned into pLVTHM plasmid through MluI and ClaI digestion were designed, annealed, and phosphorylated as communicated by Dr. Tron (http://tronolab.epfl.ch/). 19-mer gene target sequences for H1 genes were designed manually following standard rules (AAN19, GC% 30-70) to the most divergent region of H1.4 to get specific targeting, and to a common region for several H1 variants for the multi-H1 shRNA.

Inducible H1 variant knock-down T47D-MTVL cell lines were produced as described previously [97]. For the production of viral particles, $2.5x10^6$ HEK 293T cells were transfected with plasmids ptTR-KRAB-Red or pLVTHM-shH1.n (10 µg), and pCMVΔR8.91 (15 µg) and pVSVG (5 µg) in 100 mm plates using calcium phosphate. Medium was collected every 24 hours for 2 days and ultracentrifuged for 1 h 30 min at 26,000 rpm and 4ºC in a sucrose gradient, to concentrate viral particles. Pellet containing the viruses was dissolved in medium and used for the infection. Cells were infected using the spinoculation system, with centrifugation at 1,200 rpm for 2 hours at RT. Initially, a cell line expressing the Dox-responsive KRAB repressor and RedFP (ptTR-KRAB-Red) was generated. Then, this cell line was infected with viruses for expression of the different shRNAs (pLVTHM). The inducible knocked-down cell lines were sorted in a FACSvantageSE (Becton Dickinson) or MoFlo high-speed sorter (DakoCytomation, Fort Collins, Colorado, USA) for RedFP-positive and GFP-positive fluorescence after 3 days of Dox treatment. Then, cells were amplified in the absence of Dox until an experiment was performed.

shRNA	TARGET GENE	VECTOR	TARGET SEQUENCE
LMNB2_A	LMNB2	pLKO.1	CGGCAGTTCTTTGTTAAAGAT
LMNB2_B	LMNB2	pLKO.1	GCTCAAGAACAACTCGGACAA
LMNB2_C	LMNB2	pLKO.1	GCAGGAGTACGACTTCAAGAT
LMNB2_D	LMNB2	pLKO.1	GCAGCAGGAGTACGACTTCAA
LMNB2_E	LMNB2	pLKO.1	CTACAAGTTCACGCCCAAGTA
RANDOM	None	pLVTHM	ACGTAGGCTAAGAGAAGCA
120sh	H1.4	pLVTHM	GTCCGAGCTCATTACTAAA
225sh	Multi-H1	pLVTHM	GAACAACAGCCGCATCAAG
444sh	H1.4&LMNB2	pLVTHM	GAAGAGCGCCAAGAAGACC
156sh	H1.2	pLVTHM	AGAGCGTAGCGGAGTTTCT
87sh	H1X	pLVTHM	CAACGGTTCCTTCAAGCTCAA

7. STABLE EXPRESSION OF HA-TAGGED H1 VARIANTS

Generation of T47D-MTVL stably expressing HA-Tagged H1 variants was achieved as described previously [97]. Briefly, human histone H1 variants were PCR-amplified from genomic DNA and cloned into pCDNA4-HA vector provided by D. Reinberg's group (NYU Medical School). The complete H1-HA cassette was cloned into the lentiviral expression vector pEV833.GFP provided by E. Verdin (Gladstone Institute) upstream an IRES-GFP cassette. Viruses were then produced and cells were infected with pEV833-derived lentivirus. HA-tagged H1 variants-expressing cell lines were selected by sorting in a FACSvantageSE (Becton Dickinson) or in a

MoFlo high-speed sorter (DakoCytomation, Fort Collins, Colorado, USA), for GFP-positive fluorescence.

8. PROTEIN EXTRACTS

8.1. H1 extraction

Histone H1 was purified by 5% perchloric acid lysis for 1 hour at 4ºC. Soluble acid proteins were precipitated with 30% trichloroacetic acid overnight at 4ºC, washed twice with 0.5 ml of acetone and reconstituted in water. Protein concentration was determined by Micro BCA protein assay (Pierce).

8.2. Total histone extraction

Total histones were purified by 0.6N HCl lysis for 1 hour at 4ºC. Soluble histones were then precipitated adding acetone an incubating overnight at -20ºC. Histones were pelleted at maximum speed at 4ºC and reconstituted in water. Protein concentration was determined by Micro BCA protein assay (Pierce).

8.3. Whole cell extract

Cells were washed twice with cold PBS 1X, scraped with *Lysis Buffer* and boiled 5 min to 95ºC. Cell lysates were obtained by centrifugation and the protein concentration was determined by Micro BCD protein assay (Pierce). *Lysis Buffer*: 25mM Tris-HCl pH7.5, 1% SDS, 1mM EDTA pH8.0, 1mM EGTA pH8.0, 20 mM β-glycerolphosphate, 2 mM ortovanadate and 2mM PMSF.

9. GEL ELECTROPHORESIS AND IMMUNOBLOTTING

Extracts or purified proteins were subjected to 12% SDS-PAGE, transferred to a PVDF membrane, blocked with Odissey blocking buffer (LI-COR Biosciences) for 1 hour, incubated with primary antibodies overnight at 4ºC and with secondary antibodies conjugated to fluorescence (IRDye 680 goat anti-rabbit IgG and IRDye 800CW goat anti-mouse IgG, LI-COR) for 1 hour at room temperature. Bands were visualized with the Odissey Infrared Imaging System.

10. TWO-DIMENSIONAL GEL ELECTROPHORESIS

H1 extracts were first subjected to acetic acid–urea (AU) polyacrylamide gel electrophoresis (AU-PAGE) (0.0105 gr thio-urea, 15% acrylamide, 0.1% bisacrylamide, 5% acetic acid, and 2.5M urea). Next, the gel region containing H1 proteins was cut and equilibrated in *O'Farrell's buffer* (10% glycerol, 2.3% SDS and 62.5mM Tris-HCl pH6.8) 30 minutes at RT before a second run in

15% SDS-PAGE. Finally, gels were stained with 0.2% (w/v) Coomassie blue for 1 h in 25% (v/v) isopropanol and 10% (v/v) acetic acid, and destained overnight in 10% (v/v) isopropanol and 10% (v/v) acetic acid. Western blot experiments with those gels were done as described above.

11. MNase DIGESTION

Four millions of cells growing in rich medium and treated of not with Dox during 6 days were pelleted, washed with PBS 1X, and resuspended in *BufferA* (10mM Tris-HCl pH7.4, 10mM NaCl, 3mM $MgCl_2$, 0.3M sucrose and 0.2mM PMSF) plus 0.2% of NP40 and incubated for 10 min at 4ºC. Cells were then centrifuged and the nuclei pellet was dissolved in *BufferA* plus 10 mM $CaCl_2$. MNase (Sigma) digestion was performed at different concentrations in a digestion curve for 25 min at room temperature. Samples were treated with RNaseA and Proteinase K and DNA was then purified through a Qiagen column.

12. IMMUNOFLUORESCENCE

Cells treated or not with Dox in rich medium were seeded onto coverslips. After 6 days in Dox, cells were washed with PBS 1X and fixed by incubation in 4% paraformaldehyde in PBS 1X for 15 minutes at room temperature. Next, they were permeabilized by incubation in 0.2% Triton X-100 in PBS 1X for 10 minutes at room temperature. After rinsing three times for 5 minutes in PBS 1X, the coverslips were incubated for 1 hour with 3% BSA in PBS at RT to reduce non-specific staining. Cells were incubated with fluorescent Phalloidin (Sigma) for 1 hour. Then, coverslips were whased with in PBS 1X and mounted on slides with VectaShield – DAPI mounting medium (Vector laboratories). Samples were visualized in a Spinning Disk Confocal Microscope (PerkinElmer Ultraview ERS).

13. TIME LAPSE EXPERIMENTS

After 3 days of Dox treatment, T47D inducible knock-down cells were plated into 35 mm Glass Bottom Microwell Dishes (MatTek) and placed in a Spinning Disk Confocal Microscope (PerkinElmer Ultraview ERS) or a Leica TCS-SP5 Confocal Microscope, with the culture chamber at 37ºC and 5% CO_2. Cellular growth was followed until day 6 of Dox treatment monitoring GFP and RedFP self-fluorescence every 10 minutes. Images were analyzed with Volocity (Perkin Elmer) or Leica LAS AF software.

14. Z-STACK RECONSTRUCTION EXPERIMENTS

After 6 days of Dox treatment, T47D inducible knock-down cells plated into 35 mm Glass Bottom Microwell Dishes (MatTek) were visualized *in vivo* in a Spinning Disk Confocal Microscope (PerkinElmer Ultraview ERS), and cells were monitored by GFP and RedFP self-fluorescence. Measurements were performed with Volocity (Perkin Elmer) software.

15. PROLIFERATION ASSAYS

T47D-derived GFP-positive (H1-HAs expressing cells) or double RedFP/GFP-positive cells (inducible shRNA-expressing cells) were mixed 1:1 with parental T47D cells (RedFP and GFP-negative) and seeded together in a plate. Cells were split every two or three days and the percentage of GFP and RedFP-positive cells was measured by FACS in a Cytomics FC500 MPL flow cytometer (Beckman Coulter, Inc, Fullerton, CA).

16. CELL CYCLE ANALYSIS

After cells were recovered and washed with cold PBS 1X, they were fixed in 70% ethanol overnight at -20ºC. Then, cells were washed twice with PBS 1X to get rid of the ethanol and resuspended in PBS 1X. Next, they were treated with RNaseA at 1 mg/ml for 1 hour at 37ºC, and, finally, propidium iodide (PI) was added to the cells and incubated at 4ºC 4 hours or overnight. Samples were analyzed using an Epics XL flow cytometer (Coulter Corporation, Hialeah, Florida). DNA analysis (Ploidy analysis) on single fluorescence histograms was done using Multicycle software (Phoenix Flow Systems, San Diego, CA).

17. SOFT-AGAR COLONY FORMATION ASSAYS

T47D inducible knock-down cells were plated in agar after 3 days of Dox treatment. Melted agar (0.6%) in complete medium was placed at the bottom of 12-well plates, allowed to solidify and overlayed with $9X10^3$ cells resuspended in 0.4% agar/complete medium with or without Dox. After 4 weeks replacing the media every two or three days (with or w/o Dox), wells were fixed with glutaraldheide 0.5% in PBS 1X and stained with 0.025% crystal violet to visualize the colonies.

18. TRANSIENT TRANSFECTIONS

24 hours before transfection, HEK 293T cells were seeded at a density of $2x10^5$ cells in a 6-well plate in DMEM medium. Transfection was using calcium phosphate-DNA mix, prepared with 5µg of DNA into 168 µl of 250mM $CaCl_2$. This mix was added to an equal volume of 2X HBS

solution and incubated for 30 minutes at room temperature. Then, the suspension was added to the plates, and, at least six hours later, the medium was replaced by fresh medium. Extracts were prepared 48 hours after transfection.

19. RNA EXTRACTION AND RT-PCR

Total RNA was extracted using High Pure RNA isolation kit (Roche) according to the manufacturer's instructions. cDNA was obtained from 100 ng of total RNA using SuperScript VILO cDNA synthesis (Invitrogen). Gene products were analyzed by qPCR using EXPRESS SYBR GreenER qPCR SuperMix Universal (Invitrogen) and specific oligonucleotides in a Roche 480 Lightcycler. Each value was corrected by human GAPDH and expressed as relative units.

20. FORMALDEHYDE-ASSISTED ISOLATION OF REGULATORY ELEMENTS (FAIRE) ASSAYS

Cells were fixed using 1% formaldehyde, harvested and sonicated using a Diagenode Bioruptor to generate chromatin fragments between 200 and 500 bp, similar than in ChIP experiments (see below). FAIRE (Formaldehyde-Assisted Isolation of Regulatory Elements) assays were performed as described in [321]. To prepare input DNA an aliquot of chromatin was taken and treated with RNAaseA, de-crosslinked overnight at 65ºC, purified by phenol/chloroform extraction, and run on a gel to ensure average fragment sizes of 200-500 bp. FAIRE DNA was prepared processing chromatin twice with phenol/chloroform extraction to purify DNA not bound by nucleosome in the water phase. The samples were later treated with RNaseA, de-crosslinked by overnight incubation at 65ºC, and purified by GenElute PCR Clean-Up Kit (Sigma). Real-time PCR was performed on FAIRE and input DNA using EXPRESS SYBR GreenER qPCR SuperMix Universal from Invitrogen and specific oligonucleotides in a Roche 480 Lightcycler.

21. ChIP ASSAYS

Chromatin immunoprecipitation (ChIP) assays were performed as described previously [322]. Exponentially growing cells or arrested cells without serum were fixed by adding *Crosslinking solution*, containing formaldehyde, directly to culture medium to final concentration of 1% formaldehyde, and incubating for 10 minutes at 37ºC. The crosslinking reaction was stopped by adding Glycine to a final concentration of 0.1M and incubating for 5 min at RT. The medium was then removed and cells were washed twice with cold PBS 1X. Cells were scrapped in PBS 1X-containing protease and phosphatase inhibitors, and pelleted for 5 min at 4,000 rpm at 4ºC. Later, cell pellets were resuspended in 5 ml of *Lysis Buffer I* containing inhibitors and incubated for 10 min on ice. After lysis, cells were pelleted for 5 min at 4,000 rpm at 4ºC and then

resuspended in 1 ml of nuclei *Lysis Buffer II.* Lysates were then sonicated using a Diagenode Bioruptor to generate chromatin fragments between 200 and 500 bp. After sonication material was centrifuged at maximum speed 10 min at 4ºC, and supernatant was recovered (chromatin), discarding cell debris. A 50 µl aliquot of chromatin was treated with Proteinase K overnight, and DNA was recovered by phenol/chloroform extraction to quantify DNA concentration and check the size of the sheared DNA in a 1.2% agarose gel.

To perform the chromatin immunoprecipitation, 30 µg of chromatin was diluted 10-fold in *ChIP IP buffer* containing inhibitors, and immunoprecipitated overnight at 4ºC in rotation using the indicated antibody (1-5 µg, depending on the antibody). Mouse or rabbit IgG (Santa Cruz Biothechnology) was used as a control for nonspecific interaction of DNA. Input was prepared with 10% of the chromatin material used for an immunoprecipitation. Immunocomplexes were recovered using 20 µl of Protein-A magnetic beads from Millipore. Beads with bound antibody/protein/DNA complexes were washed for 5 min at 4ºC in rotation with *Washing Buffers 1, 2, and 3*, and then twice with TE 1X. Decross-linkeing was performed at 65ºC overnight, and immunoprecipitated DNA was recovered using the IPure Kit from Diagenode.

ChIP solutions:

SOLUTION	COMPOSITION
Crosslinking Solution	50mM Hepes pH8.0; 0.1M NaCl; 1mM EDTA pH8.0; 0.5mM EGTA pH8.0
Lysis Buffer I	5mM PIPES pH8.0; 85mM KCl; 0.5% NP-40
Lysis Buffer II	1% SDS; 10mM EDTA pH8.0; 50mM Tris-HCl pH8.1
ChIP IP Buffer	0.01% SDS; 1.1% Triton X-100; 1.2mM EDTA pH8.0; 16.7mM Tris-HCl pH8.1; 167mM NaCl
Washing Buffer I	0.1% SDS; 1% Triton X-100; 2mM EDTA pH8.0; 20mM Tris-HCl pH8.1; 150mM NaCl
Washing Buffer II	0.1% SDS; 1% Triton X-100; 2mM EDTA pH8.0; 20mM Tris-HCl pH8.1; 500mM NaCl
Washing Buffer III	0.25M LiCl; 1% NP-40; 1% Sodium Deoxicholate; 1mM EDTA pH8.0; 10mM Tris-HCl pH8.1
Protease & Phosphatase inhibitors	1mM Phenylmethylsulfonylfluoride (PMSF); 1µg/ml Aprotinin, 1µg/ml Pepstatin A; 1mM Sodium ortovanadate; 20mM β-Glycerophosphate; 1X Protease Inhibitors Cockatil-PIC (Roche)

21.1. CHIP-QUANTITATIVE PCR

Real-time PCR was performed on ChIP and input DNA using EXPRESS SYBR GreenER qPCR SuperMix Universal (Invitrogen) and specific oligonucleotides in a Roche 480 Lightcycler. ChIP values were corrected by the correspondent input chromatin sample.

21.2. ChIP-chip ASSAYS WITH Nimblegen PROMOTER ARRAYS

At least 10 ng of ChIP and input DNA was amplified using GenomePlex Complete Whole Genome Amplification (WGA) Kit (Sigma) and eluted with GenElute PCR Clean-Up Kit (Sigma). For ChIP-on-chip experiments we used Nimblgen HG18 Refseq Promoter 3x720K array. 1 µg ChIP and input DNA was directly labeled by Klenow random priming with Cy5 and Cy3 nonamers with Nimblegen Dual-color DNA Labeling Kit following manufacturer's user's guide Chip-chip arrays v6.2, and the labeled DNA was precipitated with 1 volume isopropanol. Hybridization mix including 15 µg labeled DNA was prepared using Nimblegen Hybridization Kit. Arrays were hybridized in Nimblegen Hybridization System 4 Station for 16-18 h at 42ºC, and then washed in 1x Wash solution I, II and III. Hybridization buffers and washes were completed using manufacturer's protocols. Arrays were scanned on a Nimblegen MS 200 Scanner per manufacturer's protocol.

ChIP-on-chip raw data was normalized and differential intensity of each probe compared to input control was calculated using the Nimblegen software DEVA. Average fold change (ChIP vs. input) each 50bp bin for a range of -3.2Kb upstream and 800bp downstream window from RefSeq TSS were calculated using in-house Perl script. LOESS smoothed line plot around the TSS were plotted using in-house script written in R statistical programming language. For ChIP-signal heat map, similarly fold change average for each individual RefSeq transcript was calculated and then data was visualized with Java Treeview [323]. Functional annotation of target genes based on Gene Ontology (GO) was performed using DAVID Software (Database for Annotation, Visualization and IntegratedDiscovery).

21.3. ChIP-seq

Library preparation for sequencing: ChIP and genomic library preparation was performed using standard Illumina protocols. Libraries were prepared with the ChIP-seq Sample Preparation Kit (Illumina) according to the manufacturer’s instructions. Briefly, 10 ng of ChIP and input DNA were repaired to overhang a 3’-dA and then adapters were ligated to the end of DNA fragments. DNA fragments with proper size (usually 100-300bp, including adaptor sequence) were selected after PCR amplification, obtaining qualified library for sequencing.

21.3.1. Sequencing, mapping and peak detection

Sequencing was performed with Illumina HiSeq 2000 system. Raw sequence reads containing more than 10% of "N", or bases with Q <=20 account for more than 50% of the total were removed and adaptor sequences were trimmed. Identified clean reads were uniquely aligned allowing at best two mismatches to the UCSC (The Genome Sequencing Consortium) reference genome (human hg18) using the program SOAP (version 2.21) [324]. Sequence matching exactly more than one place with equally quality were discarded to avoid bias. Read length and read counts of each library are listed in Table R.2. Peak caller program for histone, SICER (version 1.1) [251], was used with following parameters: redundancy threshold=1, window size=200, fragment size=150, effective genome fraction=0.75, gap size=200, FDR=0.01 and Fold Change at least 2. Differential binding of reads was also done using SICER program script with similar parameter settings. Input subtracted normalized (total mapped library size) WIG files were produced from duplicate removed aligned reads using the program javaGenomicsToolKit.

21.3.2. Binding sites to gene feature annotation

Enriched peaks were annotated to nearest gene (RefSeq genes) using Bioconductor package ChIPpeakAnno [325]. Distribution of enriched and depleted regions (peaks) to various genomic features, and continuous ChIP signal profile distribution of reads along the meta-gene were performed using software CEAS [252] and in-house Python and Perl scripts.

21.3.3. Regulatory regions, histone modification peaks, CpG and LADs abundance

Input-subtracted normalized average H1 variants read density in each enriched locations of regulatory regions, histone modification peaks, CpG and LADs were calculated, and representation in box-plot were made using in-house scripts.

21.3.4. Publicly available genome-wide location data analysis

Public ChIP-seq data, which includes H3K4me1, H3K4me2, H3K4me3, H3K27me3, H3K27ac, H3K9me3, H3K9ac, H3K36me3, P300, CTCF, FAIRE and DNase enriched genomic locations, are taken from ENCODE project. CpG island genomic location information (hg18) and the coordinates of LADs [105] were taken from UCSC database. Publicly available whole-genome data if not available on hg18 version, they were first re-mapped to the human genome version hg18 using the UCSC coordinate conversion tool (http://genome.ucsc.edu/cgi-bin/hgLiftOver).

21.3.5. Overlap analysis

Overlap of genomic position range data was done using BedTools [326]. Overlap means two genomic range data overlap by at least one base.

21.3.6. Average ChIP signal profile

For sequencing data, ChIP signal around center of each given genomic location were calculated by using normalized input subtracted-average tags number in each 50bp bins in a set window. Relative distance of each tag from above mentioned position and average signal was determined by using 'Sitepro' script of CEAS package [252] and plotting was done in R programming language.

21.3.7. Functional enrichment analysis

Functional annotation of target genes was based on Gene Ontology (GO) ([327]; http://www.geneontology.org) as extracted from EnsEMBL Biomart [328]. Accordingly, all genes were classified into ontology: genes involved in Biological Processes (BP). We took only the GO categories that had at least 10 genes annotated. We used GiTools for enrichement analysis and heat map generation [253]. Resulting p-values were adjusted for multiple testing using the Benjamin and Hochberg's method of False Discovery Rate (FDR) [329].

22. Agilent EXPRESION ARRAYS

Total RNA was extracted using High Pure RNA isolation Kit (Roche) according to the manufacturer's instructions. cDNA was obtained from 100 ng of total RNA using SuperScript VILO cDNA synthesis Kit (Invitrogen). High RNA integrity was assessed by Bioanalyzer nano 6000 assay. For each sample, 100 ng of total were reversed transcribed into cDNA with a T7 promoter and the cDNA was in vitro transcribed into cRNA in the presence of Cy3-CTP using the Low input quick Amp kit (Agilent). Labeled samples were purified using RNeasy mini spin columns (Qiagen). Then, 600 ng of cRNA were preblocked and fragmented in Agilent fragmentation buffer and mixed with Agilent GEx Hybridization mix. Hybridization mix was laid onto each sector of subarray gasket slide and sandwiched against an 8 x 65K format oligonucleotide microarray (Human v1 Sureprint G3 Human GE 8x60k Microarray, Agilent design ID 028004) inside a hybridization chamber which was hybridized overnight at 65ºC. Subsequently array chambers were disassembled submerged in Agilent Gene Expression Buffer 1 and washed 1 minute in another dish with the same solution with a magnetic stirrer at 200 rpm at room temperature, followed by 1 minute in gilent Gene Expression Buffer 2 with a

magnetic stirrer at 200 rpm at 37ºC and immediate withdrawal from the solution and air drying. Fluorescent signal was captured into TIF images with an Agilent scanner using recommended settings with Scan Control software (Agilent). Signal intensities were extracted into a tabulated text file using Feature Extraction software (Agilent) using the appropriate array configuration and annotation files. The normalized log2intensities were obtained using quantile method with normexp background correction the Bioconductor Limma package in R.

23. ACCESSION NUMBER

The data sets are available in the Gene Expression Omnibus (GEO) database under the accession number GSE49345.

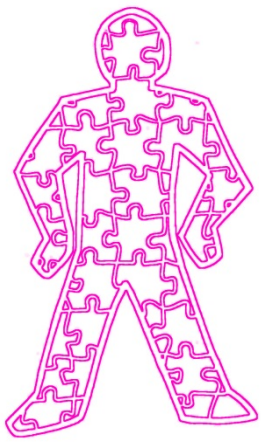

ABBREVIATIONS

5mC	5-methylcytosine
A	Adenine
ACP	Architectural chromatin proteins
ADP	Adenosine diphosphate
ATP	Adenosine triphosphate
bp	Base pair
BSA	Bovine serum albumin
C	Cytosine
CDK	Cyclin dependent kinase
cDNA	Complementary DNA
CENP	Centromeric protein
CGI	CpG island
ChIP	Chromatin immunoprecipitation
CTD	C-terminal domain
DamID	DNA adenine methyltransferase identification
DMEM	Dulbecco's modified Eagle medium
DNA	Deoxyribonucleic acid
DNase	Deoxyribonuclease
DNMT	DNA methyltransferase
Dox	Doxicycline
DSB	Double strand beaks
DTT	DL-Dithiothreitol
EDTA	Ethylene diaminetetraacetic acid
EMT	Epithelial-to-mesenchymal transition
ER	Estrogen receptor
ESC	Embryonic stem cell
EtBr	Ethidium Bromide
FACS	Fluorescence-activated cell sorting
FAIRE	Formaldehyde assisted isolation of regulatory elements
FCS	Fetal calf serum
FISH	Fluorescence *in situ* hybridization
FRAP	Fluorescence recovery after photobleaching
G	Guanine
GD	Globular domain
GFP	Green fluorescence protein
GO	Gene ontology
HA	Hemagglutinin
HAT	Histone acetyltransferase
HCP	High-CpG promoter
HDAC	Histone deacetylase
HDM	Histone demethylase

HEPES	(2-Hydroxyethyl)-1-piperazineethanesulphonic acid
HIRA	Histone cell cycle regulation-defective homolog A
HJURP	Holliday junction recognition protein
HMG	High mobility group
HMT	Histone methyltransferase
HP1	Heterochromatin protein 1
ICP	Intermediate-CpG promoter
ICR	Imprinted control region
IE	Immediate-early
INM	Inner nuclear membrane
IP	Immunoprecipitation
IRIF	Irradiation-induced foci
K	Lysine
Kb	Kilobase pair
KCl	Potassium chloride
KD	Knock-down
KDa	Kilodalton
KO	Knock-out
LAD	Lamina-associated domain
LCP	Low-CpG promoter
lincRNA	Long intergenic non-coding ribonucleic acid
LOCK	Large organized chromatin lysine 9 modifications
M	Molar
MEM	Minimum Essential Medium
miRNA	Micro ribonucleic acid
MMTV	Mouse mammary tumor virus
MNase	Micrococcal nuclease
mRNA	Messenger ribonucleic acid
NaCl	Sodium chloride
NAD	Nucleolus-associated domain
NAD	Nicotinamide adenine dinucleotide
ncRNA	Non-coding ribonucleic acid
NDR	Nucleosome depleted region
NFR	Nucleosome free region
NL	Nuclear lamina
NOMe	Nucleosome occupancy and methylome
NTD	N-terminal domain
nucB	Nucleosome B
PBS	Phosphate buffered saline
PcG	Polycomb group
PCR	Polymerase chain reaction

PI	Propidium iodide
PIC	Preinitiation complex
PIPES	1,4-Piperazinediethanesulfonic acid
PMSF	Phenylmethylsulfonyl fluoride
PRC	Polycomb-repressive complex
PTM	Post-translational modification
qPCR	Quantitative PCR
R	Arginine
RedFP or RFP	Red fluorescent protein
RNA	Ribonucleic acid
RNAi	Interference ribonucleic acid
RNApol	RNA polymerase
RNase	Ribonuclease
rpm	Revolutions per minute
RPMI	
rRNA	Ribosomal ribonucleic acid
RT	Room temperature
RT-PCR	Reverse transcription PCR
S	Serine
SAHF	Senescence-associated heterochromatic foci
SDS	Sodium-dodecyl-sulphate
shRNA	Short hairpin ribonucleic acid
SINE	Short interspersed element
siRNA	Small interference ribonucleic acid
snoRNA	Small nucleolar ribonucleic acid
snRNA	Small nuclear ribonucleic acid
T	Thymine
TAD	Topologically associating domains
TE	Tris-EDTA
TF	Transcription factor
TF	Transcription factor
Tris	Tris(hydroxymethyl)-amino-methane
tRNA	Transfer ribonucleic acid
TSS	Transcription start site
TTS	Transcription termination site
wt	Wild type

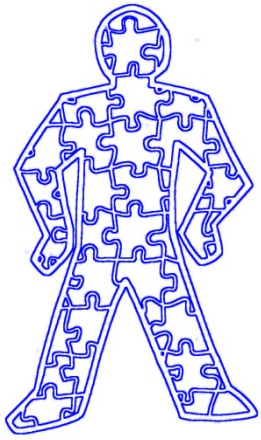

PUBLICATIONS

1.

Mapping of six somatic linker histone H1 variants in human breast cancer cells uncovers specific features of H1.2.

Lluís Millán-Ariño, Abul B.M.M.K. Islam, Andrea Izquierdo-Bouldstridge, Regina Mayor, Jean-Michel Terme, Neus Luque, Mónica Sancho, Núria López-Bigas, Albert Jordan.

Submited, 2013

Abstract: Seven linker histone H1 variants exist in human somatic cells with distinct prevalence among cell types and during differentiation. Despite being key chromatin structural components, it remains elusive how they participate in the regulation of nuclear processes. Moreover, it is not well understood whether the different variants have specific roles or are differentially distributed along the genome. By taking advantage of specific antibodies to H1 variants and HA-tagged recombinant H1 variants expressed in breast cancer cells, we have investigated the distribution of variants H1.2 to H1.5, H1.0 and H1X in promoters and genome-wide. All H1 variants bind gene promoters and are depleted from transcription start sites (TSS) in active genes. The extension of H1 depletion at promoters is dependent on the transcriptional status of the gene and differs between variants. Noteworthy, H1.2 is less abundant than other variants at the TSS of inactive genes, and promoters enriched in H1.2 upstream of TSS are different from those enriched in other variants and tend to be repressed. Additionally, H1.2 is enriched at chromosomal domains characterized by low GC content and associates with lamina-associated domains. Meanwhile, other variants associate with higher GC content, CpG islands and gene-rich domains. Altogether, histone H1 is not uniformly distributed along the genome and differences among variants exist, being H1.2 the variant showing a more specific pattern and a strongest correlation with low gene expression. Interestingly, the most structurally divergent variants H1.0 and H1X are similarly distributed to other variants such as H1.4 and H3.

2.

Progestins activate 6-phosphofructo-2-kinase/fructose-2,6-bisphosphatase 3 (PFKFB3) in breast cancer cells.

Novellasdemunt L, Obach M, **Millán-Ariño Ll**, Manzano A, Ventura F, Rosa JL, Jordan A, Navarro-Sabate A, Bartrons R.

Biochem J. 2012 Mar 1;442(2):345-56. doi: 10.1042/BJ20111418.

Abstract: PFKFB (6-phosphofructo-2-kinase/fructose-2,6-bisphosphatase) catalyses the synthesis and degradation of Fru-2,6-P2 (fructose-2,6-bisphosphate), a key modulator of glycolysis and gluconeogenesis. The PFKFB3 gene is extensively involved in cell proliferation owing to its key role in carbohydrate metabolism. In the present study we analyse its mechanism of regulation by progestins in breast cancer cells. We report that exposure of T47D cells to synthetic progestins (ORG2058 or norgestrel) leads to a rapid increase in Fru-2,6-P2 concentration. Our Western blot results are compatible with a short-term activation due to PFKFB3 isoenzyme phosphorylation and a long-term sustained action due to increased PFKFB3 protein levels. Transient transfection of T47D cells with deleted gene promoter constructs allowed us to identify a PRE (progesterone-response element) to which PR (progesterone receptor) binds and thus transactivates PFKFB3 gene transcription. PR expression in the PR-negative cell line MDA-MB-231 induces endogenous PFKFB3 expression in response to norgestrel. Direct binding of PR to the PRE box (-3490 nt) was confirmed by ChIP (chromatin immunoprecipiation) experiments. A dual mechanism affecting PFKFB3 protein and gene regulation operates in order to assure glycolysis in breast cancer cells. An immediate early response through the ERK (extracellular-signal-regulated kinase)/RSK (ribosomal S6 kinase) pathway leading to phosphorylation of PFKFB3 on Ser461 is followed by activation of mRNA transcription via cis-acting sequences on the PFKFB3 promoter.

3.

Histone H1 variants are differentially expressed and incorporated into chromatin during differentiation and reprogramming to pluripotency.

Terme JM, Sesé B, **Millán-Ariño Ll**, Mayor R, Izpisúa Belmonte JC, Barrero MJ, Jordan A.

J Biol Chem. 2011 Oct 14;286(41):35347-57. doi: 10.1074/jbc.M111.281923. Epub 2011 Aug 18.

Abstract: There are seven linker histone variants in human somatic cells (H1.0 to H1.5 and H1X), and their prevalence varies as a function of cell type and differentiation stage, suggesting that the different variants may have distinct roles. We have revisited this notion by using new methodologies to study pluripotency and differentiation, including the in vitro differentiation of human embryonic stem (ES) and teratocarcinoma cells and the reprogramming of keratinocytes to induced pluripotent stem cells. Our results show that pluripotent cells (PCs) have decreased levels of H1.0 and increased levels of H1.1, H1.3, and H1.5 compared with differentiated cells. PCs have a more diverse repertoire of H1 variants, whereas in differentiated cells, H1.0 expression represents ~80% of the H1 transcripts. In agreement with their prevalent expression in ES cells, the regulatory regions of H1.3 and H1.5 genes were found to be occupied by pluripotency factors. Moreover, the H1.0 gene promoter contains bivalent domains (H3K4me2 and H3K27me3) in PCs, suggesting that this variant is likely to have an important role during differentiation. Indeed, the knockdown of H1.0 in human ES did not affect self-renewal but impaired differentiation. Accordingly, H1.0 was recruited to the regulatory regions of differentiation and pluripotency genes during differentiation, confirming that this histone variant plays a critical role in the regulation of these genes. Thus, histone H1 variant expression is controlled by a variety of mechanisms that produce distinct but consistent H1 repertoires in pluripotent and differentiated cells that appear critical to maintain the functionality of such cells.

4.

Mutational analysis of progesterone receptor functional domains in stable cell lines delineates sets of genes regulated by different mechanisms.

Quiles I, **Millán-Ariño Ll**, Subtil-Rodríguez A, Miñana B, Spinedi N, Ballaré C, Beato M, Jordan A.

Mol Endocrinol. 2009 Jun;23(6):809-26. doi: 10.1210/me.2008-0454. Epub 2009 Mar 19.

Abstract: Steroid hormone receptors act directly in the nucleus on the chromatin organization and transcriptional activity of several promoters. Furthermore, they have an indirect effect on cytoplasmic signal transduction pathways, including MAPK, impacting ultimately on gene expression. We are interested in distinguishing between the two modes of action of progesterone receptor (PR) on the control of gene expression and cell proliferation. For this, we have stably expressed, in PR-negative breast cancer cells, tagged forms of the PR isoform B mutated at regions involved either in DNA binding (DNA-binding domain) or in its ability to interact with the estrogen receptor and to activate the c-Src/MAPK/Erk/Msk cascade (estrogen receptor-interacting domain). Both mutants impair PR-mediated activation of a well-understood model promoter in response to progestin, as well as hormone-induced cell proliferation. Additional mutants affecting transactivation activity of PR (activation function 2) or a zinc-finger implicated in dimerization (D-box) have also been tested. Microarrays and gene expression experiments on these cell lines define the subsets of hormone-responsive genes regulated by different modes of action of PR isoform B, as well as genes in which the nuclear and nongenomic pathways cooperate. Correlation between CCND1 expression in the different cell lines and their ability to support cell proliferation confirms CCND1 as a key controller gene.

5.

Progesterone induction of the 11beta-hydroxysteroid dehydrogenase type 2 promoter in breast cancer cells involves coordinated recruitment of STAT5A and progesterone receptor to a distal enhancer and polymerase tracking.

Subtil-Rodríguez A, **Millán-Ariño Ll**, Quiles I, Ballaré C, Beato M, Jordan A.

Mol Cell Biol. 2008 Jun;28(11):3830-49. doi: 10.1128/MCB.01217-07. Epub 2008 Mar 31.

Abstract: Steroid hormone receptors regulate gene expression, interacting with target DNA sequences but also activating cytoplasmic signaling pathways. Using the human 11beta-hydroxysteroid dehydrogenase type 2 (11beta-HSD2) gene as a model, we have investigated the contributions of both effects on a human progesterone-responsive promoter in breast cancer cells. Chromatin immunoprecipitation has identified two different mechanisms of hormone-induced progesterone receptor (PR) recruitment to the 11beta-HSD2 promoter: (i) direct PR binding to DNA at the proximal promoter, abrogated when PR contains a mutated DNA binding domain (DBD), and (ii) STAT5A (signal transducer and activator of transcription 5A)-mediated recruitment of PR to an upstream distal region, impaired by AG490, a JAK/STAT pathway inhibitor. The JAK/STAT inhibitor, as well as expression of dominant-negative STAT5A, impairs hormone induction of 11beta-HSD2. On the other hand, the DBD-mutated PR fully supports 11beta-HSD2 expression. These results, along with data from a deletion analysis, indicate that the distal region is crucial for hormone regulation of 11beta-HSD2. We show active RNA polymerase II tracking from the distal region upon PR and STAT5A binding, concomitant with synthesis of noncoding, hormone-dependent RNAs, suggesting that this region works as a hormone-dependent transcriptional enhancer. In conclusion, coordination of PR transcriptional effects and cytoplasmic signaling activation, in particular the JAK/STAT pathway, are critical in regulating progestin-induced endogenous 11beta-HSD2 gene expression in breast cancer cells. This is not unique to this promoter, as AG490 also alters the expression of other progesterone-regulated genes.

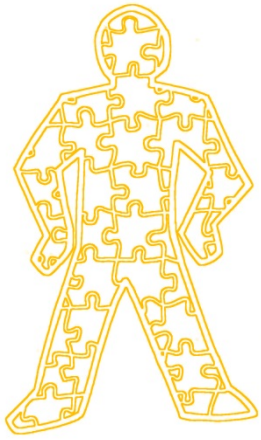

REFERENCES

1. Dahm R: **Discovering DNA: Friedrich Miescher and the early years of nucleic acid research.** *Hum Genet* 2008, **122:**565-581.
2. Watson JD, Crick FH: **Molecular structure of nucleic acids; a structure for deoxyribose nucleic acid.** *Nature* 1953, **171:**737-738.
3. Luger K, Mader AW, Richmond RK, Sargent DF, Richmond TJ: **Crystal structure of the nucleosome core particle at 2.8 A resolution.** *Nature* 1997, **389:**251-260.
4. Kornberg RD, Thomas JO: **Chromatin structure; oligomers of the histones.** *Science* 1974, **184:**865-868.
5. Tremethick DJ: **Higher-order structures of chromatin: the elusive 30 nm fiber.** *Cell* 2007, **128:**651-654.
6. Woodcock CL, Dimitrov S: **Higher-order structure of chromatin and chromosomes.** *Curr Opin Genet Dev* 2001, **11:**130-135.
7. Thoma F, Koller T, Klug A: **Involvement of histone H1 in the organization of the nucleosome and of the salt-dependent superstructures of chromatin.** *J Cell Biol* 1979, **83:**403-427.
8. Bednar J, Horowitz RA, Grigoryev SA, Carruthers LM, Hansen JC, Koster AJ, Woodcock CL: **Nucleosomes, linker DNA, and linker histone form a unique structural motif that directs the higher-order folding and compaction of chromatin.** *Proc Natl Acad Sci U S A* 1998, **95:**14173-14178.
9. Brown DT: **Histone H1 and the dynamic regulation of chromatin function.** *Biochem Cell Biol* 2003, **81:**221-227.
10. Bustin M, Catez F, Lim JH: **The dynamics of histone H1 function in chromatin.** *Mol Cell* 2005, **17:**617-620.
11. Misteli T: **Beyond the sequence: cellular organization of genome function.** *Cell* 2007, **128:**787-800.
12. Luger K, Dechassa ML, Tremethick DJ: **New insights into nucleosome and chromatin structure: an ordered state or a disordered affair?** *Nat Rev Mol Cell Biol* 2012, **13:**436-447.
13. Peterson CL, Laniel MA: **Histones and histone modifications.** *Curr Biol* 2004, **14:**R546-551.
14. Berger SL, Kouzarides T, Shiekhattar R, Shilatifard A: **An operational definition of epigenetics.** *Genes Dev* 2009, **23:**781-783.
15. Ehrlich M, Gama-Sosa MA, Huang LH, Midgett RM, Kuo KC, McCune RA, Gehrke C: **Amount and distribution of 5-methylcytosine in human DNA from different types of tissues of cells.** *Nucleic Acids Res* 1982, **10:**2709-2721.
16. Lister R, Pelizzola M, Dowen RH, Hawkins RD, Hon G, Tonti-Filippini J, Nery JR, Lee L, Ye Z, Ngo QM, et al: **Human DNA methylomes at base resolution show widespread epigenomic differences.** *Nature* 2009, **462:**315-322.
17. Takai D, Jones PA: **Comprehensive analysis of CpG islands in human chromosomes 21 and 22.** *Proc Natl Acad Sci U S A* 2002, **99:**3740-3745.
18. Jones PA: **Functions of DNA methylation: islands, start sites, gene bodies and beyond.** *Nat Rev Genet* 2012, **13:**484-492.

19. Tammen SA, Friso S, Choi SW: **Epigenetics: the link between nature and nurture.** *Mol Aspects Med* 2013, **34:**753-764.
20. Blackledge NP, Zhou JC, Tolstorukov MY, Farcas AM, Park PJ, Klose RJ: **CpG islands recruit a histone H3 lysine 36 demethylase.** *Mol Cell* 2010, **38:**179-190.
21. Zhou JC, Blackledge NP, Farcas AM, Klose RJ: **Recognition of CpG island chromatin by KDM2A requires direct and specific interaction with linker DNA.** *Mol Cell Biol* 2012, **32:**479-489.
22. Heyn H, Esteller M: **DNA methylation profiling in the clinic: applications and challenges.** *Nat Rev Genet* 2012, **13:**679-692.
23. Kulis M, Esteller M: **DNA methylation and cancer.** *Adv Genet* 2010, **70:**27-56.
24. Kouzarides T: **Chromatin modifications and their function.** *Cell* 2007, **128:**693-705.
25. Freitas MA, Sklenar AR, Parthun MR: **Application of mass spectrometry to the identification and quantification of histone post-translational modifications.** *J Cell Biochem* 2004, **92:**691-700.
26. Garcia BA: **Mass spectrometric analysis of histone variants and post-translational modifications.** *Front Biosci (Schol Ed)* 2009, **1:**142-153.
27. Tropberger P, Pott S, Keller C, Kamieniarz-Gdula K, Caron M, Richter F, Li G, Mittler G, Liu ET, Buhler M, et al: **Regulation of transcription through acetylation of H3K122 on the lateral surface of the histone octamer.** *Cell* 2013, **152:**859-872.
28. Strahl BD, Allis CD: **The language of covalent histone modifications.** *Nature* 2000, **403:**41-45.
29. Bhaumik SR, Smith E, Shilatifard A: **Covalent modifications of histones during development and disease pathogenesis.** *Nat Struct Mol Biol* 2007, **14:**1008-1016.
30. Allfrey VG, Faulkner R, Mirsky AE: **Acetylation and Methylation of Histones and Their Possible Role in the Regulation of Rna Synthesis.** *Proc Natl Acad Sci U S A* 1964, **51:**786-794.
31. Koch CM, Andrews RM, Flicek P, Dillon SC, Karaoz U, Clelland GK, Wilcox S, Beare DM, Fowler JC, Couttet P, et al: **The landscape of histone modifications across 1% of the human genome in five human cell lines.** *Genome Res* 2007, **17:**691-707.
32. Hong L, Schroth GP, Matthews HR, Yau P, Bradbury EM: **Studies of the DNA binding properties of histone H4 amino terminus. Thermal denaturation studies reveal that acetylation markedly reduces the binding constant of the H4 "tail" to DNA.** *J Biol Chem* 1993, **268:**305-314.
33. Serrano L, Vazquez BN, Tischfield J: **Chromatin structure, pluripotency and differentiation.** *Exp Biol Med (Maywood)* 2013, **238:**259-270.
34. Zeng L, Zhou MM: **Bromodomain: an acetyl-lysine binding domain.** *FEBS Lett* 2002, **513:**124-128.
35. Olsen CA: **Expansion of the lysine acylation landscape.** *Angew Chem Int Ed Engl* 2012, **51:**3755-3756.
36. Taverna SD, Li H, Ruthenburg AJ, Allis CD, Patel DJ: **How chromatin-binding modules interpret histone modifications: lessons from professional pocket pickers.** *Nat Struct Mol Biol* 2007, **14:**1025-1040.
37. Kouzarides T: **Histone methylation in transcriptional control.** *Curr Opin Genet Dev* 2002, **12:**198-209.

38. Black JC, Van Rechem C, Whetstine JR: **Histone lysine methylation dynamics: establishment, regulation, and biological impact.** *Mol Cell* 2012, **48:**491-507.
39. Shi Y, Lan F, Matson C, Mulligan P, Whetstine JR, Cole PA, Casero RA, Shi Y: **Histone demethylation mediated by the nuclear amine oxidase homolog LSD1.** *Cell* 2004, **119:**941-953.
40. Liu W, Tanasa B, Tyurina OV, Zhou TY, Gassmann R, Liu WT, Ohgi KA, Benner C, Garcia-Bassets I, Aggarwal AK, et al: **PHF8 mediates histone H4 lysine 20 demethylation events involved in cell cycle progression.** *Nature* 2010, **466:**508-512.
41. Chang B, Chen Y, Zhao Y, Bruick RK: **JMJD6 is a histone arginine demethylase.** *Science* 2007, **318:**444-447.
42. Zentner GE, Henikoff S: **Regulation of nucleosome dynamics by histone modifications.** *Nat Struct Mol Biol* 2013, **20:**259-266.
43. Azuara V, Perry P, Sauer S, Spivakov M, Jorgensen HF, John RM, Gouti M, Casanova M, Warnes G, Merkenschlager M, Fisher AG: **Chromatin signatures of pluripotent cell lines.** *Nat Cell Biol* 2006, **8:**532-538.
44. Bernstein BE, Mikkelsen TS, Xie X, Kamal M, Huebert DJ, Cuff J, Fry B, Meissner A, Wernig M, Plath K, et al: **A bivalent chromatin structure marks key developmental genes in embryonic stem cells.** *Cell* 2006, **125:**315-326.
45. Pedersen MT, Helin K: **Histone demethylases in development and disease.** *Trends Cell Biol* 2010, **20:**662-671.
46. Banerjee T, Chakravarti D: **A peek into the complex realm of histone phosphorylation.** *Mol Cell Biol* 2011, **31:**4858-4873.
47. Paull TT, Rogakou EP, Yamazaki V, Kirchgessner CU, Gellert M, Bonner WM: **A critical role for histone H2AX in recruitment of repair factors to nuclear foci after DNA damage.** *Curr Biol* 2000, **10:**886-895.
48. Green GR, Poccia DL: **Phosphorylation of sea urchin sperm H1 and H2B histones precedes chromatin decondensation and H1 exchange during pronuclear formation.** *Dev Biol* 1985, **108:**235-245.
49. Mahadevan LC, Willis AC, Barratt MJ: **Rapid histone H3 phosphorylation in response to growth factors, phorbol esters, okadaic acid, and protein synthesis inhibitors.** *Cell* 1991, **65:**775-783.
50. Fischle W, Tseng BS, Dormann HL, Ueberheide BM, Garcia BA, Shabanowitz J, Hunt DF, Funabiki H, Allis CD: **Regulation of HP1-chromatin binding by histone H3 methylation and phosphorylation.** *Nature* 2005, **438:**1116-1122.
51. Hirota T, Lipp JJ, Toh BH, Peters JM: **Histone H3 serine 10 phosphorylation by Aurora B causes HP1 dissociation from heterochromatin.** *Nature* 2005, **438:**1176-1180.
52. Barth TK, Imhof A: **Fast signals and slow marks: the dynamics of histone modifications.** *Trends Biochem Sci* 2010, **35:**618-626.
53. Ausio J: **Histone variants--the structure behind the function.** *Brief Funct Genomic Proteomic* 2006, **5:**228-243.
54. Vardabasso C, Hasson D, Ratnakumar K, Chung CY, Duarte LF, Bernstein E: **Histone variants: emerging players in cancer biology.** *Cell Mol Life Sci* 2013.
55. Skene PJ, Henikoff S: **Histone variants in pluripotency and disease.** *Development* 2013, **140:**2513-2524.

56. Luk E, Ranjan A, Fitzgerald PC, Mizuguchi G, Huang Y, Wei D, Wu C: **Stepwise histone replacement by SWR1 requires dual activation with histone H2A.Z and canonical nucleosome.** *Cell* 2010, **143:**725-736.
57. Lukas J, Lukas C, Bartek J: **More than just a focus: The chromatin response to DNA damage and its role in genome integrity maintenance.** *Nat Cell Biol* 2011, **13:**1161-1169.
58. van Attikum H, Gasser SM: **Crosstalk between histone modifications during the DNA damage response.** *Trends Cell Biol* 2009, **19:**207-217.
59. Han W, Li X, Fu X: **The macro domain protein family: structure, functions, and their potential therapeutic implications.** *Mutat Res* 2011, **727:**86-103.
60. Gamble MJ, Frizzell KM, Yang C, Krishnakumar R, Kraus WL: **The histone variant macroH2A1 marks repressed autosomal chromatin, but protects a subset of its target genes from silencing.** *Genes Dev* 2010, **24:**21-32.
61. Bernstein E, Muratore-Schroeder TL, Diaz RL, Chow JC, Changolkar LN, Shabanowitz J, Heard E, Pehrson JR, Hunt DF, Allis CD: **A phosphorylated subpopulation of the histone variant macroH2A1 is excluded from the inactive X chromosome and enriched during mitosis.** *Proc Natl Acad Sci U S A* 2008, **105:**1533-1538.
62. Barrero MJ, Sese B, Marti M, Izpisua Belmonte JC: **Macro histone variants are critical for the differentiation of human pluripotent cells.** *J Biol Chem* 2013, **288:**16110-16116.
63. Creppe C, Posavec M, Douet J, Buschbeck M: **MacroH2A in stem cells: a story beyond gene repression.** *Epigenomics* 2012, **4:**221-227.
64. Hake SB, Garcia BA, Duncan EM, Kauer M, Dellaire G, Shabanowitz J, Bazett-Jones DP, Allis CD, Hunt DF: **Expression patterns and post-translational modifications associated with mammalian histone H3 variants.** *J Biol Chem* 2006, **281:**559-568.
65. Jin C, Zang C, Wei G, Cui K, Peng W, Zhao K, Felsenfeld G: **H3.3/H2A.Z double variant-containing nucleosomes mark 'nucleosome-free regions' of active promoters and other regulatory regions.** *Nat Genet* 2009, **41:**941-945.
66. Chow CM, Georgiou A, Szutorisz H, Maia e Silva A, Pombo A, Barahona I, Dargelos E, Canzonetta C, Dillon N: **Variant histone H3.3 marks promoters of transcriptionally active genes during mammalian cell division.** *EMBO Rep* 2005, **6:**354-360.
67. Goldberg AD, Banaszynski LA, Noh KM, Lewis PW, Elsaesser SJ, Stadler S, Dewell S, Law M, Guo X, Li X, et al: **Distinct factors control histone variant H3.3 localization at specific genomic regions.** *Cell* 2010, **140:**678-691.
68. Jin C, Felsenfeld G: **Distribution of histone H3.3 in hematopoietic cell lineages.** *Proc Natl Acad Sci U S A* 2006, **103:**574-579.
69. Dunleavy EM, Roche D, Tagami H, Lacoste N, Ray-Gallet D, Nakamura Y, Daigo Y, Nakatani Y, Almouzni-Pettinotti G: **HJURP is a cell-cycle-dependent maintenance and deposition factor of CENP-A at centromeres.** *Cell* 2009, **137:**485-497.
70. Foltz DR, Jansen LE, Bailey AO, Yates JR, 3rd, Bassett EA, Wood S, Black BE, Cleveland DW: **Centromere-specific assembly of CENP-a nucleosomes is mediated by HJURP.** *Cell* 2009, **137:**472-484.
71. De Rop V, Padeganeh A, Maddox PS: **CENP-A: the key player behind centromere identity, propagation, and kinetochore assembly.** *Chromosoma* 2012, **121:**527-538.

72. Consortium EP, Bernstein BE, Birney E, Dunham I, Green ED, Gunter C, Snyder M: **An integrated encyclopedia of DNA elements in the human genome.** *Nature* 2012, **489:**57-74.
73. Consortium EP, Birney E, Stamatoyannopoulos JA, Dutta A, Guigo R, Gingeras TR, Margulies EH, Weng Z, Snyder M, Dermitzakis ET, et al: **Identification and analysis of functional elements in 1% of the human genome by the ENCODE pilot project.** *Nature* 2007, **447:**799-816.
74. Lee RC, Feinbaum RL, Ambros V: **The C. elegans heterochronic gene lin-4 encodes small RNAs with antisense complementarity to lin-14.** *Cell* 1993, **75:**843-854.
75. Derrien T, Guigo R, Johnson R: **The Long Non-Coding RNAs: A New (P)layer in the "Dark Matter".** *Front Genet* 2011, **2:**107.
76. Derrien T, Johnson R, Bussotti G, Tanzer A, Djebali S, Tilgner H, Guernec G, Martin D, Merkel A, Knowles DG, et al: **The GENCODE v7 catalog of human long noncoding RNAs: analysis of their gene structure, evolution, and expression.** *Genome Res* 2012, **22:**1775-1789.
77. Amaral PP, Dinger ME, Mercer TR, Mattick JS: **The eukaryotic genome as an RNA machine.** *Science* 2008, **319:**1787-1789.
78. Clapier CR, Cairns BR: **The biology of chromatin remodeling complexes.** *Annu Rev Biochem* 2009, **78:**273-304.
79. Manning BJ, Peterson CL: **Releasing the brakes on a chromatin-remodeling enzyme.** *Nat Struct Mol Biol* 2013, **20:**5-7.
80. Gaspar-Maia A, Alajem A, Meshorer E, Ramalho-Santos M: **Open chromatin in pluripotency and reprogramming.** *Nat Rev Mol Cell Biol* 2011, **12:**36-47.
81. Vicent GP, Zaurin R, Nacht AS, Li A, Font-Mateu J, Le Dily F, Vermeulen M, Mann M, Beato M: **Two chromatin remodeling activities cooperate during activation of hormone responsive promoters.** *PLoS Genet* 2009, **5:**e1000567.
82. Vicent GP, Nacht AS, Font-Mateu J, Castellano G, Gaveglia L, Ballare C, Beato M: **Four enzymes cooperate to displace histone H1 during the first minute of hormonal gene activation.** *Genes Dev* 2011, **25:**845-862.
83. Clapier CR, Cairns BR: **Regulation of ISWI involves inhibitory modules antagonized by nucleosomal epitopes.** *Nature* 2012, **492:**280-284.
84. Murawska M, Brehm A: **CHD chromatin remodelers and the transcription cycle.** *Transcription* 2011, **2:**244-253.
85. Gkikopoulos T, Schofield P, Singh V, Pinskaya M, Mellor J, Smolle M, Workman JL, Barton GJ, Owen-Hughes T: **A role for Snf2-related nucleosome-spacing enzymes in genome-wide nucleosome organization.** *Science* 2011, **333:**1758-1760.
86. Papamichos-Chronakis M, Watanabe S, Rando OJ, Peterson CL: **Global regulation of H2A.Z localization by the INO80 chromatin-remodeling enzyme is essential for genome integrity.** *Cell* 2011, **144:**200-213.
87. Sadeh R, Allis CD: **Genome-wide "re"-modeling of nucleosome positions.** *Cell* 2011, **147:**263-266.
88. Struhl K, Segal E: **Determinants of nucleosome positioning.** *Nat Struct Mol Biol* 2013, **20:**267-273.
89. Segal E, Fondufe-Mittendorf Y, Chen L, Thastrom A, Field Y, Moore IK, Wang JP, Widom J: **A genomic code for nucleosome positioning.** *Nature* 2006, **442:**772-778.

90. Nelson HC, Finch JT, Luisi BF, Klug A: **The structure of an oligo(dA).oligo(dT) tract and its biological implications.** *Nature* 1987, **330:**221-226.
91. Tillo D, Hughes TR: **G+C content dominates intrinsic nucleosome occupancy.** *BMC Bioinformatics* 2009, **10:**442.
92. Valouev A, Johnson SM, Boyd SD, Smith CL, Fire AZ, Sidow A: **Determinants of nucleosome organization in primary human cells.** *Nature* 2011, **474:**516-520.
93. Zhang Y, Moqtaderi Z, Rattner BP, Euskirchen G, Snyder M, Kadonaga JT, Liu XS, Struhl K: **Intrinsic histone-DNA interactions are not the major determinant of nucleosome positions in vivo.** *Nat Struct Mol Biol* 2009, **16:**847-852.
94. Zhang Z, Wippo CJ, Wal M, Ward E, Korber P, Pugh BF: **A packing mechanism for nucleosome organization reconstituted across a eukaryotic genome.** *Science* 2011, **332:**977-980.
95. Arya G, Maitra A, Grigoryev SA: **A structural perspective on the where, how, why, and what of nucleosome positioning.** *J Biomol Struct Dyn* 2010, **27:**803-820.
96. Fan Y, Nikitina T, Zhao J, Fleury TJ, Bhattacharyya R, Bouhassira EE, Stein A, Woodcock CL, Skoultchi AI: **Histone H1 depletion in mammals alters global chromatin structure but causes specific changes in gene regulation.** *Cell* 2005, **123:**1199-1212.
97. Sancho M, Diani E, Beato M, Jordan A: **Depletion of human histone H1 variants uncovers specific roles in gene expression and cell growth.** *PLoS Genet* 2008, **4:**e1000227.
98. Schones DE, Cui K, Cuddapah S, Roh TY, Barski A, Wang Z, Wei G, Zhao K: **Dynamic regulation of nucleosome positioning in the human genome.** *Cell* 2008, **132:**887-898.
99. Gaffney DJ, McVicker G, Pai AA, Fondufe-Mittendorf YN, Lewellen N, Michelini K, Widom J, Gilad Y, Pritchard JK: **Controls of nucleosome positioning in the human genome.** *PLoS Genet* 2012, **8:**e1003036.
100. Kelly TK, Liu Y, Lay FD, Liang G, Berman BP, Jones PA: **Genome-wide mapping of nucleosome positioning and DNA methylation within individual DNA molecules.** *Genome Res* 2012, **22:**2497-2506.
101. Bickmore WA: **The Spatial Organization of the Human Genome.** *Annu Rev Genomics Hum Genet* 2013.
102. Cremer T, Cremer C: **Chromosome territories, nuclear architecture and gene regulation in mammalian cells.** *Nat Rev Genet* 2001, **2:**292-301.
103. Caron H, van Schaik B, van der Mee M, Baas F, Riggins G, van Sluis P, Hermus MC, van Asperen R, Boon K, Voute PA, et al: **The human transcriptome map: clustering of highly expressed genes in chromosomal domains.** *Science* 2001, **291:**1289-1292.
104. Bickmore WA, van Steensel B: **Genome architecture: domain organization of interphase chromosomes.** *Cell* 2013, **152:**1270-1284.
105. Guelen L, Pagie L, Brasset E, Meuleman W, Faza MB, Talhout W, Eussen BH, de Klein A, Wessels L, de Laat W, van Steensel B: **Domain organization of human chromosomes revealed by mapping of nuclear lamina interactions.** *Nature* 2008, **453:**948-951.
106. Meuleman W, Peric-Hupkes D, Kind J, Beaudry JB, Pagie L, Kellis M, Reinders M, Wessels L, van Steensel B: **Constitutive nuclear lamina-genome interactions are highly conserved and associated with A/T-rich sequence.** *Genome Res* 2013, **23:**270-280.

107. van Koningsbruggen S, Gierlinski M, Schofield P, Martin D, Barton GJ, Ariyurek Y, den Dunnen JT, Lamond AI: **High-resolution whole-genome sequencing reveals that specific chromatin domains from most human chromosomes associate with nucleoli.** *Mol Biol Cell* 2010, **21:**3735-3748.
108. Filion GJ, van Bemmel JG, Braunschweig U, Talhout W, Kind J, Ward LD, Brugman W, de Castro IJ, Kerkhoven RM, Bussemaker HJ, van Steensel B: **Systematic protein location mapping reveals five principal chromatin types in Drosophila cells.** *Cell* 2010, **143:**212-224.
109. Ernst J, Kellis M: **Discovery and characterization of chromatin states for systematic annotation of the human genome.** *Nat Biotechnol* 2010, **28:**817-825.
110. Ram O, Goren A, Amit I, Shoresh N, Yosef N, Ernst J, Kellis M, Gymrek M, Issner R, Coyne M, et al: **Combinatorial patterning of chromatin regulators uncovered by genome-wide location analysis in human cells.** *Cell* 2011, **147:**1628-1639.
111. de Wit E, de Laat W: **A decade of 3C technologies: insights into nuclear organization.** *Genes Dev* 2012, **26:**11-24.
112. Cremer T, Cremer M: **Chromosome territories.** *Cold Spring Harb Perspect Biol* 2010, **2:**a003889.
113. Lieberman-Aiden E, van Berkum NL, Williams L, Imakaev M, Ragoczy T, Telling A, Amit I, Lajoie BR, Sabo PJ, Dorschner MO, et al: **Comprehensive mapping of long-range interactions reveals folding principles of the human genome.** *Science* 2009, **326:**289-293.
114. Sexton T, Yaffe E, Kenigsberg E, Bantignies F, Leblanc B, Hoichman M, Parrinello H, Tanay A, Cavalli G: **Three-dimensional folding and functional organization principles of the Drosophila genome.** *Cell* 2012, **148:**458-472.
115. Dixon JR, Selvaraj S, Yue F, Kim A, Li Y, Shen Y, Hu M, Liu JS, Ren B: **Topological domains in mammalian genomes identified by analysis of chromatin interactions.** *Nature* 2012, **485:**376-380.
116. Hou C, Li L, Qin ZS, Corces VG: **Gene density, transcription, and insulators contribute to the partition of the Drosophila genome into physical domains.** *Mol Cell* 2012, **48:**471-484.
117. Nora EP, Lajoie BR, Schulz EG, Giorgetti L, Okamoto I, Servant N, Piolot T, van Berkum NL, Meisig J, Sedat J, et al: **Spatial partitioning of the regulatory landscape of the X-inactivation centre.** *Nature* 2012, **485:**381-385.
118. Gondor A: **Nuclear architecture and chromatin structure on the path to cancer.** *Semin Cancer Biol* 2013, **23:**63-64.
119. van Steensel B: **Chromatin: constructing the big picture.** *EMBO J* 2011, **30:**1885-1895.
120. Jost KL, Bertulat B, Cardoso MC: **Heterochromatin and gene positioning: inside, outside, any side?** *Chromosoma* 2012, **121:**555-563.
121. Kasinsky HE, Lewis JD, Dacks JB, Ausio J: **Origin of H1 linker histones.** *FASEB J* 2001, **15:**34-42.
122. Talbert PB, Ahmad K, Almouzni G, Ausio J, Berger F, Bhalla PL, Bonner WM, Cande WZ, Chadwick BP, Chan SW, et al: **A unified phylogeny-based nomenclature for histone variants.** *Epigenetics Chromatin* 2012, **5:**7.
123. Izzo A, Kamieniarz K, Schneider R: **The histone H1 family: specific members, specific functions?** *Biol Chem* 2008, **389:**333-343.

124. Harshman SW, Young NL, Parthun MR, Freitas MA: **H1 histones: current perspectives and challenges.** *Nucleic Acids Res* 2013.
125. Happel N, Doenecke D: **Histone H1 and its isoforms: contribution to chromatin structure and function.** *Gene* 2009, **431:**1-12.
126. Happel N, Warneboldt J, Hanecke K, Haller F, Doenecke D: **H1 subtype expression during cell proliferation and growth arrest.** *Cell Cycle* 2009, **8:**2226-2232.
127. Coles LS, Wells JR: **An H1 histone gene-specific 5' element and evolution of H1 and H5 genes.** *Nucleic Acids Res* 1985, **13:**585-594.
128. Doenecke D, Albig W, Bouterfa H, Drabent B: **Organization and expression of H1 histone and H1 replacement histone genes.** *J Cell Biochem* 1994, **54:**423-431.
129. Eilers A, Bouterfa H, Triebe S, Doenecke D: **Role of a distal promoter element in the S-phase control of the human H1.2 histone gene transcription.** *Eur J Biochem* 1994, **223:**567-574.
130. Gokhman D, Livyatan I, Sailaja BS, Melcer S, Meshorer E: **Multilayered chromatin analysis reveals E2f, Smad and Zfx as transcriptional regulators of histones.** *Nat Struct Mol Biol* 2013, **20:**119-126.
131. Albig W, Meergans T, Doenecke D: **Characterization of the H1.5 gene completes the set of human H1 subtype genes.** *Gene* 1997, **184:**141-148.
132. Ohe Y, Hayashi H, Iwai K: **Human spleen histone H1. Isolation and amino acid sequences of three minor variants, H1a, H1c, and H1d.** *J Biochem* 1989, **106:**844-857.
133. Parseghian MH, Clark RF, Hauser LJ, Dvorkin N, Harris DA, Hamkalo BA: **Fractionation of human H1 subtypes and characterization of a subtype-specific antibody exhibiting non-uniform nuclear staining.** *Chromosome Res* 1993, **1:**127-139.
134. Lennox RW, Cohen LH: **The histone H1 complements of dividing and nondividing cells of the mouse.** *J Biol Chem* 1983, **258:**262-268.
135. Seyedin SM, Kistler WS: **H1 histone subfractions of mammalian testes. 1. Organ specificity in the rat.** *Biochemistry* 1979, **18:**1371-1375.
136. McBryant SJ, Hansen JC: **Dynamic fuzziness during linker histone action.** *Adv Exp Med Biol* 2012, **725:**15-26.
137. McBryant SJ, Lu X, Hansen JC: **Multifunctionality of the linker histones: an emerging role for protein-protein interactions.** *Cell Res* 2010, **20:**519-528.
138. Crane-Robinson C: **Where is the globular domain of linker histone located on the nucleosome?** *Trends Biochem Sci* 1997, **22:**75-77.
139. Oberg C, Belikov S: **The N-terminal domain determines the affinity and specificity of H1 binding to chromatin.** *Biochem Biophys Res Commun* 2012, **420:**321-324.
140. Vila R, Ponte I, Collado M, Arrondo JL, Jimenez MA, Rico M, Suau P: **DNA-induced alpha-helical structure in the NH2-terminal domain of histone H1.** *J Biol Chem* 2001, **276:**46429-46435.
141. Caterino TL, Fang H, Hayes JJ: **Nucleosome linker DNA contacts and induces specific folding of the intrinsically disordered H1 carboxyl-terminal domain.** *Mol Cell Biol* 2011, **31:**2341-2348.
142. Caterino TL, Hayes JJ: **Structure of the H1 C-terminal domain and function in chromatin condensation.** *Biochem Cell Biol* 2011, **89:**35-44.
143. Misteli T, Gunjan A, Hock R, Bustin M, Brown DT: **Dynamic binding of histone H1 to chromatin in living cells.** *Nature* 2000, **408:**877-881.

144. Hashimoto H, Takami Y, Sonoda E, Iwasaki T, Iwano H, Tachibana M, Takeda S, Nakayama T, Kimura H, Shinkai Y: **Histone H1 null vertebrate cells exhibit altered nucleosome architecture.** *Nucleic Acids Res* 2010, **38:**3533-3545.
145. Fan Y, Nikitina T, Morin-Kensicki EM, Zhao J, Magnuson TR, Woodcock CL, Skoultchi AI: **H1 linker histones are essential for mouse development and affect nucleosome spacing in vivo.** *Mol Cell Biol* 2003, **23:**4559-4572.
146. Woodcock CL, Skoultchi AI, Fan Y: **Role of linker histone in chromatin structure and function: H1 stoichiometry and nucleosome repeat length.** *Chromosome Res* 2006, **14:**17-25.
147. Oberg C, Izzo A, Schneider R, Wrange O, Belikov S: **Linker histone subtypes differ in their effect on nucleosomal spacing in vivo.** *J Mol Biol* 2012, **419:**183-197.
148. Lu X, Hansen JC: **Identification of specific functional subdomains within the linker histone H10 C-terminal domain.** *J Biol Chem* 2004, **279:**8701-8707.
149. Garcia BA, Busby SA, Barber CM, Shabanowitz J, Allis CD, Hunt DF: **Characterization of phosphorylation sites on histone H1 isoforms by tandem mass spectrometry.** *J Proteome Res* 2004, **3:**1219-1227.
150. Wisniewski JR, Zougman A, Kruger S, Mann M: **Mass spectrometric mapping of linker histone H1 variants reveals multiple acetylations, methylations, and phosphorylation as well as differences between cell culture and tissue.** *Mol Cell Proteomics* 2007, **6:**72-87.
151. Wood C, Snijders A, Williamson J, Reynolds C, Baldwin J, Dickman M: **Post-translational modifications of the linker histone variants and their association with cell mechanisms.** *FEBS J* 2009, **276:**3685-3697.
152. Bonet-Costa C, Vilaseca M, Diema C, Vujatovic O, Vaquero A, Omenaca N, Castejon L, Bernues J, Giralt E, Azorin F: **Combined bottom-up and top-down mass spectrometry analyses of the pattern of post-translational modifications of Drosophila melanogaster linker histone H1.** *J Proteomics* 2012, **75:**4124-4138.
153. Lesner A, Kartvelishvili A, Lesniak J, Nikolov D, Kartvelishvili M, Trillo-Pazos G, Zablotna E, Simm M: **Monoubiquitinated histone H1B is required for antiviral protection in CD4(+)T cells resistant to HIV-1.** *Biochemistry* 2004, **43:**16203-16211.
154. Wisniewski JR, Zougman A, Mann M: **Nepsilon-formylation of lysine is a widespread post-translational modification of nuclear proteins occurring at residues involved in regulation of chromatin function.** *Nucleic Acids Res* 2008, **36:**570-577.
155. Deterding LJ, Bunger MK, Banks GC, Tomer KB, Archer TK: **Global changes in and characterization of specific sites of phosphorylation in mouse and human histone H1 Isoforms upon CDK inhibitor treatment using mass spectrometry.** *J Proteome Res* 2008, **7:**2368-2379.
156. Chu CS, Hsu PH, Lo PW, Scheer E, Tora L, Tsai HJ, Tsai MD, Juan LJ: **Protein kinase A-mediated serine 35 phosphorylation dissociates histone H1.4 from mitotic chromosome.** *J Biol Chem* 2011, **286:**35843-35851.
157. Happel N, Stoldt S, Schmidt B, Doenecke D: **M phase-specific phosphorylation of histone H1.5 at threonine 10 by GSK-3.** *J Mol Biol* 2009, **386:**339-350.
158. Hergeth SP, Dundr M, Tropberger P, Zee BM, Garcia BA, Daujat S, Schneider R: **Isoform-specific phosphorylation of human linker histone H1.4 in mitosis by the kinase Aurora B.** *J Cell Sci* 2011, **124:**1623-1628.

159. Talasz H, Sarg B, Lindner HH: **Site-specifically phosphorylated forms of H1.5 and H1.2 localized at distinct regions of the nucleus are related to different processes during the cell cycle.** *Chromosoma* 2009, **118:**693-709.
160. Telu KH, Abbaoui B, Thomas-Ahner JM, Zynger DL, Clinton SK, Freitas MA, Mortazavi A: **Alterations of Histone H1 Phosphorylation During Bladder Carcinogenesis.** *J Proteome Res* 2013.
161. Koop R, Di Croce L, Beato M: **Histone H1 enhances synergistic activation of the MMTV promoter in chromatin.** *EMBO J* 2003, **22:**588-599.
162. Vicent GP, Koop R, Beato M: **Complex role of histone H1 in transactivation of MMTV promoter chromatin by progesterone receptor.** *J Steroid Biochem Mol Biol* 2002, **83:**15-23.
163. Zheng Y, John S, Pesavento JJ, Schultz-Norton JR, Schiltz RL, Baek S, Nardulli AM, Hager GL, Kelleher NL, Mizzen CA: **Histone H1 phosphorylation is associated with transcription by RNA polymerases I and II.** *J Cell Biol* 2010, **189:**407-415.
164. Trojer P, Zhang J, Yonezawa M, Schmidt A, Zheng H, Jenuwein T, Reinberg D: **Dynamic Histone H1 Isotype 4 Methylation and Demethylation by Histone Lysine Methyltransferase G9a/KMT1C and the Jumonji Domain-containing JMJD2/KDM4 Proteins.** *J Biol Chem* 2009, **284:**8395-8405.
165. Daujat S, Zeissler U, Waldmann T, Happel N, Schneider R: **HP1 binds specifically to Lys26-methylated histone H1.4, whereas simultaneous Ser27 phosphorylation blocks HP1 binding.** *J Biol Chem* 2005, **280:**38090-38095.
166. Vaquero A, Scher M, Lee D, Erdjument-Bromage H, Tempst P, Reinberg D: **Human SirT1 interacts with histone H1 and promotes formation of facultative heterochromatin.** *Mol Cell* 2004, **16:**93-105.
167. Weiss T, Hergeth S, Zeissler U, Izzo A, Tropberger P, Zee BM, Dundr M, Garcia BA, Daujat S, Schneider R: **Histone H1 variant-specific lysine methylation by G9a/KMT1C and Glp1/KMT1D.** *Epigenetics Chromatin* 2010, **3:**7.
168. Kamieniarz K, Izzo A, Dundr M, Tropberger P, Ozretic L, Kirfel J, Scheer E, Tropel P, Wisniewski JR, Tora L, et al: **A dual role of linker histone H1.4 Lys 34 acetylation in transcriptional activation.** *Genes Dev* 2012, **26:**797-802.
169. Poirier GG, de Murcia G, Jongstra-Bilen J, Niedergang C, Mandel P: **Poly(ADP-ribosyl)ation of polynucleosomes causes relaxation of chromatin structure.** *Proc Natl Acad Sci U S A* 1982, **79:**3423-3427.
170. Krishnakumar R, Gamble MJ, Frizzell KM, Berrocal JG, Kininis M, Kraus WL: **Reciprocal binding of PARP-1 and histone H1 at promoters specifies transcriptional outcomes.** *Science* 2008, **319:**819-821.
171. Krishnakumar R, Kraus WL: **PARP-1 regulates chromatin structure and transcription through a KDM5B-dependent pathway.** *Mol Cell* 2010, **39:**736-749.
172. Wright RH, Castellano G, Bonet J, Le Dily F, Font-Mateu J, Ballare C, Nacht AS, Soronellas D, Oliva B, Beato M: **CDK2-dependent activation of PARP-1 is required for hormonal gene regulation in breast cancer cells.** *Genes Dev* 2012, **26:**1972-1983.
173. Shan L, Li X, Liu L, Ding X, Wang Q, Zheng Y, Duan Y, Xuan C, Wang Y, Yang F, et al: **GATA3 cooperates with PARP1 to regulate CCND1 transcription through modulating histone H1 incorporation.** *Oncogene* 2013.

174. Kassner I, Barandun M, Fey M, Rosenthal F, Hottiger MO: **Crosstalk between SET7/9-dependent methylation and ARTD1-mediated ADP-ribosylation of histone H1.4.** *Epigenetics Chromatin* 2013, **6:**1.
175. Hill DA: **Influence of linker histone H1 on chromatin remodeling.** *Biochem Cell Biol* 2001, **79:**317-324.
176. Schlissel MS, Brown DD: **The transcriptional regulation of Xenopus 5s RNA genes in chromatin: the roles of active stable transcription complexes and histone H1.** *Cell* 1984, **37:**903-913.
177. Nishiyama M, Skoultchi AI, Nakayama KI: **Histone H1 recruitment by CHD8 is essential for suppression of the Wnt-beta-catenin signaling pathway.** *Mol Cell Biol* 2012, **32:**501-512.
178. Nishiyama M, Oshikawa K, Tsukada Y, Nakagawa T, Iemura S, Natsume T, Fan Y, Kikuchi A, Skoultchi AI, Nakayama KI: **CHD8 suppresses p53-mediated apoptosis through histone H1 recruitment during early embryogenesis.** *Nat Cell Biol* 2009, **11:**172-182.
179. Maclean JA, Bettegowda A, Kim BJ, Lou CH, Yang SM, Bhardwaj A, Shanker S, Hu Z, Fan Y, Eckardt S, et al: **The rhox homeobox gene cluster is imprinted and selectively targeted for regulation by histone h1 and DNA methylation.** *Mol Cell Biol* 2011, **31:**1275-1287.
180. Bouvet P, Dimitrov S, Wolffe AP: **Specific regulation of Xenopus chromosomal 5S rRNA gene transcription in vivo by histone H1.** *Genes Dev* 1994, **8:**1147-1159.
181. Kandolf H: **The H1A histone variant is an in vivo repressor of oocyte-type 5S gene transcription in Xenopus laevis embryos.** *Proc Natl Acad Sci U S A* 1994, **91:**7257-7261.
182. Shen X, Gorovsky MA: **Linker histone H1 regulates specific gene expression but not global transcription in vivo.** *Cell* 1996, **86:**475-483.
183. Vujatovic O, Zaragoza K, Vaquero A, Reina O, Bernues J, Azorin F: **Drosophila melanogaster linker histone dH1 is required for transposon silencing and to preserve genome integrity.** *Nucleic Acids Res* 2012, **40:**5402-5414.
184. Chubb JE, Rea S: **Core and linker histone modifications involved in the DNA damage response.** *Subcell Biochem* 2010, **50:**17-42.
185. Hashimoto H, Sonoda E, Takami Y, Kimura H, Nakayama T, Tachibana M, Takeda S, Shinkai Y: **Histone H1 variant, H1R is involved in DNA damage response.** *DNA Repair (Amst)* 2007, **6:**1584-1595.
186. De S, Brown DT, Lu ZH, Leno GH, Wellman SE, Sittman DB: **Histone H1 variants differentially inhibit DNA replication through an affinity for chromatin mediated by their carboxyl-terminal domains.** *Gene* 2002, **292:**173-181.
187. Cascone A, Bruelle C, Lindholm D, Bernardi P, Eriksson O: **Destabilization of the outer and inner mitochondrial membranes by core and linker histones.** *PLoS One* 2012, **7:**e35357.
188. Konishi A, Shimizu S, Hirota J, Takao T, Fan Y, Matsuoka Y, Zhang L, Yoneda Y, Fujii Y, Skoultchi AI, Tsujimoto Y: **Involvement of histone H1.2 in apoptosis induced by DNA double-strand breaks.** *Cell* 2003, **114:**673-688.
189. Hale TK, Contreras A, Morrison AJ, Herrera RE: **Phosphorylation of the linker histone H1 by CDK regulates its binding to HP1alpha.** *Mol Cell* 2006, **22:**693-699.

190. Kuzmichev A, Jenuwein T, Tempst P, Reinberg D: **Different EZH2-containing complexes target methylation of histone H1 or nucleosomal histone H3.** *Mol Cell* 2004, **14:**183-193.
191. Fan Y, Sirotkin A, Russell RG, Ayala J, Skoultchi AI: **Individual somatic H1 subtypes are dispensable for mouse development even in mice lacking the H1(0) replacement subtype.** *Mol Cell Biol* 2001, **21:**7933-7943.
192. Hellauer K, Sirard E, Turcotte B: **Decreased expression of specific genes in yeast cells lacking histone H1.** *J Biol Chem* 2001, **276:**13587-13592.
193. Downs JA, Kosmidou E, Morgan A, Jackson SP: **Suppression of homologous recombination by the Saccharomyces cerevisiae linker histone.** *Mol Cell* 2003, **11:**1685-1692.
194. Barra JL, Rhounim L, Rossignol JL, Faugeron G: **Histone H1 is dispensable for methylation-associated gene silencing in Ascobolus immersus and essential for long life span.** *Mol Cell Biol* 2000, **20:**61-69.
195. Jedrusik MA, Schulze E: **A single histone H1 isoform (H1.1) is essential for chromatin silencing and germline development in Caenorhabditis elegans.** *Development* 2001, **128:**1069-1080.
196. Jedrusik MA, Schulze E: **Linker histone HIS-24 (H1.1) cytoplasmic retention promotes germ line development and influences histone H3 methylation in Caenorhabditis elegans.** *Mol Cell Biol* 2007, **27:**2229-2239.
197. Jedrusik MA, Vogt S, Claus P, Schulze E: **A novel linker histone-like protein is associated with cytoplasmic filaments in Caenorhabditis elegans.** *J Cell Sci* 2002, **115:**2881-2891.
198. Prymakowska-Bosak M, Przewloka MR, Slusarczyk J, Kuras M, Lichota J, Kilianczyk B, Jerzmanowski A: **Linker histones play a role in male meiosis and the development of pollen grains in tobacco.** *Plant Cell* 1999, **11:**2317-2329.
199. Wierzbicki AT, Jerzmanowski A: **Suppression of histone H1 genes in Arabidopsis results in heritable developmental defects and stochastic changes in DNA methylation.** *Genetics* 2005, **169:**997-1008.
200. Lu X, Wontakal SN, Emelyanov AV, Morcillo P, Konev AY, Fyodorov DV, Skoultchi AI: **Linker histone H1 is essential for Drosophila development, the establishment of pericentric heterochromatin, and a normal polytene chromosome structure.** *Genes Dev* 2009, **23:**452-465.
201. Takami Y, Nishi R, Nakayama T: **Histone H1 variants play individual roles in transcription regulation in the DT40 chicken B cell line.** *Biochem Biophys Res Commun* 2000, **268:**501-508.
202. Steinbach OC, Wolffe AP, Rupp RA: **Somatic linker histones cause loss of mesodermal competence in Xenopus.** *Nature* 1997, **389:**395-399.
203. Brown DT, Alexander BT, Sittman DB: **Differential effect of H1 variant overexpression on cell cycle progression and gene expression.** *Nucleic Acids Res* 1996, **24:**486-493.
204. Gunjan A, Alexander BT, Sittman DB, Brown DT: **Effects of H1 histone variant overexpression on chromatin structure.** *J Biol Chem* 1999, **274:**37950-37956.
205. Alami R, Fan Y, Pack S, Sonbuchner TM, Besse A, Lin Q, Greally JM, Skoultchi AI, Bouhassira EE: **Mammalian linker-histone subtypes differentially affect gene expression in vivo.** *Proc Natl Acad Sci U S A* 2003, **100:**5920-5925.

206. Gabrilovich DI, Cheng P, Fan Y, Yu B, Nikitina E, Sirotkin A, Shurin M, Oyama T, Adachi Y, Nadaf S, et al: **H1(0) histone and differentiation of dendritic cells. A molecular target for tumor-derived factors.** *J Leukoc Biol* 2002, **72:**285-296.
207. Sirotkin AM, Edelmann W, Cheng G, Klein-Szanto A, Kucherlapati R, Skoultchi AI: **Mice develop normally without the H1(0) linker histone.** *Proc Natl Acad Sci U S A* 1995, **92:**6434-6438.
208. Drabent B, Saftig P, Bode C, Doenecke D: **Spermatogenesis proceeds normally in mice without linker histone H1t.** *Histochem Cell Biol* 2000, **113:**433-442.
209. Fantz DA, Hatfield WR, Horvath G, Kistler MK, Kistler WS: **Mice with a targeted disruption of the H1t gene are fertile and undergo normal changes in structural chromosomal proteins during spermiogenesis.** *Biol Reprod* 2001, **64:**425-431.
210. Lin Q, Sirotkin A, Skoultchi AI: **Normal spermatogenesis in mice lacking the testis-specific linker histone H1t.** *Mol Cell Biol* 2000, **20:**2122-2128.
211. Lin Q, Inselman A, Han X, Xu H, Zhang W, Handel MA, Skoultchi AI: **Reductions in linker histone levels are tolerated in developing spermatocytes but cause changes in specific gene expression.** *J Biol Chem* 2004, **279:**23525-23535.
212. Martianov I, Brancorsini S, Catena R, Gansmuller A, Kotaja N, Parvinen M, Sassone-Corsi P, Davidson I: **Polar nuclear localization of H1T2, a histone H1 variant, required for spermatid elongation and DNA condensation during spermiogenesis.** *Proc Natl Acad Sci U S A* 2005, **102:**2808-2813.
213. Tanaka H, Iguchi N, Isotani A, Kitamura K, Toyama Y, Matsuoka Y, Onishi M, Masai K, Maekawa M, Toshimori K, et al: **HANP1/H1T2, a novel histone H1-like protein involved in nuclear formation and sperm fertility.** *Mol Cell Biol* 2005, **25:**7107-7119.
214. Murga M, Jaco I, Fan Y, Soria R, Martinez-Pastor B, Cuadrado M, Yang SM, Blasco MA, Skoultchi AI, Fernandez-Capetillo O: **Global chromatin compaction limits the strength of the DNA damage response.** *J Cell Biol* 2007, **178:**1101-1108.
215. Eirin-Lopez JM, Gonzalez-Tizon AM, Martinez A, Mendez J: **Birth-and-death evolution with strong purifying selection in the histone H1 multigene family and the origin of orphon H1 genes.** *Mol Biol Evol* 2004, **21:**1992-2003.
216. Ponte I, Vidal-Taboada JM, Suau P: **Evolution of the vertebrate H1 histone class: evidence for the functional differentiation of the subtypes.** *Mol Biol Evol* 1998, **15:**702-708.
217. Meergans T, Albig W, Doenecke D: **Varied expression patterns of human H1 histone genes in different cell lines.** *DNA Cell Biol* 1997, **16:**1041-1049.
218. Pina B, Martinez P, Suau P: **Changes in H1 complement in differentiating rat-brain cortical neurons.** *Eur J Biochem* 1987, **164:**71-76.
219. Pina B, Suau P: **Changes in the proportions of histone H1 subtypes in brain cortical neurons.** *FEBS Lett* 1987, **210:**161-164.
220. Parseghian MH, Hamkalo BA: **A compendium of the histone H1 family of somatic subtypes: an elusive cast of characters and their characteristics.** *Biochem Cell Biol* 2001, **79:**289-304.
221. Happel N, Schulze E, Doenecke D: **Characterisation of human histone H1x.** *Biol Chem* 2005, **386:**541-551.
222. Zlatanova J, Doenecke D: **Histone H1 zero: a major player in cell differentiation?** *FASEB J* 1994, **8:**1260-1268.

223. Helliger W, Lindner H, Grubl-Knosp O, Puschendorf B: **Alteration in proportions of histone H1 variants during the differentiation of murine erythroleukaemic cells.** *Biochem J* 1992, **288 (Pt 3):**747-751.
224. Terme JM, Sese B, Millan-Arino L, Mayor R, Izpisua Belmonte JC, Barrero MJ, Jordan A: **Histone H1 variants are differentially expressed and incorporated into chromatin during differentiation and reprogramming to pluripotency.** *J Biol Chem* 2011, **286:**35347-35357.
225. Zhang Y, Cooke M, Panjwani S, Cao K, Krauth B, Ho PY, Medrzycki M, Berhe DT, Pan C, McDevitt TC, Fan Y: **Histone h1 depletion impairs embryonic stem cell differentiation.** *PLoS Genet* 2012, **8:**e1002691.
226. Lim CY, Reversade B, Knowles BB, Solter D: **Optimal histone H3 to linker histone H1 chromatin ratio is vital for mesodermal competence in Xenopus.** *Development* 2013, **140:**853-860.
227. Lin CJ, Conti M, Ramalho-Santos M: **Histone variant H3.3 maintains a decondensed chromatin state essential for mouse preimplantation development.** *Development* 2013, **140:**3624-3634.
228. Sato S, Takahashi S, Asamoto M, Nakanishi M, Wakita T, Ogura Y, Yatabe Y, Shirai T: **Histone H1 expression in human prostate cancer tissues and cell lines.** *Pathol Int* 2012, **62:**84-92.
229. Medrzycki M, Zhang Y, McDonald JF, Fan Y: **Profiling of linker histone variants in ovarian cancer.** *Front Biosci* 2012, **17:**396-406.
230. Sjoblom T, Jones S, Wood LD, Parsons DW, Lin J, Barber TD, Mandelker D, Leary RJ, Ptak J, Silliman N, et al: **The consensus coding sequences of human breast and colorectal cancers.** *Science* 2006, **314:**268-274.
231. Hechtman JF, Beasley MB, Kinoshita Y, Ko HM, Hao K, Burstein DE: **Promyelocytic leukemia zinc finger and histone H1.5 differentially stain low- and high-grade pulmonary neuroendocrine tumors: a pilot immunohistochemical study.** *Hum Pathol* 2013, **44:**1400-1405.
232. Lever MA, Th'ng JP, Sun X, Hendzel MJ: **Rapid exchange of histone H1.1 on chromatin in living human cells.** *Nature* 2000, **408:**873-876.
233. Vyas P, Brown DT: **N- and C-terminal domains determine differential nucleosomal binding geometry and affinity of linker histone isotypes H1(0) and H1c.** *J Biol Chem* 2012, **287:**11778-11787.
234. Th'ng JP, Sung R, Ye M, Hendzel MJ: **H1 family histones in the nucleus. Control of binding and localization by the C-terminal domain.** *J Biol Chem* 2005, **280:**27809-27814.
235. Clausell J, Happel N, Hale TK, Doenecke D, Beato M: **Histone H1 subtypes differentially modulate chromatin condensation without preventing ATP-dependent remodeling by SWI/SNF or NURF.** *PLoS One* 2009, **4:**e0007243.
236. Orrego M, Ponte I, Roque A, Buschati N, Mora X, Suau P: **Differential affinity of mammalian histone H1 somatic subtypes for DNA and chromatin.** *BMC Biol* 2007, **5:**22.
237. Kalashnikova AA, Winkler DD, McBryant SJ, Henderson RK, Herman JA, DeLuca JG, Luger K, Prenni JE, Hansen JC: **Linker histone H1.0 interacts with an extensive network of proteins found in the nucleolus.** *Nucleic Acids Res* 2013, **41:**4026-4035.

238. Lee H, Habas R, Abate-Shen C: **MSX1 cooperates with histone H1b for inhibition of transcription and myogenesis.** *Science* 2004, **304:**1675-1678.
239. Mackey-Cushman SL, Gao J, Holmes DA, Nunoya JI, Wang R, Unutmaz D, Su L: **FoxP3 interacts with linker histone H1.5 to modulate gene expression and program Treg cell activity.** *Genes Immun* 2011, **12:**559-567.
240. Kim K, Choi J, Heo K, Kim H, Levens D, Kohno K, Johnson EM, Brock HW, An W: **Isolation and characterization of a novel H1.2 complex that acts as a repressor of p53-mediated transcription.** *J Biol Chem* 2008, **283:**9113-9126.
241. Kim K, Jeong KW, Kim H, Choi J, Lu W, Stallcup MR, An W: **Functional interplay between p53 acetylation and H1.2 phosphorylation in p53-regulated transcription.** *Oncogene* 2012, **31:**4290-4301.
242. Bhan S, May W, Warren SL, Sittman DB: **Global gene expression analysis reveals specific and redundant roles for H1 variants, H1c and H1(0), in gene expression regulation.** *Gene* 2008, **414:**10-18.
243. Parseghian MH, Harris DA, Rishwain DR, Hamkalo BA: **Characterization of a set of antibodies specific for three human histone H1 subtypes.** *Chromosoma* 1994, **103:**198-208.
244. Parseghian MH, Newcomb RL, Hamkalo BA: **Distribution of somatic H1 subtypes is non-random on active vs. inactive chromatin II: distribution in human adult fibroblasts.** *J Cell Biochem* 2001, **83:**643-659.
245. Parseghian MH, Newcomb RL, Winokur ST, Hamkalo BA: **The distribution of somatic H1 subtypes is non-random on active vs. inactive chromatin: distribution in human fetal fibroblasts.** *Chromosome Res* 2000, **8:**405-424.
246. Braunschweig U, Hogan GJ, Pagie L, van Steensel B: **Histone H1 binding is inhibited by histone variant H3.3.** *EMBO J* 2009, **28:**3635-3645.
247. Li JY, Patterson M, Mikkola HK, Lowry WE, Kurdistani SK: **Dynamic distribution of linker histone H1.5 in cellular differentiation.** *PLoS Genet* 2012, **8:**e1002879.
248. Cao K, Lailler N, Zhang Y, Kumar A, Uppal K, Liu Z, Lee EK, Wu H, Medrzycki M, Pan C, et al: **High-resolution mapping of h1 linker histone variants in embryonic stem cells.** *PLoS Genet* 2013, **9:**e1003417.
249. Izzo A, Kamieniarz-Gdula K, Ramirez F, Noureen N, Kind J, Manke T, van Steensel B, Schneider R: **The Genomic Landscape of the Somatic Linker Histone Subtypes H1.1 to H1.5 in Human Cells.** *Cell Rep* 2013.
250. Kalhor R, Tjong H, Jayathilaka N, Alber F, Chen L: **Genome architectures revealed by tethered chromosome conformation capture and population-based modeling.** *Nat Biotechnol* 2012, **30:**90-98.
251. Zang C, Schones DE, Zeng C, Cui K, Zhao K, Peng W: **A clustering approach for identification of enriched domains from histone modification ChIP-Seq data.** *Bioinformatics* 2009, **25:**1952-1958.
252. Shin H, Liu T, Manrai AK, Liu XS: **CEAS: cis-regulatory element annotation system.** *Bioinformatics* 2009, **25:**2605-2606.
253. Perez-Llamas C, Lopez-Bigas N: **Gitools: analysis and visualisation of genomic data using interactive heat-maps.** *PLoS One* 2011, **6:**e19541.

254. Gamallo C, Moreno-Bueno G, Sarrio D, Calero F, Hardisson D, Palacios J: **The prognostic significance of P-cadherin in infiltrating ductal breast carcinoma.** *Mod Pathol* 2001, **14:**650-654.
255. Peralta Soler A, Knudsen KA, Salazar H, Han AC, Keshgegian AA: **P-cadherin expression in breast carcinoma indicates poor survival.** *Cancer* 1999, **86:**1263-1272.
256. Kinkade JM, Jr., Cole RD: **A structural comparison of different lysine-rich histones of calf thymus.** *J Biol Chem* 1966, **241:**5798-5805.
257. Kinkade JM, Jr., Cole RD: **The resolution of four lysine-rich histones derived from calf thymus.** *J Biol Chem* 1966, **241:**5790-5797.
258. Toyama BH, Savas JN, Park SK, Harris MS, Ingolia NT, Yates JR, 3rd, Hetzer MW: **Identification of long-lived proteins reveals exceptional stability of essential cellular structures.** *Cell* 2013, **154:**971-982.
259. Barski A, Cuddapah S, Cui K, Roh TY, Schones DE, Wang Z, Wei G, Chepelev I, Zhao K: **High-resolution profiling of histone methylations in the human genome.** *Cell* 2007, **129:**823-837.
260. Thakar A, Gupta P, Ishibashi T, Finn R, Silva-Moreno B, Uchiyama S, Fukui K, Tomschik M, Ausio J, Zlatanova J: **H2A.Z and H3.3 histone variants affect nucleosome structure: biochemical and biophysical studies.** *Biochemistry* 2009, **48:**10852-10857.
261. Clayton AL, Mahadevan LC: **MAP kinase-mediated phosphoacetylation of histone H3 and inducible gene regulation.** *FEBS Lett* 2003, **546:**51-58.
262. Drobic B, Perez-Cadahia B, Yu J, Kung SK, Davie JR: **Promoter chromatin remodeling of immediate-early genes is mediated through H3 phosphorylation at either serine 28 or 10 by the MSK1 multi-protein complex.** *Nucleic Acids Res* 2010, **38:**3196-3208.
263. Healy S, Khan P, He S, Davie JR: **Histone H3 phosphorylation, immediate-early gene expression, and the nucleosomal response: a historical perspective.** *Biochem Cell Biol* 2012, **90:**39-54.
264. Garber M, Yosef N, Goren A, Raychowdhury R, Thielke A, Guttman M, Robinson J, Minie B, Chevrier N, Itzhaki Z, et al: **A high-throughput chromatin immunoprecipitation approach reveals principles of dynamic gene regulation in mammals.** *Mol Cell* 2012, **47:**810-822.
265. Mavrich TN, Ioshikhes IP, Venters BJ, Jiang C, Tomsho LP, Qi J, Schuster SC, Albert I, Pugh BF: **A barrier nucleosome model for statistical positioning of nucleosomes throughout the yeast genome.** *Genome Res* 2008, **18:**1073-1083.
266. Teif VB, Vainshtein Y, Caudron-Herger M, Mallm JP, Marth C, Hofer T, Rippe K: **Genome-wide nucleosome positioning during embryonic stem cell development.** *Nat Struct Mol Biol* 2012, **19:**1185-1192.
267. Kratzmeier M, Albig W, Meergans T, Doenecke D: **Changes in the protein pattern of H1 histones associated with apoptotic DNA fragmentation.** *Biochem J* 1999, **337 (Pt 2):**319-327.
268. Hawkins RD, Hon GC, Lee LK, Ngo Q, Lister R, Pelizzola M, Edsall LE, Kuan S, Luu Y, Klugman S, et al: **Distinct epigenomic landscapes of pluripotent and lineage-committed human cells.** *Cell Stem Cell* 2010, **6:**479-491.
269. Krejci J, Uhlirova R, Galiova G, Kozubek S, Smigova J, Bartova E: **Genome-wide reduction in H3K9 acetylation during human embryonic stem cell differentiation.** *J Cell Physiol* 2009, **219:**677-687.

270. Wen B, Wu H, Shinkai Y, Irizarry RA, Feinberg AP: **Large histone H3 lysine 9 dimethylated chromatin blocks distinguish differentiated from embryonic stem cells.** *Nat Genet* 2009, **41:**246-250.
271. Meshorer E, Yellajoshula D, George E, Scambler PJ, Brown DT, Misteli T: **Hyperdynamic plasticity of chromatin proteins in pluripotent embryonic stem cells.** *Dev Cell* 2006, **10:**105-116.
272. Melcer S, Hezroni H, Rand E, Nissim-Rafinia M, Skoultchi A, Stewart CL, Bustin M, Meshorer E: **Histone modifications and lamin A regulate chromatin protein dynamics in early embryonic stem cell differentiation.** *Nat Commun* 2012, **3:**910.
273. Gondor A: **Dynamic chromatin loops bridge health and disease in the nuclear landscape.** *Semin Cancer Biol* 2013, **23:**90-98.
274. Reddy KL, Feinberg AP: **Higher order chromatin organization in cancer.** *Semin Cancer Biol* 2013, **23:**109-115.
275. Timp W, Feinberg AP: **Cancer as a dysregulated epigenome allowing cellular growth advantage at the expense of the host.** *Nat Rev Cancer* 2013, **13:**497-510.
276. Munoz P, Iliou MS, Esteller M: **Epigenetic alterations involved in cancer stem cell reprogramming.** *Mol Oncol* 2012, **6:**620-636.
277. McDonald OG, Wu H, Timp W, Doi A, Feinberg AP: **Genome-scale epigenetic reprogramming during epithelial-to-mesenchymal transition.** *Nat Struct Mol Biol* 2011, **18:**867-874.
278. Chow KH, Factor RE, Ullman KS: **The nuclear envelope environment and its cancer connections.** *Nat Rev Cancer* 2012, **12:**196-209.
279. Hansen KD, Timp W, Bravo HC, Sabunciyan S, Langmead B, McDonald OG, Wen B, Wu H, Liu Y, Diep D, et al: **Increased methylation variation in epigenetic domains across cancer types.** *Nat Genet* 2011, **43:**768-775.
280. Popova EY, Grigoryev SA, Fan Y, Skoultchi AI, Zhang SS, Barnstable CJ: **Developmentally regulated linker histone H1c promotes heterochromatin condensation and mediates structural integrity of rod photoreceptors in mouse retina.** *J Biol Chem* 2013, **288:**17895-17907.
281. Chodavarapu RK, Feng S, Bernatavichute YV, Chen PY, Stroud H, Yu Y, Hetzel JA, Kuo F, Kim J, Cokus SJ, et al: **Relationship between nucleosome positioning and DNA methylation.** *Nature* 2010, **466:**388-392.
282. Felle M, Hoffmeister H, Rothammer J, Fuchs A, Exler JH, Langst G: **Nucleosomes protect DNA from DNA methylation in vivo and in vitro.** *Nucleic Acids Res* 2011, **39:**6956-6969.
283. Portela A, Liz J, Nogales V, Setien F, Villanueva A, Esteller M: **DNA methylation determines nucleosome occupancy in the 5'-CpG islands of tumor suppressor genes.** *Oncogene* 2013.
284. Berdasco M, Esteller M: **Aberrant epigenetic landscape in cancer: how cellular identity goes awry.** *Dev Cell* 2010, **19:**698-711.
285. Cui P, Zhang L, Lin Q, Ding F, Xin C, Fang X, Hu S, Yu J: **A novel mechanism of epigenetic regulation: nucleosome-space occupancy.** *Biochem Biophys Res Commun* 2010, **391:**884-889.
286. Ball DJ, Gross DS, Garrard WT: **5-methylcytosine is localized in nucleosomes that contain histone H1.** *Proc Natl Acad Sci U S A* 1983, **80:**5490-5494.

287. Campoy FJ, Meehan RR, McKay S, Nixon J, Bird A: **Binding of histone H1 to DNA is indifferent to methylation at CpG sequences.** *J Biol Chem* 1995, **270:**26473-26481.
288. McArthur M, Thomas JO: **A preference of histone H1 for methylated DNA.** *EMBO J* 1996, **15:**1705-1714.
289. Nightingale K, Wolffe AP: **Methylation at CpG sequences does not influence histone H1 binding to a nucleosome including a Xenopus borealis 5 S rRNA gene.** *J Biol Chem* 1995, **270:**4197-4200.
290. Strom R, Santoro R, D'Erme M, Mastrantonio S, Reale A, Marenzi S, Zardo G, Caiafa P: **Specific variants of H1 histone regulate CpG methylation in eukaryotic DNA.** *Gene* 1995, **157:**253-256.
291. Zardo G, Santoro R, D'Erme M, Reale A, Guidobaldi L, Caiafa P, Strom R: **Specific inhibitory effect of H1e histone somatic variant on in vitro DNA-methylation process.** *Biochem Biophys Res Commun* 1996, **220:**102-107.
292. Yang SM, Kim BJ, Norwood Toro L, Skoultchi AI: **H1 linker histone promotes epigenetic silencing by regulating both DNA methylation and histone H3 methylation.** *Proc Natl Acad Sci U S A* 2013, **110:**1708-1713.
293. Roll JD, Rivenbark AG, Jones WD, Coleman WB: **DNMT3b overexpression contributes to a hypermethylator phenotype in human breast cancer cell lines.** *Mol Cancer* 2008, **7:**15.
294. Ruike Y, Imanaka Y, Sato F, Shimizu K, Tsujimoto G: **Genome-wide analysis of aberrant methylation in human breast cancer cells using methyl-DNA immunoprecipitation combined with high-throughput sequencing.** *BMC Genomics* 2010, **11:**137.
295. Hon GC, Hawkins RD, Caballero OL, Lo C, Lister R, Pelizzola M, Valsesia A, Ye Z, Kuan S, Edsall LE, et al: **Global DNA hypomethylation coupled to repressive chromatin domain formation and gene silencing in breast cancer.** *Genome Res* 2012, **22:**246-258.
296. Rhee JK, Kim K, Chae H, Evans J, Yan P, Zhang BT, Gray J, Spellman P, Huang TH, Nephew KP, Kim S: **Integrated analysis of genome-wide DNA methylation and gene expression profiles in molecular subtypes of breast cancer.** *Nucleic Acids Res* 2013.
297. Sun Z, Asmann YW, Kalari KR, Bot B, Eckel-Passow JE, Baker TR, Carr JM, Khrebtukova I, Luo S, Zhang L, et al: **Integrated analysis of gene expression, CpG island methylation, and gene copy number in breast cancer cells by deep sequencing.** *PLoS One* 2011, **6:**e17490.
298. Fang F, Turcan S, Rimner A, Kaufman A, Giri D, Morris LG, Shen R, Seshan V, Mo Q, Heguy A, et al: **Breast cancer methylomes establish an epigenomic foundation for metastasis.** *Sci Transl Med* 2011, **3:**75ra25.
299. Ernst J, Kheradpour P, Mikkelsen TS, Shoresh N, Ward LD, Epstein CB, Zhang X, Wang L, Issner R, Coyne M, et al: **Mapping and analysis of chromatin state dynamics in nine human cell types.** *Nature* 2011, **473:**43-49.
300. Jackson AL, Bartz SR, Schelter J, Kobayashi SV, Burchard J, Mao M, Li B, Cavet G, Linsley PS: **Expression profiling reveals off-target gene regulation by RNAi.** *Nat Biotechnol* 2003, **21:**635-637.
301. Jackson AL, Linsley PS: **Recognizing and avoiding siRNA off-target effects for target identification and therapeutic application.** *Nat Rev Drug Discov* 2010, **9:**57-67.

302. Petri S, Meister G: **siRNA design principles and off-target effects.** *Methods Mol Biol* 2013, **986:**59-71.
303. Harborth J, Elbashir SM, Bechert K, Tuschl T, Weber K: **Identification of essential genes in cultured mammalian cells using small interfering RNAs.** *J Cell Sci* 2001, **114:**4557-4565.
304. Steen RL, Collas P: **Mistargeting of B-type lamins at the end of mitosis: implications on cell survival and regulation of lamins A/C expression.** *J Cell Biol* 2001, **153:**621-626.
305. Okamura H, Yoshida K, Amorim BR, Haneji T: **Histone H1.2 is translocated to mitochondria and associates with Bak in bleomycin-induced apoptotic cells.** *J Cell Biochem* 2008, **103:**1488-1496.
306. Funayama R, Saito M, Tanobe H, Ishikawa F: **Loss of linker histone H1 in cellular senescence.** *J Cell Biol* 2006, **175:**869-880.
307. Kind J, van Steensel B: **Genome-nuclear lamina interactions and gene regulation.** *Curr Opin Cell Biol* 2010, **22:**320-325.
308. Malhas A, Lee CF, Sanders R, Saunders NJ, Vaux DJ: **Defects in lamin B1 expression or processing affect interphase chromosome position and gene expression.** *J Cell Biol* 2007, **176:**593-603.
309. Shimi T, Pfleghaar K, Kojima S, Pack CG, Solovei I, Goldman AE, Adam SA, Shumaker DK, Kinjo M, Cremer T, Goldman RD: **The A- and B-type nuclear lamin networks: microdomains involved in chromatin organization and transcription.** *Genes Dev* 2008, **22:**3409-3421.
310. Goldman RD, Shumaker DK, Erdos MR, Eriksson M, Goldman AE, Gordon LB, Gruenbaum Y, Khuon S, Mendez M, Varga R, Collins FS: **Accumulation of mutant lamin A causes progressive changes in nuclear architecture in Hutchinson-Gilford progeria syndrome.** *Proc Natl Acad Sci U S A* 2004, **101:**8963-8968.
311. Shah PP, Donahue G, Otte GL, Capell BC, Nelson DM, Cao K, Aggarwala V, Cruickshanks HA, Rai TS, McBryan T, et al: **Lamin B1 depletion in senescent cells triggers large-scale changes in gene expression and the chromatin landscape.** *Genes Dev* 2013, **27:**1787-1799.
312. Prokocimer M, Davidovich M, Nissim-Rafinia M, Wiesel-Motiuk N, Bar DZ, Barkan R, Meshorer E, Gruenbaum Y: **Nuclear lamins: key regulators of nuclear structure and activities.** *J Cell Mol Med* 2009, **13:**1059-1085.
313. Taddei A, Hediger F, Neumann FR, Gasser SM: **The function of nuclear architecture: a genetic approach.** *Annu Rev Genet* 2004, **38:**305-345.
314. Albergaria A, Ribeiro AS, Vieira AF, Sousa B, Nobre AR, Seruca R, Schmitt F, Paredes J: **P-cadherin role in normal breast development and cancer.** *Int J Dev Biol* 2011, **55:**811-822.
315. Ribeiro AS, Albergaria A, Sousa B, Correia AL, Bracke M, Seruca R, Schmitt FC, Paredes J: **Extracellular cleavage and shedding of P-cadherin: a mechanism underlying the invasive behaviour of breast cancer cells.** *Oncogene* 2010, **29:**392-402.
316. Ribeiro AS, Sousa B, Carreto L, Mendes N, Nobre AR, Ricardo S, Albergaria A, Cameselle-Teijeiro JF, Gerhard R, Soderberg O, et al: **P-cadherin functional role is dependent on E-cadherin cellular context: a proof of concept using the breast cancer model.** *J Pathol* 2013, **229:**705-718.

317. Paredes J, Correia AL, Ribeiro AS, Milanezi F, Cameselle-Teijeiro J, Schmitt FC: **Breast carcinomas that co-express E- and P-cadherin are associated with p120-catenin cytoplasmic localisation and poor patient survival.** *J Clin Pathol* 2008, **61:**856-862.
318. Albergaria A, Ribeiro AS, Pinho S, Milanezi F, Carneiro V, Sousa B, Sousa S, Oliveira C, Machado JC, Seruca R, et al: **ICI 182,780 induces P-cadherin overexpression in breast cancer cells through chromatin remodelling at the promoter level: a role for C/EBPbeta in CDH3 gene activation.** *Hum Mol Genet* 2010, **19:**2554-2566.
319. Paredes J, Albergaria A, Oliveira JT, Jeronimo C, Milanezi F, Schmitt FC: **P-cadherin overexpression is an indicator of clinical outcome in invasive breast carcinomas and is associated with CDH3 promoter hypomethylation.** *Clin Cancer Res* 2005, **11:**5869-5877.
320. Paredes J, Stove C, Stove V, Milanezi F, Van Marck V, Derycke L, Mareel M, Bracke M, Schmitt F: **P-cadherin is up-regulated by the antiestrogen ICI 182,780 and promotes invasion of human breast cancer cells.** *Cancer Res* 2004, **64:**8309-8317.
321. Simon JM, Giresi PG, Davis IJ, Lieb JD: **Using formaldehyde-assisted isolation of regulatory elements (FAIRE) to isolate active regulatory DNA.** *Nat Protoc* 2012, **7:**256-267.
322. Strutt H, Paro R: **Mapping DNA target sites of chromatin proteins in vivo by formaldehyde crosslinking.** *Methods Mol Biol* 1999, **119:**455-467.
323. Saldanha AJ: **Java Treeview--extensible visualization of microarray data.** *Bioinformatics* 2004, **20:**3246-3248.
324. Li R, Yu C, Li Y, Lam TW, Yiu SM, Kristiansen K, Wang J: **SOAP2: an improved ultrafast tool for short read alignment.** *Bioinformatics* 2009, **25:**1966-1967.
325. Zhu LJ, Gazin C, Lawson ND, Pages H, Lin SM, Lapointe DS, Green MR: **ChIPpeakAnno: a Bioconductor package to annotate ChIP-seq and ChIP-chip data.** *BMC Bioinformatics* 2010, **11:**237.
326. Quinlan AR, Hall IM: **BEDTools: a flexible suite of utilities for comparing genomic features.** *Bioinformatics* 2010, **26:**841-842.
327. Lander ES, Linton LM, Birren B, Nusbaum C, Zody MC, Baldwin J, Devon K, Dewar K, Doyle M, FitzHugh W, et al: **Initial sequencing and analysis of the human genome.** *Nature* 2001, **409:**860-921.
328. Hubbard TJ, Aken BL, Beal K, Ballester B, Caccamo M, Chen Y, Clarke L, Coates G, Cunningham F, Cutts T, et al: **Ensembl 2007.** *Nucleic Acids Res* 2007, **35:**D610-617.
329. Benjamini Y, Hochberg, Y.: **Controlling the false discovery rate: A practical and powerful approach to multiple testing.** *Journal of the Royal Statistical Society* 1995, **57:**289-300.